A fine-scale lidar-based habitat suitability mapping methodology for the marbled murrelet (*Brachyramphus marmoratus*) on Vancouver Island, British Columbia

by

Georgia Emily Clyde
BSc., University of Victoria, 2013

A Thesis Submitted in Partial Fulfillment
of the Requirements for the Degree of

MASTER OF SCIENCE

in the Department of Geography

Supervisory Committee

A fine-scale lidar-based habitat suitability mapping methodology for the marbled murrelet (*Brachyramphus marmoratus*) on Vancouver Island, British Columbia

by

Georgia Emily Clyde
BSc., University of Victoria, 2013

Supervisory Committee

Dr. K. Olaf Niemann (Department of Geography)
Supervisor

Dr. Mark S. Flaherty (Department of Geography)
Departmental Member

Abstract

Supervisory Committee

Dr. K. Olaf Niemann (Department of Geography)
Supervisor

Dr. Mark S. Flaherty (Department of Geography)
Departmental Member

The marbled murrelet (*Brachyramphus marmoratus*) is a Threatened seabird with very particular nesting requirements. They choose to nest almost exclusively on mossy platforms, provided by large branches or deformities, in the upper canopies of coniferous old-growth trees located within 50 km of the ocean. Due primarily to a loss of this nesting habitat, populations in B.C. have seen significant decline over the past several decades. As such, reliable spatial habitat data are required to facilitate efficient management of the species and its remaining habitats. Current habitat mapping methodologies are limited by their qualitative assessment of habitat attributes and the large, stand-based spatial scale at which they classify and map habitat. This research aimed to address these limitations by utilizing light detection and ranging (lidar) technologies to develop an object-based habitat mapping methodology capable of quantitatively mapping habitat suitability at the scale of an individual tree on Northern Vancouver Island, British Columbia (B.C.). Using a balanced random forest (BRF) classification algorithm and in-field habitat suitability data derived from low-level aerial surveys (LLAS), a series of lidar-derived terrain and canopy descriptors were used to predict the habitat suitability (Rank 1: Very High Suitability – Rank 6: Nil Suitability) of lidar-derived individual tree objects. The classification model reported an overall classification accuracy of 71%, with Rank 1 – Rank 5 reporting individual class accuracies of 90%, 86%, 74%, 67%, and 98%, respectively. Evaluation of the object-based predictive habitat suitability maps provided evidence that this new methodology is capable of identifying and quantifying within-stand habitat variability at the scale of an individual tree. This improved quantification provides a superior level of habitat differentiation currently unattainable using existing habitat mapping methods. As the total amount of suitable nesting habitat in B.C. is expected to continue to decline, this improved quantification is a critical advancement for strategic managers, facilitating improved habitat and species management.

Table of Contents

List of Tables

List of Figures

Acknowledgements

There are many people who are owed an innumerable number of thanks for their continued support of this research and their unwavering belief in me.

First, to Western Forest Products Inc. and the Natural Sciences and Engineering Research Council of Canada for their generous financial support, which made this research possible. With special and sincere thanks to Christine Petrovcic and Sue McDonald for their dedication to this project and their constant guidance and expertise. Without you, this would not have been possible. To Louise Waterhouse and Dr. Alan Burger, for their expert advice and invaluable feedback, and to Dr. Mark Flaherty, for your helpful insights.

To my fellow grad school victims, Robin Kite, Michael Branion-calles, Michael Grilliot, Terri Evans, Gillian Harvey, Dr. Jessica Fitterer, and my friends far and wide, thank you for keeping me sane and never letting me feel alone on this grueling journey.

To my mom, dad and brother, who have supported me from the very beginning, this achievement is as much mine as it is yours. To Traian, thank you for being your calm, grounding, loving, and goofy self. Without your unconditional support, I would never have made it through this process.

Lastly, I give thanks to my lab family, to whom I owe everything. To Diana, for your friendship, truly unwavering support, and mutual love of wine and fries. To Roger, Geoff, Fabio, and Rob, thank you for making the last six years of my life both miserable and unforgettable. I love you guys, and I will consider taking you out of the burn book. Finally, to my supervisor and friend Olaf, thank you for taking a chance on a kid who knew nothing about remote sensing, it has been an extraordinary adventure. Please, never hesitate to give me a call if you're ever in need of a life coach, and remember, I told you that you'd miss me when I was gone.

Dedication

I dedicate this thesis to the marbled murrelet, best of luck.

Chapter 1: Introduction

1.1 Research Rational

The marbled murrelet (*Brachyramphus marmoratus*) is a small, Threatened seabird from the family Alcidae (Auks). The global distribution of marbled murrelets extends from central California northwards through Southern British Columbia (B.C.) to the Aleutian Islands, Alaska (Environment Canada, 2014). They feed in the coastal waters of the Pacific Ocean. However, unlike most seabirds, marbled murrelets fly extensive distances inland to nest, traveling up to 125 km between feeding and nesting sites daily (Lorenz et al., 2016). They are habitat specialists, requiring a suite of biophysical and geographical characteristics at landscape, stand, and individual tree - based scales (COSEWIC, 2012). In B.C., they nest almost exclusively on mossy platforms provided by large branches or deformities in the upper canopies of coniferous old-growth trees within 50 km of the ocean (Environment Canada, 2014; Mather et al., 2010; Nelson, 1997). The amount of old-growth forests that exhibit these biophysical attributes is directly linked to the abundance of marbled murrelets (Burger & Waterhouse, 2009). Troublingly, marbled murrelet populations in B.C. and the United States (U.S.) have seen significant decline over the past several decades due in large part to a loss of this nesting habitat (Environment Canada, 2014). Accordingly, they are listed as Threatened under the Canadian *Species at Risk Act* (SARA), Threatened under the United States *Endangered Species Act* (ESA), Blue Listed by the B.C. Conservation Data Center, Identified Wildlife under the B.C. *Forest and Range Practices Act* (FRPA), and managed as a focal species under Ecosystem Based Management in B.C. (B.C. Ministy of Environment, 2004;

Burger, 2001; COSEWIC, 2012; Environment Canada, 2014; Horn et al., 2009; USFWS, 1997).

In response to their decline and as per the requirements of these legislative designations, extensive research efforts have been focused on the identification of critical terrestrial habitat. A considerable collaborative effort has been made in B.C. and the U.S. by government, industry, and academia over the past several decades to understand what characteristics comprise suitable nesting habitat (Bradley & Cooke, 2001; Burger, 2002; Burger et al., 2010; Burger & Bahn, 2004; Burger & Chatwin, 2002; Burger & Waterhouse, 2009; Manley et al., 1999; CMMRT, 2003; Mather et al., 2010; Silvergieter & Lank, 2011b, 2011a; Wilk, et al., 2016), and what methods can be used to identify, classify, and map such habitats (Burger, 2004; Burger, Manley, et al., 2009; Burger & Waterhouse, 2009; Burger, Waterhouse, et al., 2009; Hagar et al., 2014; Hamer et al., 2008; Mather et al., 2010). Through this work there is now an understanding of the biophysical and geographical characteristics that comprise suitable nesting habitat. Yet there is continued uncertainty about the reliability of how habitat is classified and mapped (Burger & Waterhouse, 2009; Donald et al., 2010; Mather et al., 2010). Research that focuses on improving the identification of critical nesting habitat is therefore imperative for the recovery of the species.

Habitat in B.C. is classified using a six-class ranking system, where Rank 1 indicates the most suitable habitat, and Rank 6 indicates the least suitable habitat, essentially representing non-forested areas. These rankings are qualitatively assigned to habitat areas

based on the interpretation of structural forest characteristics known to influence habitat suitability. The qualitative nature of these assessments can create inconsistencies in the habitat rankings assigned between geographical regions and even between surveys within the same region, as well as negatively influence the accuracy of the habitat suitability rankings assigned to habitat areas. Furthermore, the large, stand-based spatial scale that habitat is currently mapped at creates uncertainty regarding the reliability of the habitat data, as the stand-based polygons are not likely to be entirely homogenous in forest characteristics. Instead, they are likely to be variable, containing patches of habitat that may be more or less suitable than the overall polygon ranking represents. Variability that is undetectable at the current stand-based scale (Cober et al., 2014; Donald et al., 2010; Hamer et al., 1995; Waterhouse et al., 2009; Waterhouse et al., 2010; Zharikov et al., 2006). Note that a *patch* is defined for this research simply as a smaller area of habitat contained within a larger habitat area. Not in relation to use of *patch* in the context of *minimum patch size* concerning edge effects and predation (Burger, 2016) or the required area surrounding a suitable nest tree, inclusive of the tree itself and the nest grove within a nest stand (Silvergieter & Lank, 2011b). Given that species recovery is dependent on the maintenance of suitable nesting habitat (Environment Canada, 2014), methods that result in inconsistent habitat classifications and potentially overgeneralize habitat suitability are problematic, and may be limiting the implementation of current habitat management strategies for the marbled murrelet (Environment Canada, 2014). Advanced remote sensing technologies such as light detection and ranging (lidar) provide an opportunity to improve upon the methods currently used for classifying and mapping marbled murrelet nesting habitat, by facilitating the quantitative measurement of habitat

attributes at a refined spatial scale, thus reducing uncertainty in spatial habitat management and facilitating improved habitat and species management.

1.2 Research Focus

This thesis focused on the improvement of methods currently used to map marbled murrelet nesting habitat in B.C. Particular focus was placed on the improvement of the spatial scale at which habitat is currently mapped and the qualitative assessments currently used to determine habitat suitability. The most common approaches currently used to generate predictive habitat suitability maps for the marbled murrelet in B.C. rely predominantly on either air photo interpretation (API) or low-level aerial surveys (LLAS). The former visually interpret attributes associated with murrelet nesting habitat, such as tree size and canopy complexity, from air photos at a scale of 1:20000 (Burger, 2004). Based on these interpretations, polygons are then delineated around contiguous areas of habitat interpreted to be of a particular suitability for nesting. LLAS visually assess attributes associated with nesting habitat, such as canopy closure and the presence of nesting platforms, through in-field helicopter surveys (Burger, 2004). Data collected from the in-field surveys are then used to classify the suitability of large, stand-based polygons. The specific habitat maps that this research aimed to improve upon were derived using a LLAS method. To do so this research evaluated the development of an object-based methodology capable of mapping habitat at an individual tree – based scale, using habitat descriptors that were quantitatively measured from a lidar point cloud.

Airborne lidar utilizes an active remote sensing technology capable of capturing highly accurate, three-dimensional information about terrain and above ground vegetation (Lim et al., 2003). Lidar technologies offer a non-invasive approach for accessing remote regions and repeatedly collecting data across large spatial extents, both of which are challenging if not impossible though field-based surveys alone (Bradbury et al., 2005). This ability to directly quantify forest structures in three dimensions makes lidar highly advantageous for mapping wildlife habitats, particularly for species with specialized structural requirements (Lefsky et al., 2002; Turner et al., 2003). Furthermore, sensor advancements have resulted in increasingly higher point densities, now allowing for reliable quantification of forest structure at an individual tree - based scale (Casas et al., 2016; Heurich et al., 2003; Holmgren & Soderman, 2002; Jakubowski et al., 2013; Vierling et al., 2008). This improved spatial scale has been shown to be ideal for capturing bird-habitat relationships (Bradbury et al., 2005). Lidar-derived habitat predictors have also demonstrated improved classification accuracies in predictive wildlife habitat models (Ackers et al., 2015; Graf et al., 2009). Lidar-based predictive modelling for marbled murrelet nesting habitat has been explored in the U.S. (Hagar et al., 2014), however its application here in B.C., and the utilization of an object-based scale are novel.

Complex interactions between many variables are intrinsic to ecological systems. Random forests are a robust non-parametric statistical classification or regression technique that offer the ability to handle these complex interactions by allowing for mixed variable types, accounting for higher order interactions between predictors and

non-linear relationships, imputing missing values, and report on variable importance while producing high classification accuracies (Branion-calles, 2015; Breiman, 2001; Cutler et al., 2007). They make no distributional assumptions about predictors and require only two user-defined parameters when implemented in R: the number of trees to include in the forest and the number of predictors to consider in each tree (Williams, 2011; Cutler et al., 2007). Random forests have demonstrated several instances of comparable and superior performance for ecological applications when compared to other machine leaning algorithms such as support vector machines, artificial neural nets, and simple classification trees, as well as more traditional methods such as linear regressions (Breiman, 2001; Cutler et al., 2007; Lawler et al., 2006; Meyer et al., 2003; Peters et al., 2007; Svetnik et al., 2003). Moreover, in ecological modelling the features of most interest are often rare events. Thus, data representing ecological phenomena frequently contain an uneven distribution in the number of samples per category, with the critical category having the least number of samples. This creates imbalanced datasets. The most significant advantage of a random forest classifier is its ability to handle these imbalanced datasets using a balanced variant of the classifier (Chen et al., 2004). This balanced random forest (BRF) classifier ensures that the minority class is equally represented in the model and not dominated by observations from the majority classes. Because the most suitable nesting habitat for the marbled murrelet occurs in smaller quantities when compared to lower quality habitats, nesting habitat suitability data are often imbalanced. The use of a BRF statistical classifier was therefore highly advantageous for the methodology developed here.

Lastly, while predictive occupancy models are often the most desirable modelling product for species and habitat management, nest site and occupancy data are inherently challenging to collect for the marbled murrelet, due to their secretive behavior and elusive nesting patterns. Because of this, predictive habitat suitability models are often built instead, identifying areas of potentially suitable nesting habitat that can then be investigated through in-field surveys to evaluate occupancy and nest site presence. Because there were no nest site or occupancy data available within our study sites, this research focused on the development of a predictive habitat suitability model utilizing LLAS waypoint data of known habitat suitability. LLAS waypoint data were utilized for two reasons: (1) there was already an existing database of LLAS waypoint data for the study sites, and (2) a large network of these LLAS waypoint data also exists across much of B.C. Therefore, facilitating the efficient replication of this methodology as a standard, operationally-based habitat mapping approach across B.C. as more lidar data become available.

1.3 Research Goal

The goal of this research was to investigate the development of a quantitative, lidar-based, predictive habitat mapping methodology capable of producing predictive nesting habitat suitability maps for the marbled murrelet at the scale of the individual tree. This was achieved by evaluating the ability of a series of lidar-derived habitat descriptors to predict habitat suitability of mature and old-growth trees on Northern Vancouver Island, B.C., determined by LLAS waypoint data. This new methodology aimed to overcome the limitations often associated with current mapping methods regarding the spatial scale of

habitat data and the qualitative nature of habitat classifications. By mapping habitat at this refined, individual tree - based scale, small patches of suitable habitat situated within larger unsuitable areas can be identified and mapped. Lastly, this research aimed to make recommendations to industry and government concerning data collection and processing methods best suited for future habitat mapping initiatives for the marbled murrelet. The methodology developed here allows for a more accurate and consistent identification of suitable nesting habitat when compared to the mixed approaches currently used in B.C., and provides object-based datasets that can be scaled up based on preferred clustering methods and parameter settings. This thesis contributed towards improving the spatial scale, accuracy, and availability of habitat data for the marbled murrelet in B.C., a valuable contribution for strategic planning and conservation initiatives focused on the recovery of the marbled murrelet in multi-use landscapes.

1.4 Research Questions and Objectives

1) First, can lidar-derived structural habitat descriptors be used to predict habitat suitability at the scale of an individual tree using habitat data derived from ranked LLAS waypoints?
    - Identify and extract individual tree objects from lidar data to be used as the objects for modelling and mapping.
    - Extract a series of habitat predictors from the lidar data based on expert knowledge and literature that can be used to effectively predict the suitability of habitat using LLAS waypoint data and a BRF statistical classifier.

- Use the predictive classification model developed in objective two to predict a habitat suitability ranking for all trees identified in objective one and map all trees by their predicted rankings to create the object-based predictive habitat suitability maps.

2) If so, can this object-based mapping methodology be used to identify smaller patches of suitably ranked habitat within larger areas previously identified as less suitable by existing methods?
    - Compare the predicted rankings of the individual trees to the overall rankings of existing stand-based habitat suitability maps and visually inspect the object-based habitat maps to evaluate if the new methodology can be used to identify patches of suitably ranked trees within larger unsuitable areas.

3) Lastly, based on results, can a lidar-based approach be recommended for future marbled murrelet habitat mapping initiatives in B.C.?
    - Evaluate accuracy of results and costs associated with method to make recommendations about the appropriate data and modelling techniques for future marbled murrelet habitat studies

1.5 Thesis Outline

This thesis is comprised of six chapters. Chapter one provided an introduction to the research, discussing its rational, its focus, its main goal, and the specific research questions and objectives it aimed to answered and meet. Chapter two provides the background information, gathered through an extensive literature review, used to guide this research and shape the methodology that was developed. Chapter three outlines the methods used, including information on the study sites where this research was conducted and the data that were used. Chapter four presents the key results. Chapter five discusses the results and their significance, and makes recommendations for future habitat studies. Finally, Chapter six presents the conclusions and research contributions.

Chapter 2: Background

2.1 The Marbled Murrelet

2.1.1 Biology and behaviour

The marbled murrelet is a diving seabird from the Alcidae family. They have stout but streamlined bodies, resulting in a high body mass to wing size ratio (avg. adult: 24-25 cm long, 122-149 mm wing length, and 188-269 g) (Nelson, 1997). This ratio creates an imbalance and results in high wing loading. This imbalance makes takeoff and landing challenging and requires specific structural attributes of nesting sites to facilitate their stall landings and jump-off takeoffs. This imbalance also requires rapid wing movement in order to sustain flight (Nelson, 1997). This rapid wing movement allows them to reach exceptional flight speeds of up to 158 km/h (average ≥ 70 km/h), but also requires a high caloric intake to sustain (Burger, 1997, 2002; Environment Canada, 2014) .

Like all alcids, marbled murrelets dive below the surface and use their wings to propel themselves or "fly" underwater in pursuit of their prey. Their streamlined bodies allow them to move rapidly when diving, resulting in relatively short dive times (~30 seconds) (Wong et al., 2008). Diving depths are relatively unknown. However, based on the behaviour of their most common prey, Pacific sand lance (*Ammodytes hexapterus*), it is estimated they dive primarily within the top 5 m of the water column (Burger, 2002). They are opportunistic feeders, but prefer small schooling fish and large crustaceans. They feed in shallow (< 30 m), nearshore (0.5 – 2.0 km) ocean waters (Environment Canada, 2014). Although feeding has also been observed in freshwater lakes (Carter &

Sealy, 1986). Foraging adults fly to and from feeding sites in the hours just before dawn and shortly after dusk, and occur on the water at very low densities as singles or pairs of birds (Ralph et al., 1995; Strachan et al., 1995). These elusive flight patterns make them challenging to identify and track.

Marbled murrelets are a long-lived species, and while exact generation time is unknown, they are estimated to live approximately 10 years (Burger, 2002). Average age of first breed is also unconfirmed, but is estimated to be relatively late, between 2-5 years old (Environment Canada, 2014). Unlike most alcids, the marbled murrelet does not nest in colonies. Instead they mostly nest as solitary pairs at very low densities (0.11 nests//ha) (Burger, 2001; Conroy et al., 2002). The breeding season lasts from mid-April to August, with nest site prospecting and selection generally occurring between March and May (Nelson, 1997). Research suggests that nests are only likely to be re-used if extensive habitat loss has occurred in the area (Burger, Manley, et al., 2009). If the area is relatively undisturbed, re-use of nest sites is considered to be rare (Burger, Manley, et al., 2009; Nelson, 1997). They have low reproduction rates, with females laying only one egg per clutch and not all mature females breeding within a given year (Hamer & Nelson, 1995). These low reproductive rates make them highly sensitive to changes in their environment and slow to recover from population declines.

2.1.2 Threats

The main threat to the marbled murrelet in B.C. is the loss of their nesting habitat, due in large part to forestry operations (Environment Canada, 2014). In the U.S. the situation is

much the same, with Washington, Oregon, and California noting the loss of nesting habitat as the primary threat to the species, and Alaska reporting it as a contributing factor (McShane et al., 2004; Miller et al., 2012; Piatt, 2007; Ralph et al., 1995). It has been estimate that from 1978 to 2008, 22% of total suitable nesting habitat in B.C. was long (Long et al., 2011), with some regions experiencing even higher rates of loss, 70%, 80%, and 77% for the Sunshine Coast, Desolation Sound, and eastern Vancouver Island, respectively (Burger, 2002; Zharikov et al., 2006). Furthermore, more recent work by Environment Canada (2014) suggests that an additional 5.4% of suitable nesting habitat in B.C. was lost between 2002 and 2011. The rate of loss is estimated to slow as the provincial Allowable Annual Cuts (AAC) decreases. However, it is estimated that regardless, suitable habitat will continue to be lost to harvesting, urban development, and energy development (Environment Canada, 2014). Intensifying this threat, studies have also shown that murrelets will not nest at higher densities in smaller pockets of remaining habitat in fragmented landscapes, instead population numbers will decline (Burger, 2001; Raphael et al., 2002). COSEWIC (2012) infers that this loss of habitat has, and will continue to, have a direct and proportional impact on population numbers. Other terrestrial threats to the marbled murrelet include industrial activities that fragment habitat, creating "hard edges" that increase the exposure of nest sites to predation (Burger, 2002; COSEWIC, 2012; Environment Canada, 2014; Gabriel & Golightly, 2014; Malt & Lank, 2007, 2009). Marine threats to the species include entanglement in gill-nets, oil spills, boater traffic, and possibly rising ocean temperatures (Environment Canada, 2014).

2.1.3 Population

The global population is estimated to be 357,900 birds (Environment Canada, 2014). Alaska contains the largest proportion of the total population with an estimated 237,500 birds (66%) (Piatt, 2007). B.C. contains the second largest proportion of the population, with approximately 99,100 birds (28%) (estimates range 72,600-125,600) (Bertram et al., 2015). The southern U.S. contains the smallest proportion of the total population with 21,300 birds (6%), distributed across Washington, Oregon, and California (Falxa et al., 2013). Count data in B.C. are insufficient to draw definitive conclusions about the provinces' overall population trends, however recent work by Bertram et al. (2015) suggests an annual decline of 1.6% across all B.C. conservation regions, with annual declines as high as 9% in the eastern Vancouver Island conservation region. Declines within smaller, localized, populations have also been demonstrated (Bertram et al., 2015; Burger, 2002; COSEWIC, 2012). Overall, the total B.C. population is expected to decline by 30% over the next 30 years (COSEWIC, 2012).

2.1.4 Current status and recovery planning

In Canada, the marbled murrelet was designated as Threatened in 1990 by COSEWIC and confirmed at this status again in 2000 and 2012 (COSEWIC, 2012). In 2003, they became a Federal, Schedule 1 Threatened species under SARA, granting the implementation of their protection and recovery measures (Environment Canada, 2014). In B.C., they are on the provincial Blue List, identifying them as a species of special concern and vulnerable to extirpation or extinction, and as an Identified Wildlife species under the FRPA, allowing for the establishment of Wildlife Habitat Areas (WHA) and

the implementation of their Identified Wildlife Management Strategy (IWMS) (B.C. Conservation Data Center, 2016). In U.S., they are listed as Threatened species under the U.S. ESA, and listed as state-designated Endangered species in California (USFWS, 2016).

The current Federal Recovery Strategy for the species (Environment Canada, 2014) states that the overall short-term recovery objective for the species is to slow, and then halt, the decline of the species and its nesting habitat over the 30-year period from 2002 to 2032. This is to be done by stabilizing the total amount of nesting habitat area in the province to above 70% of levels present in 2002. Original work by Mather et al. (2010), further refined by Environment Canada (2014), estimated that there was just short of 1.5 million (1,471,954) ha of suitable nesting habitat in B.C. in 2002. Meaning 1,039,648 ha (70%) must be maintained and protected for the species declines to slow and ultimately halt. As of 2011, only an estimated 1,392,351 ha remained - just 352,703 ha above the minimum habitat retention levels (Environment Canada, 2014). Of additional concern, in 2009 only 515,411 ha (35%) of suitable nesting habitat in B.C. was legally protected in areas such as parks, conservancies, and ecological reserves (B.C. Ministry of Environment, 2004; Mather et al., 2010).

The current long-term recovery objective for the species is based on continued research and monitoring, with a focus on improving techniques for terrestrial and marine habitat characterization (Environment Canada, 2014). While significant progress has been made towards the recovery of the marbled murrelet through comprehensive research, policy

implementation, and designation of protected habitat areas, the current Recovery Strategy document for the marbled murrelet outlines some critical tasks for the future, including but not limited to: (1) refinement of baseline data for 2002 habitat levels, (2) continued habitat identification and mapping at a stand-based scale or better, (3) determination of a minimum patch size for critical habitat, (4) identification of critical habitat within priority conservation regions, and (5) development of methods and protocols for monitoring changes in the amount of suitable nesting habitat (Environment Canada, 2014). This research aimed to directly address several of these long-term goals, by providing more refined and reliable spatial habitat data.

2.1.5 Nesting habitat

While the marbled murrelet itself was first described in 1789, it was not until 1974 that the first definitive tree nest was discovered, found in a large Douglas-fir (*Pseudotsuga menziesii*) tree on the central coast of California (Binford et al., 1975). To date, only 240 confirmed nests have been found in B.C. (B.C. Conservation Data Center, 2013; Bloxton & Raphael, 2009; Environment Canada, 2014; Falxa et al., 2013; Ryder et al., 2012). As previously stated, the marbled murrelet is a habitat specialist with extremely particular requirements regarding the biophysical and geographic characteristics of its nest sites (Burger & Waterhouse, 2009). With the exception of a small number of nests found on cliffs or in large deciduous trees (Bradley & Cooke, 2001; Ryder et al., 2012), most nests are found on large moss or duff covered branches or deformities within the mid to upper canopies of large coniferous trees (Environment Canada, 2014). These structural characteristics are most commonly found in old-growth coniferous forests (≥ 250 years)

and, to a lesser extent, in mature coniferous forests (>141 years) with remnant old-growth components (Burger, 2002; CMMRT, 2003; Raphael, 2006). While this generally describes the characteristics of suitable nesting habitat, there are an additional number of characteristics at the landscape, forest, and individual tree - based scales that influence the potential suitability of nesting habitat.

At the landscape-scale, suitable nesting habitat in B.C. is predominantly found from 0 – 50 km inland, with suitable habitat from 0.5 – 30 km inland being the most likely to be used for nesting (Burger, 2002; Environment Canada, 2014; CMMRT, 2003). Nests have been found up to 1532 m above mean sea level (AMSL). However, on Vancouver island, the most likely elevations for suitable nesting habitat range from 0 to 600 m AMSL, with elevations from 600 to 900 m AMSL and > 900 m AMSL being moderately and least likely to contain suitable nesting habitat, respectively (Burger, 2002; CMMRT, 2003). The species also often use large-scale geomorphological features such as rivers valleys, stream channels, and avalanche chutes as flight corridors between feeding and nesting sites (Burger, 1997; Hamer & Nelson, 1995; Mack et al., 2003; Nelson, 1997; Rodway & Regehr, 2002). Provincial Biogeoclimatic Ecological Classification (BEC) zones, delineated based on climate, climax vegetation and soil conditions, have been loosely associated with forest types that provide potentially suitable nesting habitat (Horn et al., 2009; Meidinger & Pojar, 1991; Rodway & Regehr, 2002). While all BEC zones can contain suitable nesting habitat, the Coastal Western Hemlock (CWH) zone is the most used by nesting marbled murrelets as it often contains the moist, productive, low elevation forests that provide the structural requirements of suitable nesting habitat

(Donald et al., 2010; Horn et al., 2009). Results have been inconsistent when evaluating the effect of slope on habitat suitability, however it has been hypothesized that steeper slopes increase the ease of access to the middle portion of canopy, where suitable nesting platforms are most likely to occur (Burger, 2002). Studies in Clayoquot Sound and Desolation Sound have shown positive correlations between steep slopes and the presence of suitable nesting habitat and/or increased breeding success (Burger & Chatwin, 2002; Zharikov et al., 2006), while others have demonstrated negative or neutral correlations (Burger, 2002). Topographic variability is thought to potentially influence habitat suitability, with topographic irregularities such as rock outcrops or small gullies altering the vertical canopy complexity above, improving access for the birds (CMMRT, 2003). While aspect has not been widely considered, it could be hypothesized that aspect is related to moss growth and thus nesting platform suitability. Building on this, a north facing slope would theoretically be wetter and support better conditions for moss growth, whereas a south facing slope would be drier and less likely to support sufficient moss growth. However, in regions with dominantly wet climates, there may be no difference in moss growth based on topographic aspect. Furthermore, most valley bottoms exhibit a "flat" aspect, yet often contain prime Rank 1 habitat in the form of small isolated pockets of old-growth on gravel bars or flood plains (Burger & Bahn, 2004).

At the forest-based scale, habitat suitability is influenced predominantly by the complexity of the canopy. Canopy complexity can be defined by the structural attributes of canopy closure and vertical canopy complexity. In this context, canopy closure is

defined as the percentage of ground that is covered by canopy vegetation within a given area. Following this definition, suitable nesting habitat typically has a canopy closure of 30 – 70%, with the most suitable nesting habitat having 40 – 60% canopy closure (Burger, 2002). Vertical canopy complexity can generally be defined as a relative measure of canopy surface uniformity. It is an important descriptor of habitat, as stands with higher vertical complexities, indicated by greater height differentials between trees, can improve access to nesting platforms (Burger, 2004). The number of vertical layers within the canopy can also be used to define vertical canopy complexity, with optimal layering allowing the birds to navigate efficiently within the canopy (Hagar et al., 2014), while maintaining enough overhead coverage for protection against predation (Burger, 2004; Environment Canada, 2014).

At the scale of an individual tree, typical suitable nesting habitat is comprised of trees that are generally > 28.5 m tall (Burger, 2004). Trees below 28.5 m are less likely to contain sufficient nesting platforms and the heights required for stall landings and jump-off takeoffs (Environment Canada, 2014). The exception being at higher elevations, where suitable trees may be shorter due to site conditions (Burger, 2004). Trees with nests have also been found to be larger relative to surrounding trees by 15 – 20% (Silvergieter & Lank, 2011a). While there is no definitive relationship between suitable nesting habitat and tree species, as murrelets are most likely to select a tree based its structural requirements regardless of its species, regional patterns do exist (Burger, 2002; CMMRT, 2003). On western Vancouver Island, Sitka spruce (*Picea sitchensis*), Douglas-fir (*Pseudotsuga menziesii*), and Yellow-cedar (*Chamaecyparis nootkatensis*) are

consistently more likely to provide suitable nesting platforms, while Western redcedar (*Thuja plicata*) is consistently less likely to provide platforms, and Amabilis (*Abies amabilis*) and Grand fir (*Abies grandis*) and Western hemlock (*Tsuga heterophylla*) are inconsistent in providing platforms (Burger et al., 2010). Further, Sitka spruce located on flood plains, Douglas-fir located in drier BEC zones, and Yellow-cedar located at generally higher elevations will provide nest platforms more often than other species (Burger et al., 2010). Within the tree, the presence and density of nesting platforms is the most important indicator of suitable nesting habitat (Burger et al., 2010; Silvergieter & Lank, 2011a). A suitable nesting platform is defined as a branch or deformity > 15 cm in diameter and > 25 m from the ground (Burger et al., 2010). The platform must also have sufficient coverage and thickness of moss, duff or other epiphytes (Environment Canada, 2014). The moss or duff coverage creates a padded layer where the birds can create a nest cup, usually located within approximately 1 m of the tree bole (Hamer & Nelson, 1995; Nelson, 1997). In addition to nesting on the platform, murrelets will also use them as pseudo runways to help them land and takeoff (Burger, 2002). While airborne lidar is not yet capable of reliably detecting and measuring individual braches that would constitute suitable nesting platforms, the aforementioned structural characteristics of the landscape, canopy and individual tree can be used as proxy indicators to identify trees that would be most likely to contain suitable nesting platforms, and thus provide suitable nesting habitat for the species.

2.2 Existing Methods for Habitat Modelling and Mapping

Understanding species-habitat interactions has been, and continues to be, an essential component of ecological science (Guisan & Zimmermann, 2000). Through this understanding it has been long recognized that environmental factors influence resource and habitat occurrence and thus species occurrence. Therefore, by quantifying environmental factors, the distributions of a species and or its habitat can be predicted. Modelling these distributions allows for the identification of priority areas within a larger landscape, a critical tool for strategic planning and conservation (Donald et al., 2001), both of which have become increasingly important as terrestrial and marine environments become progressively fragmented, polluted, and exploited through anthropogenic change. For the marbled murrelet, understanding the distribution of its nesting habitat is paramount for recovery (Environment Canada, 2014). As such, extensive efforts have been placed on developing methods to accurately classify, model and map suitable nesting habitat over the past two decades.

Occupancy or selectivity models that use bird detections or known nest sites and biophysical attributes to predict which habitats the species will select and use for nesting are often the most important models from a resource and species management perspective. Hamer et al. (2008) developed the first predictive occupancy model for the marbled murrelet, evaluating habitat in Washington State on the Olympic Peninsula. The model was designed to evaluate the use of existing structural habitat data from previous inventories, in combination with known nest site locations, to predict occupancy of a given forest patch by the birds. They used a logistic regression model to assess 15

different structural attributes collected during field inventories evaluating their ability to predict occupancy. The final model utilized 12 predictors: canopy access, canopy closure, canopy layers, mean diameter at breast height (DBH), mistletoe index, moss cover, slope, number of trees with a > 60 cm, > 81 cm, > 99 cm DBH and > 1 potential platform, number of trees with a >60 cm DBH with high mistletoe index, and the number of potential nest platforms/ha. The predictive model reported an overall classification accuracy of 75% (90% when predicting only occupied detections). The number of canopy layers and the mistletoe index were determined to be the most significant model predictors (Hamer et al., 2008).

This method was further refined by Raphael et al. (2011), and then by Hagar et al. (2014), with the novel implementation of lidar-derived habitat descriptors. Hagar et al. (2014) used a logistic regression model to predict murrelet occupancy along the Oregon Coast using known nest site locations and six model predictors: distance to the Pacific Ocean (not lidar-derived), percentage of all returns above mean canopy height – indicating cover in the upper canopy, 99^{th} percentile of first returns – indicating height of tallest trees, 10^{th} percentile of first returns – indicating the maximum height of the bottom of the canopy, percentage of first return above the modal height – indicating variation in the upper canopy, and the minimum kurtosis of height distribution – indicating the distribution of vegetation across canopy height intervals. All metrics were generated at a 22.9 m spatial resolution, the assumed size of a nest grove (~ 525 m^2) as defined by Hagar et al. (2014). The use of lidar data allowed for the direct and more accurate measurement of habitat characteristics than had previously been available. The lidar-derived predictors were

evaluated against predictors from Gradient Nearest Neighbor (GNN) imputation using data from field plots, Landsat imagery, and other mapped environmental data. These GNN predictors were previously found to be the most important predictors of occupancy in Oregon (Raphael et al., 2011). However, the lidar-based model outperformed the GNN model in every scenario, and produced refined estimates of marbled murrelet nesting habitat. The study concluded by suggesting that lidar-derived predictors can more accurately represent nesting habitat, better discriminate between habitats that look similar by human interpretation, and should be incorporated in future models (Hagar et al., 2014). While this research introduced the novel application of lidar-derived habitat descriptors, it did not evaluate the mapping of habitat at an individual tree - based spatial scale.

Because the marbled murrelet exhibits such elusive movement and nesting patterns, occupancy and nest data are challenging to collect, particularly in samples large enough for statistical modelling. As such, habitat suitability models are often used, predicting the distribution and amount of potentially suitable nesting habitat. The first regional habitat suitability model in B.C. was developed by Bahn & Newsome (2002) and evaluated habitat suitability in Clayoquot Sound. The Habitat Suitability Index (HSI) Model classified habitats in four habitat suitability classes using data predominantly from Vegetation Resource Inventory (VRI) polygons. Seven different vegetation characteristics were selected as indicators of habitat suitability: tree height, tree age, basal area, vertical complexity, tree canopy closure, distance to sea and elevation. Habitat polygons, based off of the VRI polygon boundaries, were created and each assigned a

Suitability Index score determined by evaluating each of the seven vegetation characteristics. These scores were then combined for an overall polygon score that ranged from 0 to 1 (Excellent = > 0.875; Good = 0.78 – 0.875; Sub-optimal = 0.65 – 0.78; and Unsuitable = < 0.65).

Next, the B.C. Model (Mather et al., 2010) was built using habitat metrics from the Seamless Forest Cover Inventory (SFCI) and data from the Terrain Resources Information Management (TRIM) program. The B.C. Model is bivariate, classifying polygons from the SFCI as either (1) Suitable or (2) Not Suitable. It was designed to be used as a broad-scale tool for establishing and monitoring habitat levels for recovery planning (Mather et al., 2010). The model uses four predictors, tree height, tree age, distance inland and elevation, all derived from the SFCI. The resultant habitat maps are defined by large-scale polygons, each assigned a single habitat suitability ranking. While this was the first large-scale habitat suitability model for B.C., and provided valuable data for habitat quantification, it relies on only four habitat descriptors, most of which are qualitatively interpreted and mapped at a coarse spatial scale. This method is beneficial for broad-scale habitat mapping, but does not have the ability to produce the fine-scale habitat data that are required for localized strategic species and habitat management.

In addition to these habitat suitability models, API is a standardized method that has been widely used across B.C. for habitat classification and mapping (Burger, 2004; Donald et al., 2010; Environment Canada, 2014). Structural characteristics (vertical complexity, canopy complexity, tree height and stand age) are interpreted from high-resolution (30

cm) air photos and used to assign a habitat suitability rankings from the provincial standard six class ranking system (Burger, 2004; Environment Canada, 2014). However, a key limitation of API is that it is unable to detect the presence or absence of microhabitat features such as nesting platforms and moss or duff coverage. Additionally, while all attributes are interpreted following well-defined protocols and standards, the final classification of habitat suitability is qualitative rather than quantitative. Because of this, API is most valuable as a pre-stratification tool to define areas for further evaluation though more fine-scale methods such LLAS (Burger, Waterhouse, et al., 2009).

LLAS are field-based assessments that use low flying helicopter flights to assess biophysical attributes indicative of nesting habitat suitability. They are considered to be the most robust method for habitat classification and as such, have been conducted extensively across B.C. (Burger, 2004; Environment Canada, 2014; McDonald & Leigh-Spencer, 2014). However, they are sensitive to survey scale (i.e. the size of the area surveyed and the distance to the canopy during the survey) and intensity (i.e. the time spent evaluating the canopy and associated biophysical attributes). Thus, surveys conducted with different scales and intensities are likely to yield different habitat classifications for the same regions (Burger, 2004). LLAS use the same standard six-class habitat ranking system as API, however they are more advantageous than the top-down assessments of API, because they provide an oblique view into the canopy. This angle allows observers to assess both nesting platforms and moss presence, both of which are generally not visible through API (Burger, 2004). Habitat characteristics typically assessed during LLAS include: percentage of large trees, percentage of emergent trees

with platforms, percentage of emergent trees with suitable moss coverage, the percentage of canopy closure, vertical canopy complexity, topographic complexity, slope position, estimated age class, and dominant and co-dominant tree species. Based on the quality of these characteristics, an overall habitat suitability rank is assigned to the habitat unit being surveyed. LLAS were initially recommended to confirm or re-adjust rankings estimated during API (Burger, 2004), but direct habitat classification and mapping using only LLAS evolved due to their efficiency and ability to directly assess microhabitat features. In B.C., typically either API or LLAS are used to map habitat suitability; both methods are not usually used in conjunction unless fine-scale verification is required (Cober et al., 2014, Donald et al., 2010). As previously mentioned, the specific habitat maps this research aimed to improve upon were generated using a LLAS approach (McDonald & Leigh-Spencer, 2014).

Both API and LLAS have their own distinct advantages and have been able to provide critical information regarding habitat distributions for decision-makers to date (Environment Canada, 2014). However, an opportunity exists to improve the scale of predictive habitat maps in B.C. from a stand-based (polygon) scale to an object-based (individual tree) scale, making quantification of within polygon variability attainable. Furthermore, current methods in B.C. lack the ability to directly measure forest structure and instead rely on qualitatively estimated and interpreted measurements. By utilizing lidar data, habitat attributes can be directly, quantitatively measured.

2.3 Background Summary

This chapter presented the background information used to guide the development of a new habitat mapping methodology. A brief description of the marbled murrelet, its behaviour, the main threats to the species and the current focuses of its recovery plan were provided. The structural characteristics known to influence the suitability of marbled murrelet nesting habitat were reviewed, information that was used to guide the selection of model predictors for this research. Finally, to highlight the opportunity for an improved habitat mapping approach, existing habitat modelling and mapping approaches were reviewed. The following chapter outlines the key components of the new proposed methodological framework.

Chapter 3: Methods

3.1 Study Sites

This research was conducted at three separate sites on Northern Vancouver Island, B.C. (Figure 3.1). The sites were selected based on the availability of data, as well as the presence of general characteristics likely to provide suitable nesting habitat: proximity to near-shore feeding sites and the presence of mature and old-growth forests (>= 141 years). From North to South the study sites encompass: (1) the *Holberg* region (155.12 km^2), extending northeast from the end of Holberg inlet and including the areas northeast and northwest of the town of Holberg, (2) the *Koprino* region (87.53 km^2), located on the peninsula between Holberg Inlet and Quatsino Sound, west of the town of Quatsino, and (3) the *Jeune Landing* region (405.62 km^2), inclusive of areas surrounding Neroutsos Inlet and the towns of Jeune Landing and Port Alice. Together the sites covered 648.27 km^2, ranged from 0 - 1400 m AMSL, and extended from the Pacific Ocean coastline to 12.57 km inland.

All three regions have mild climates, with an average annual temperature of 10°C. However, they experience considerable precipitation throughout the year, with an average annual precipitation of 2543 mm (Environment Canada, 2016). These wet and nutrient rich conditions support a variety of habitat structures including large stands of mature and old-growth coniferous forests where this research was focused. The study sites fell into two main provincial BEC zones, the Coastal Western Hemlock (CWH) zone and Mountain Hemlock (MH) zone.

The CWH zone typically occupies elevations from sea level to ~ 900 – 1000 m AMSL. It is the rainiest BEC zone in B.C., with the most common tree species being Western hemlock (Meidinger & Pojar, 1991). Western redcedar and Douglas fir are common in drier areas, while Amabilis fir and Yellow-cedar are more likely to be found in wetter areas, with the Amabilis fir typically dominating at higher elevations. Red alder (*Alnus rubra*) is common in disturbed areas and Sitka spruce can be found in restricted pockets of specialized environmental conditions such as floodplains or exposed beaches. Forests in this BEC zone generally consist of young seral forests, managed second-growth mature forests, and smaller pockets of old-growth coniferous forests. Rocky cliffs and other exposed rock outcroppings are common, as are riparian areas along the many river, stream and creek channels that are often found in this zone (Meidinger & Pojar, 1991). The MH zone is typically found adjacent to and above the CWH zone. Its dominant tree species are Mountain hemlock, Amabilis fir and Yellow-cedar. Rugged terrain, rock outcroppings and talus slopes are more common in this BEC zone, while riparian areas and wetlands are limited. Forests in this BEC zone are often comprised of mature and old-growth coniferous trees (Meidinger & Pojar, 1991).

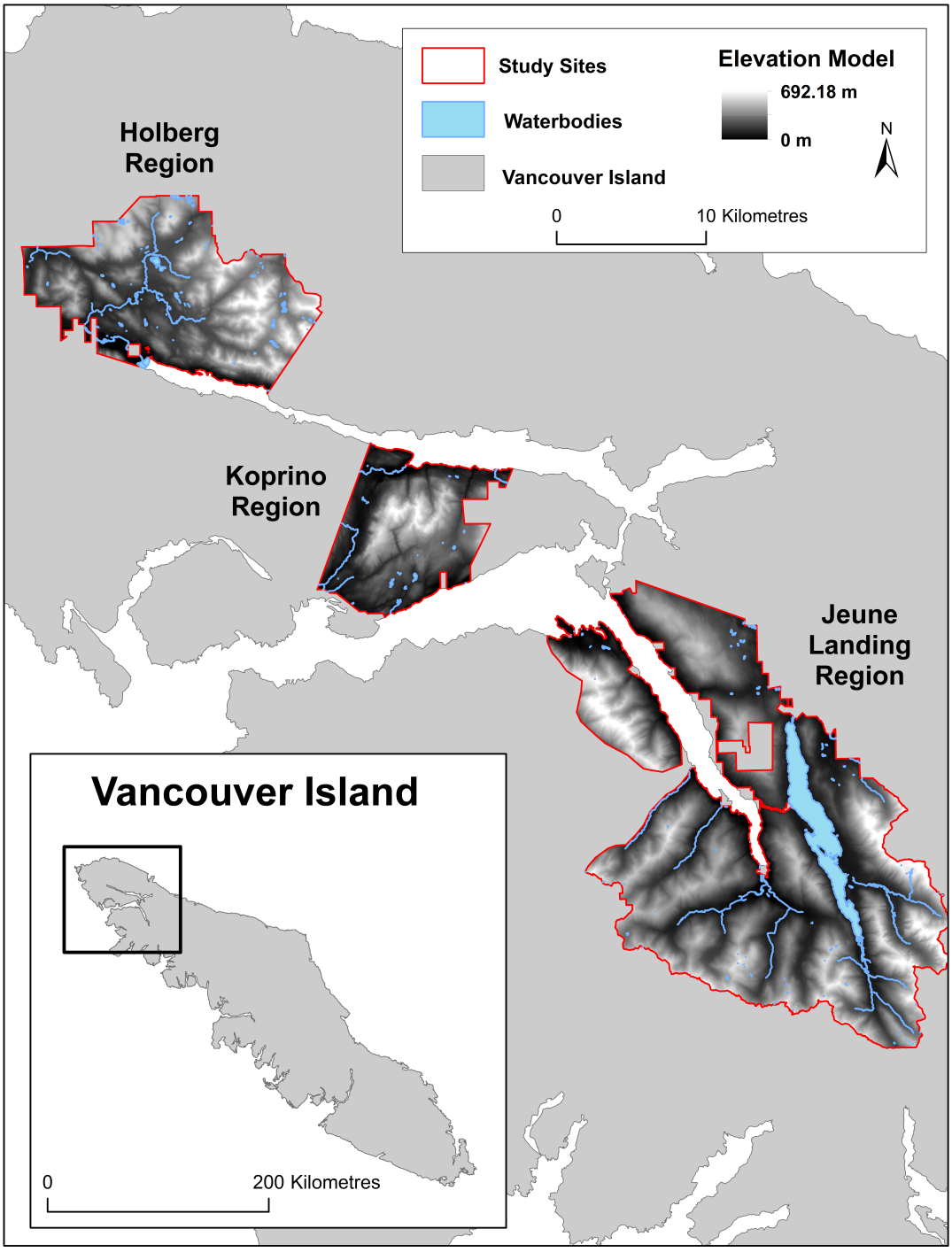

Figure 3.1. Study sites defined by data coverage on Northern Vancouver Island, B.C.

3.2 Data

3.2.1 Lidar data

Terrestrial lidar applications use a near infrared laser typically centered at 1064 nm (Jensen, 2000). The sensor emits hundreds of thousands of laser pulses per second that diverge as they travel towards the ground forming a circular footprint once reaching the ground (Wehr & Lohr, 1999). The pulses reflected from the surface return to the sensor, where the position and elevation of each point can be calculated using data from the emission angle, pulse travel time, differential global positioning system (GPS), and onboard inertial measurement unit (IMU). Each pulse can yield multiple returns as the footprint reflects off multiple levels of the target object, with the first return generally representing the top of the canopy and last return representing the ground surface (Jensen, 2000). Unlike passive remote sensing technologies, lidar systems are non-weather dependent. The resultant data product is a three-dimensional georeferenced point cloud with a typical horizontal and vertical positional accuracy of ~ 0.15 m and 0.20 m respectively (Liu, 2008). Output point densities are sensor dependent and vary dependent on a number of factors, including laser pulse frequency, aircraft speed and height, field of view, and flight line overlap. Depending on these factors, point densities from aerial acquisitions typically range from 1 – 2 pts/m^2 (low density) to 10 – 12 pts/m^2 (high density) (Leberl et al., 2010).

High-density discrete airborne lidar data were acquired from Western Forest Products Inc. Data were collected between August and October 2012 using an OPTECH 3100EA sensor (1064 nm wavelength) mounted on a Piper PA31 Navajo. Data were collected

from 700 m AG with 75% overlap, using a pulse repetition rate of 100 KHz and up to 4 returns per pulse. The data had a vertical accuracy of +/- 0.16 m, an average point density of 17 pts/m^2, and an average point spacing of 0.24 m when considering all returns (Table 3.1). While the point cloud had been previously classified, the original classification was performed primarily for the production of terrain-based descriptors, not vegetation-based descriptors. As a result, there were issues regarding an over-aggressive ground classification that had misclassified vegetation features as ground. Because of this, the data were re-classified using the TerraSoild processing package in MicroStation (Version 8.5.1.25). This ensured the data were more reliable for the future extraction of individual tree objects and area-based canopy descriptors.

To do so the lidar data were gridded into 1000 m square blocks on even easting and northing coordinates to ensure processing remained manageable. An automated classification was executed using a macro algorithm in TerraScan, utilizing a sequential three-step process. First, the algorithm ran a ground classification to identify all returns representing ground features. Next, noise was removed from the point cloud by using an algorithm that searched for isolated points that represented pits and air hits; returns that had penetrated the ground surface or contacted birds, dense atmospheric constituents, or were a result of sensor error. In the final step, the algorithm classified all remaining points as above ground vegetation. The parameter settings for the automated macro algorithm were determined using recommendations from the TerraScan users guide and analyst experience taking into consideration the structure of the terrain and vegetation present at the study sites (Table 3.2) (TerraSolid, 2013). Because the accuracy of the

point cloud classification impacts the accuracy of all data products derived from it, the point cloud was then manually edited to ensure the most accurate classification was produced. Through manual classification any remaining noise points were removed and any misclassified points were reassigned to their correct classes to the best of the interpreters' abilities. It should be noted that remnant snow pack features were miss-identified as ground by the automated classification algorithm in some of the valley bottoms in the southeast corner of the Jeune Landing study site. Attempts were made through manual classification to remove these features from the ground class, however some terrain data from these areas may be unreliable and should be interpreted with caution.

Table 3.1. Average point density and spacing of lidar data by study site.

	Average point density (pts/m^2)	Average point spacing (m)	Study site area (km^2)
Holberg	14.77	0.26	155.12
Koprino	16.24	0.25	87.53
Jeune Landing	19.87	0.22	405.61
Total	16.96	0.24	648.27

Table 3.2. Parameter settings of classification algorithm used to classify lidar point cloud in TerraScan.

Parameter	Setting
Ground classification	
Maximum building size	20.00 m
Terrain angle	89.00 °
Iteration terrain angle	10.00 °
Iteration distance	1.4 m
Reduce triangulation	NO
Stop triangulation	YES, when triangles < 0.1 m
Isolated points classification	
From class	1 or 2
To class	7
If fewer than	2 Points
Are within	7.00 m

3.2.2 LLAS waypoint data

The habitat maps that this research aimed to improve upon were generated using a three-step approach. First, habitat polygons were delineated using forest cover variables representing certain key marbled murrelet habitat features (e.g. stand age, tree height). Second, medium-intensity LLAS were then flown to qualitatively assess the suitability of the habitat within the polygons. During the LLAS, waypoint data were collected and ranked to indicate the particular suitability of the habitat at the given waypoint locations. Finally, these LLAS waypoints and their associated habitat rankings were then used to confirm or re-adjust the initial polygon boundaries where necessary, and assign an overall habitat suitability ranking to each polygon based on the rankings of all waypoints falling within a given polygon (McDonald & Leigh-Spencer, 2014). These LLAS waypoint data were acquired from Western Forest Products Inc. and treated as ground truth data of known habitat suitability used to inform the selection of model training data.

The helicopter surveys that collected the LLAS waypoint data were designed using guidelines from the provincial LLAS standard methods (Burger, 2004), whereby each waypoint was assigned a habitat ranking from the standard provincial six-class habitat suitability ranking scheme (Table 3.3). From an operational species management perspective, Rank 1, Rank 2 and Rank 3 are considered to indicate suitable nesting habitat, while Rank 4, Rank 5 and Rank 6 are considered to indicate unsuitable habitat. The LLAS began by evaluating several calibration sites before assessing the habitat, allowing observers to re-familiarize themselves with the habitat classification process. At each calibration site, the standard datasheet for aerial assessment of marbled murrelet nesting habitat (Appendix A) was filled out assessing each of the standard habitat attributes following the standard definitions and criteria for habitat assessment (Appendix B). Each of the habitat attributes were assessed independently, then based on their suitability, an overall habitat suitability ranking was assigned to the waypoint location. While canopy closure, canopy complexity, topographic complexity, age class, tree species, and slope position and grade are all ranked based on distinct threshold values determined by the overall characteristics of the habitat unit, the first three attributes, % large trees, % platforms and moss development are all assessed using a proportional method. For example, if >= 50% of the trees visible within the habitat unit are large (> 25.4 m), Rank 1 is assigned to the % large trees attribute, if >= 25% of trees visible within the habitat unit are large, Rank 2 would be assigned, and so on and so forth, until <= 1% of visible trees were large or none of the trees visible were large then Rank 5 or Rank 6 would be assigned to attribute, respectively. Once observers felt confident with their calibration assessments, the intended surveys began.

Fight transects were flown over each of the habitat polygons that were originally delineated from forest cover data in a pattern that optimized viewing of the habitat, i.e. trying to maximize visibility into the canopy to assess platform and moss presence. However, the helicopter did not stop to evaluate habitat at a more in-depth scale at any given point. Instead, it moved on a slow but continuous path. Following standard practice, at each LLAS waypoint location, all of the habitat attributes on the standard datasheet were considered, but the datasheet was not filled out. Instead at each location, only the overall habitat suitability ranking of the waypoint was recorded (McDonald & Leigh-Spencer, 2014). The LLAS waypoints were collected using OziExplorer GPS Mapping software, with a positional accuracy of approximately +/- 15 m. The LLAS waypoints were taken at fairly regular intervals, as well as boundaries where habitat transitioned from one suitability ranking to another, and any other noteworthy locations.

Table 3.3. Standard six-class habitat suitability ranking scheme used for LLAS habitat assessments for marbled murrelet habitat in B.C. (Burger, 2004).

Rank	Habitat suitability	Operational ranking	General description	% polygon with suitable features
1	Very High	Suitable	Key habitat features present in abundance; nesting highly likely	50 – 100%
2	High	Suitable	Key habitat features common and widespread; nesting likely	25 – 50%
3	Moderate	Suitable	Key habitat features present but uncommon and patchy; nesting likely but at moderate to low densities	6 – 25%
4	Low	Unsuitable	Key habitat features evident but patchy and sparse; nesting possible but unlikely or at low densities	2 – 5%
5	Very Low	Unsuitable	Key habitat features sparse and might not all be present; nesting highly unlikely	~ 1%
6	Nil	Unsuitable	All key habitat features absent (i.e. bogs, bare rock, not forested); nesting impossible	0%

Several LLAS waypoints were collected within each of the habitat polygons, with the largest polygons containing several flight lines and many LLAS waypoints. The final dataset contained ~ 800 LLAS waypoints distributed across all three study sites. The LLAS waypoints were then clipped to the study area boundaries. All Rank 6 waypoints were removed from the dataset as the identification of Rank 6 habitat is straightforward and does not require the use of a predictive habitat model (exposed rock outcrops, un-forested areas etc.). The waypoints were quality checked by expert biologists, removing any waypoints denoting transitional boundaries between habitat of differing suitability, and relocating any waypoints obviously meant to represent an adjacent area, i.e. if located within a riverbed with no trees the waypoint was moved to the adjacent forested area it was originally intended to represent. Only a total of eight waypoints were spatially relocated. Using harvest data current to 2012, the waypoints were then filtered to ensure any waypoints representing forest that had been harvested between the LLAS waypoint acquisition (2005/2006) and the lidar acquisition (2012) were removed. This quality checking process insured only waypoints with definitive habitat rankings were used to inform the selection of model training data. After post-processing, the final dataset contained 787 waypoint observations.

However, due to the medium-intensity (non-stopping flights) and point-based scale of these surveys, there was potential for two types of error in the data: *attribute error* (i.e. the accuracy of the habitat suitability ranking assigned, dependent on the attributes visible at the time the LLAS waypoint was recorded and the specific tendencies of the individual observer assessing the habitat) and *spatial error* (i.e. the spatial location of the

actual LLAS waypoint, depended on helicopter movement and the observers timing). As the predictive habitat model relied on the ability of the LLAS waypoint data to accurately represent habitat suitability, a sample of the LLAS waypoint data we re-assessed to determine the reliability of their assigned habitat suitability rankings. By evaluating the accuracy of the data, increased reliability could then be placed in the operational applicability of model results and recommendations could be made for future studies wishing to utilize the extensive network of LLAS waypoint data that already exists across B.C. for future habitat modelling purposes.

3.2.3 LLAS waypoint re-assessment

In order to include observations from all habitat suitability rankings a semi-random, stratified approach was used to select waypoints for re-assessment. The waypoint data were stratified by their associated habitat suitability rank and each study site was considered individually to ensure regional differences were accounted for in the re-assessment survey. Random observations were then drawn from each study site. However, the sample selection was considered to be semi-random because a preference was given to Rank 3 and Rank 4 waypoints. Differentiating between these two habitat rankings is critical for decision-making as their division represents the transition between operationally suitable (Rank 1, Rank 2, and Rank 3) and unsuitable (Rank 4, Rank 5, and Rank 6) habitat. Furthermore, it is often challenging to differentiate between these habitats during aerial surveys because their identifying characteristics can appear similar. These middle-ranked habitats were also the most common naturally occurring ranks across the study sites, and thus represented the largest percentage of the total LLAS

waypoint dataset. The resultant re-assessment sample included 68 LLAS waypoint observations (23 from the Holberg region, 21 from the Koprino region, and 24 from the Jeune Landing region) that were considered to be representative of the total population. The sample was made up of 46 primary waypoints and 22 contingency waypoints; only to be collected if a primary waypoint was inaccessible or had been disturbed since the original surveys. Ultimately, time and spatial proximity allowed for a total of 54 waypoints to be re-assessed, all 46 primary points and 8 contingencies (Figure 3.2).

The selected LLAS waypoints were re-assessed using a refined LLAS methodology capable of yielding more reliable habitat classifications by utilizing a high-intensity (stopped and circling slights), plot-based (refined spatial scale) approach (Burger, 2004). A 100-m radius circle (~3 ha area) centered on the location of the existing LLAS waypoints was used to define the discrete habitat plots, the characteristics of these habitat plots were used to determine the habitat suitability ranking assigned to the waypoint during the re-assessment surveys. This plot-based scale significantly improved upon the coarser scale used in the original surveys, which considered all habitat visible within the entire forest cover polygon when assigning a waypoint ranking (average forest cover polygon area ~ 26 ha). This 100-m radius plot size was selected to maintain consistency with existing verification survey methods (Donald et al., 2010).

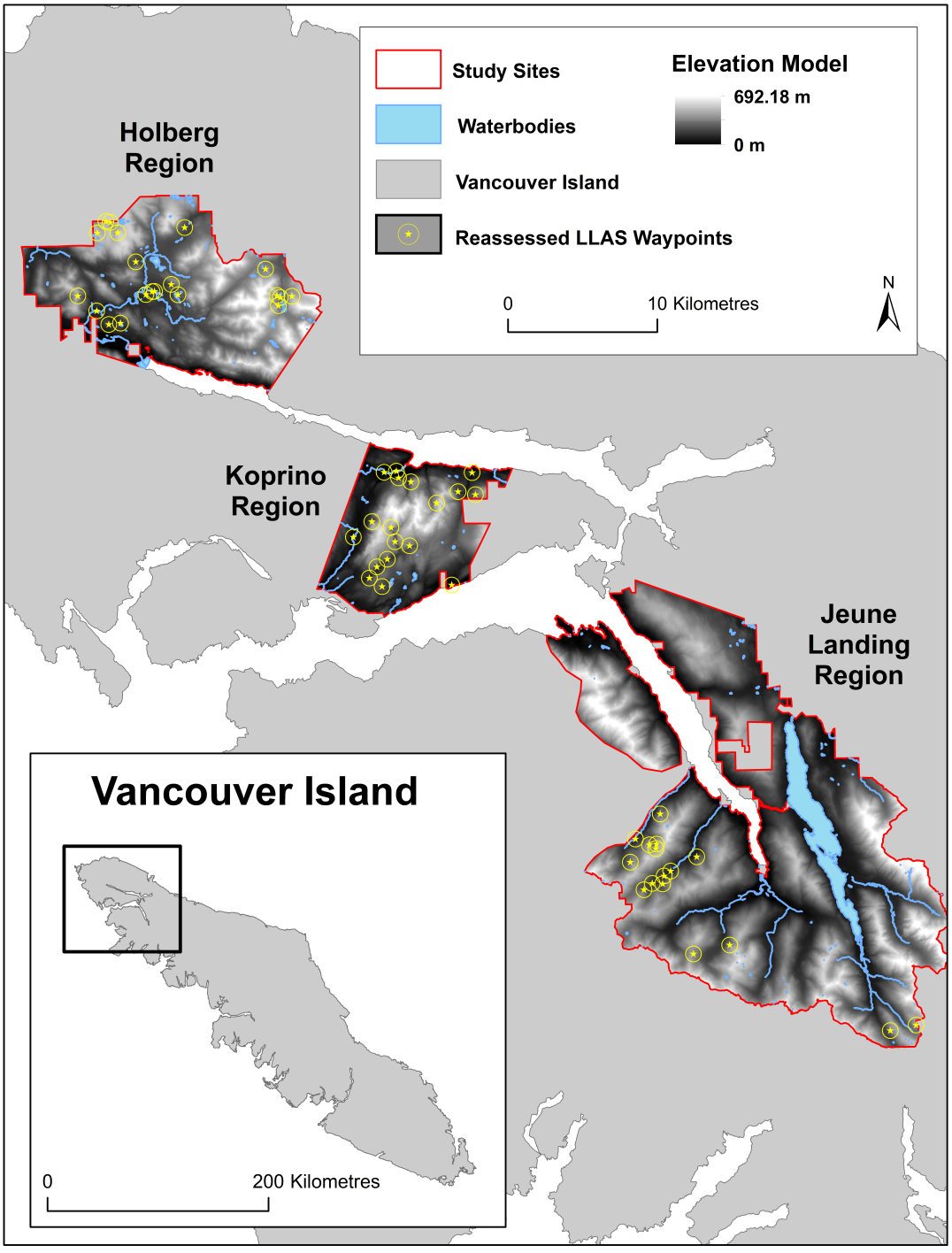

Figure 3.2. Locations of the 54 LLAS waypoints re-assessed with the high-intensity plot-based LLAS method.

In addition to the refined intensity and scale, the re-assessment surveys also introduced the novel assessment of two new attributes: (1) the *Best Tree* attribute and (2) the *Surrounding Area* attribute. Despite the finer plot-based scale of the refined surveys, habitat variation was still likely to exist within the plot area. Previous LLAS have not assessed the suitability of individual trees, as the standard classification system relies on the number of trees within a given area to assess several of its attributes, not possible when evaluating the suitability of an individual tree. The Best Tree attribute was assessed after the plot area had been considered and ranked. To do so, observers evaluated if there were any trees within the plot area that would constitute a higher habitat suitability ranking than was assigned to plot itself using an augmented classification scheme that considering only the attributes relevant to a single tree: the size of the tree, the presence of suitable nesting platforms within the tree, and the presence of moss on the platforms. By assessing the variation of habitat suitability within the plot area, data could be gathered on the appropriate scale for future LLAS and habitat mapping methods. Once the Best Tree assessment was complete, the helicopter exited the plot area to assess the suitability of the habitat in the surround area. A 250-m radius buffer centered on the waypoint location was used to restrict the assessment and define the surrounding area (~20 ha). The helicopter circled briefly around the surrounding area while observers evaluated if the habitat quality was the same as, or different, when compared to that of the plot area. If different, the habitat was assessed using the same habitat classification scheme used to assess the plot areas, and a habitat suitability ranking was assigned to the Surrounding Area attribute. When the surrounding area was determined to be less suitable than the plot area, it indicated that the plot area was a small patch of suitable

habitat situated within a larger, less suitable habitat area. Again, providing important information about habitat variability and the appropriate scale for future habitat mapping studies.

As suggested by Burger (2004) the optimal crew size of three members, exclusive of the pilot, was used. There were two observers, both with considerable experience conducting LLAS for marbled murrelet habitat assessment, and one field assistant. To control for observer bias and maintain consistency, one of the observers had participated in the original LLAS used to the waypoint data. As an added benefit, the helicopter pilot was highly experienced with LLAS for marbled murrelet habitat assessment. Prior to leaving, several maps and data tables were prepared. A digital map displaying the locations and IDs of all 68 LLAS waypoints selected for re-assessment was created. Each waypoint was displayed as single point surrounded by its 100 m (plot) and 250 m (surrounding area) - radius buffers. The map did not contain any information regarding the existing habitat suitability rankings of the waypoints. The map was loaded into the GPS moving map program OziExplorer on a laptop and used for navigation by the observer navigator seated in the front left of the helicopter. The map was also loaded on to a tablet used for visual reference by the observer biologist and field assistant in the back left and right of the helicopter, respectively. Paper copies were printed and brought for backup. The pilot loaded all data into an independent GPS system that was used to navigate efficiently to each waypoint location and circle around the plot and surround area buffers. A digital map displaying the existing LLAS polygon-based habitat maps and all 787 LLAS waypoints displayed by their existing habitat suitability ranking was also created. This

map was not viewed by either of the observers or the pilot and was only to be used by the field assistant if all contingency points were inaccessible and completely new waypoints were needed; the map was not used. In order to select appropriate contingency waypoints when necessary, a master reference table was created listing all of the re-assessment waypoints by their associated habitat suitability rank and ID. It was used by the field assistant to determine a like-ranked contingency waypoint when a when a primary waypoint was either disturbed or inaccessible.

The re-assessment surveys were conducted over October 25th and 26th, 2015. Both days fell outside the breeding season for marbled murrelets in accordance with suggestions made by Burger (2004) to avoid any impacts surveys may have on their breeding success, but inside a suitable weather window. Surveys were conducted using a Bell 206 Jet Ranger Helicopter. Data were not collected in any precise order; instead order was determined by accessibility. The flight path was continuously tracked using OziExplorer. While the pilot navigated to the plot center (LLAS waypoint coordinate), the observer navigator collected a new reference point (high-intensity LLAS waypoint) in OziExplorer, and the observer biologist took still photos for future reference. The pilot circled the helicopter around the plot area counter clockwise to ensure both observers had optimal and comparable views into the canopy. Evaluation of the plot then began using an updated version of the datasheet for aerial assessment of marbled murrelet nesting habitats (Appendix C).

At each location, all attributes on the updated datasheet were assessed and ranked based on the characteristics of the habitat within the plot area. Based on their suitability the observers then assigned an overall habitat suitability ranking the waypoint location. The observers verbally conferred their assessments, while the observer biologist noted them on a paper copy of the updated standard datasheet. If their rankings of any of the attributes or the plot area overall differed, they discussed why and came to an agreement. The Best Tree attribute was then assessed, if there were any trees within the plot constituting a higher habitat suitability ranking based on the classification scheme reviewed above, the tree(s) were assigned a Best Tree ranking, which was verbally conferred and recorded. The helicopter then exited the plot area and circled briefly around the surrounding area. If different, the observers assigned a habitat suitability ranking to the Surrounding Area attribute, which was again verbally conferred and recorded. Once the surrounding area had been assessed the total assessment was complete and the crew moved to the next LLAS waypoint location.

During each assessment, the field assistant concurrently recorded all rankings, discussions, and other noteworthy comments. Each total assessment took approximately 5 minutes. Yet, it should be noted that the first few plots took moderately longer, approximately 10 minutes, as the observers were re-familiarizing themselves with the habitat and ranking criteria. When a plot could not be reached due to weather restrictions or site disturbance the field assistant consulted the master reference table, determined the habitat rank of the intended location, and selected a contingent waypoint of the same

rank. Once all intended and additional waypoints had been reassessed the crew returned to base. All records were then cross-referenced to ensure no errors were made.

Post-survey analysis was conducted to evaluate how the new high-intensity LLAS waypoint rankings compared to those of the original LLAS waypoints. Overall consistency was evaluated, as was the consistency of each habitat suitability ranking individually, indicating if some rankings were more or less consistent than others. The directionality of change was also evaluated to determine if the original LLAS waypoint data were over or underestimating habitat suitability. Lastly, the operational implications of any ranking inconsistencies were assessed by evaluating if any of the LLAS waypoints reported a re-assessed ranking that was from a different operational ranking category (i.e. did any waypoints shift from a Suitable Rank (1 – 3) to an unsuitable rank (4 – 5) or vice versa.

3.2.4 LLAS polygon data

As discussed, the LLAS waypoint data were used to adjust or confirm the boundaries of forest cover polygons and assign an overall habitat suitability ranking the polygons. These habitat polygons, hereon referred to as LLAS polygons, constitute the existing habitat suitability maps this research aimed to improve upon. These LLAS polygon data were also acquired from Western Forest Products Inc. The LLAS polygons were adjusted using harvest data current to 2012, removing any polygons that had been harvested between polygon delineation (2005/2006) and lidar acquisition (2012). However, natural disturbance events such as wind throw and landslides could not be accounted for.

Therefore, predictions may include some habitat that has since been altered or disturbed. All Rank 6 polygons were also removed from the dataset for the same reason as previously mentioned. A sample of both the LLAS waypoints and the LLAS polygons is presented in Figure 3.3.

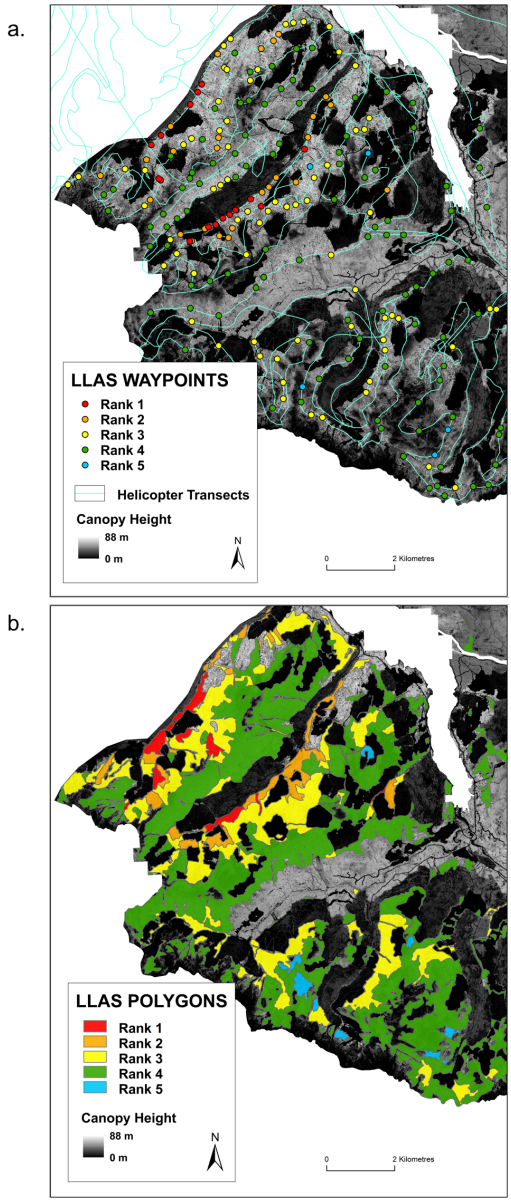

Figure 3.3. Examples of the LLAS polygon data (a) and LLAS waypoint data (b) data from the Jeune Landing study site.

3.3 Data Processing

3.3.1 Canopy height models (CHMs)

In order to achieve representative height measurements of surface objects, i.e. vegetation, the lidar ground returns were normalized using the height from ground classification function in TerraScan (Niemann, 2009). The Multiscale Curvature Classification (MCC) algorithm (Evans & Hudak, 2007) and the LAStools lidar processing package (Isenburg, 2014) were both evaluated for the normalization process, however both methods proved to be too computationally intensive and slow for the large volume of data to be processed. The normalization process works by iteratively subtracting the height of the nearest ground point from every vegetation point above. This accounts for the influence of elevation, resulting in representative heights for all vegetation points. However, there are some limitations that can be associated with this terrain normalization process when there is poor ground return coverage, typically occurring on steep slopes or occluded areas (overhangs) (Breidenbach et al., 2008). In this scenario, the nearest ground point can be too far away from the vegetation point above, and thus not representative of the true ground surface below the given vegetation point. In this case, the process can fail and produce negative or unrealistically high height values for the vegetation features or alter the physical shape of the vegetation (tilted trees) (Figure 3.4).

To identify and remove any of these normalization artifacts, a biological rational of realistic tree heights known for the area was used. All vegetation points exceeding 95 m in height and that reported negative height values were removed from the normalized point cloud. The normalized point cloud was then gridded at a 1 m spatial resolution, and

populated with the height value from the highest vegetation point within each pixel, producing the final canopy height models (CHMs) (Niemann, 2009). The 1 m spatial resolution was selected to optimize the high point density of the dataset and allow for improved representation of the crowns of mature and old-growth trees, ensuring multiple pixels would fall within a given tree crown. The CHM surfaces were then visually assessed to ensure that any remnant normalization artifacts were removed.

3.3.2 Digital elevation models (DEMs)

In order to calculate terrain descriptors, digital elevation models (DEMs) were generated from the non-normalized ground points. The non-normalized ground points were gridded at a 2 m spatial resolution, and each pixel was populated with the average height value from all ground points within the given pixel (Niemann, 2009). The DEMs were smoothed, filling up to three pixels using nearest neighbor bilinear interpolation (Guo et al., 2010; Smith, 2004). Negative elevation values surrounding coastlines, most likely due to tidal movements between acquisition days or slight penetration of the water column, were removed from the data. While several methods have been developed to quantifiably select an appropriate spatial resolution for DEMs generated from lidar data (Agarwal et al., 2006; Behan, 2000; Hengl, 2006; Hu, 2003; Holland & Longley, 2005; Liu, 2008), the appropriate resolution is highly data and objective dependent. As such, there is no standard approach. The 2 m spatial resolution used for this research was selected to optimize the high ground point density. Examples of both the CHM and DEM surfaces are presented in Figure 3.5.

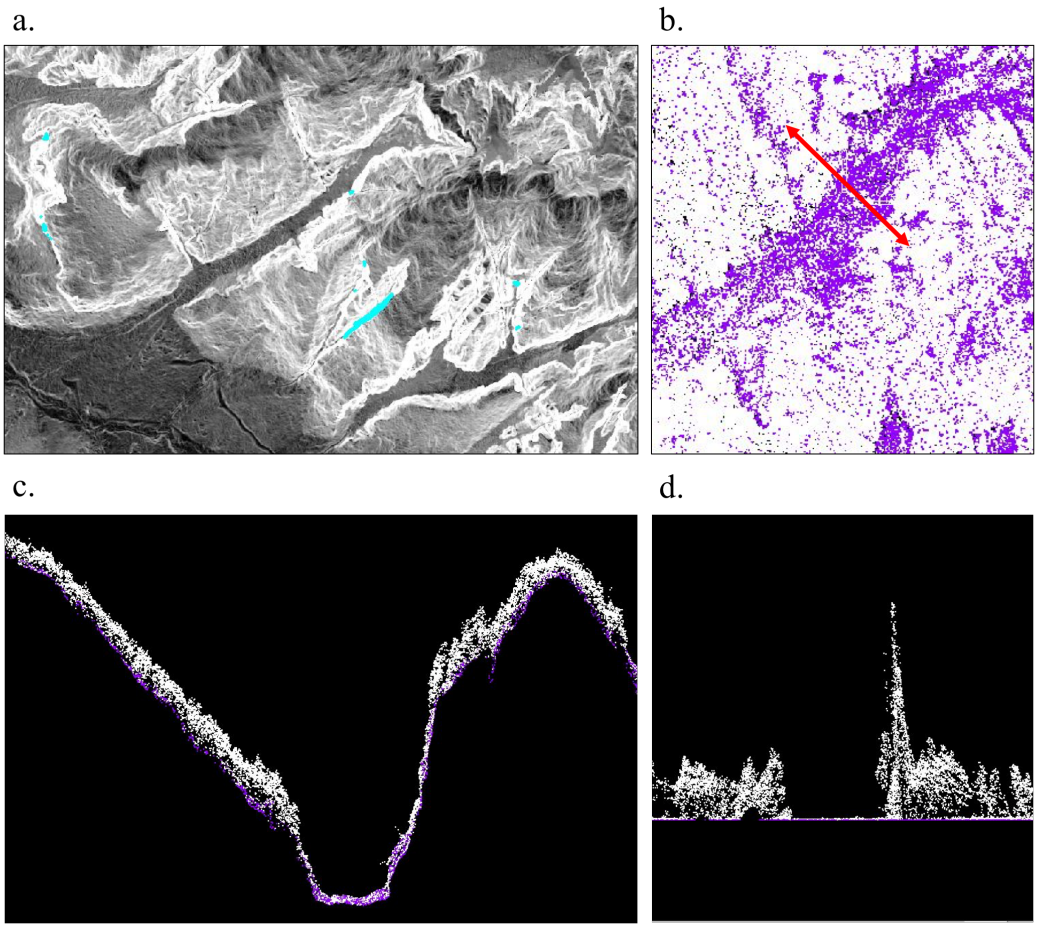

Figure 3.4. Example of the normalization issues associated with poor ground coverage and steep slopes: plot (a) represents a slope raster with problem areas highlighted in light blue, steeper slopes are indicated by brighter pixel values; plot (b) presents a top down view of the point cloud in one of these regions, and shows the location of a cross section taken, vegetation returns are in white and ground returns in purple; plot (c) presents the cross-sectional view of the point cloud taken in plot (b) before the normalization process was applied; and plot (d) gives an example of a normalization artifact from this area after the normalization process, indicated by the exaggerated height and altered shape of the vegetation.

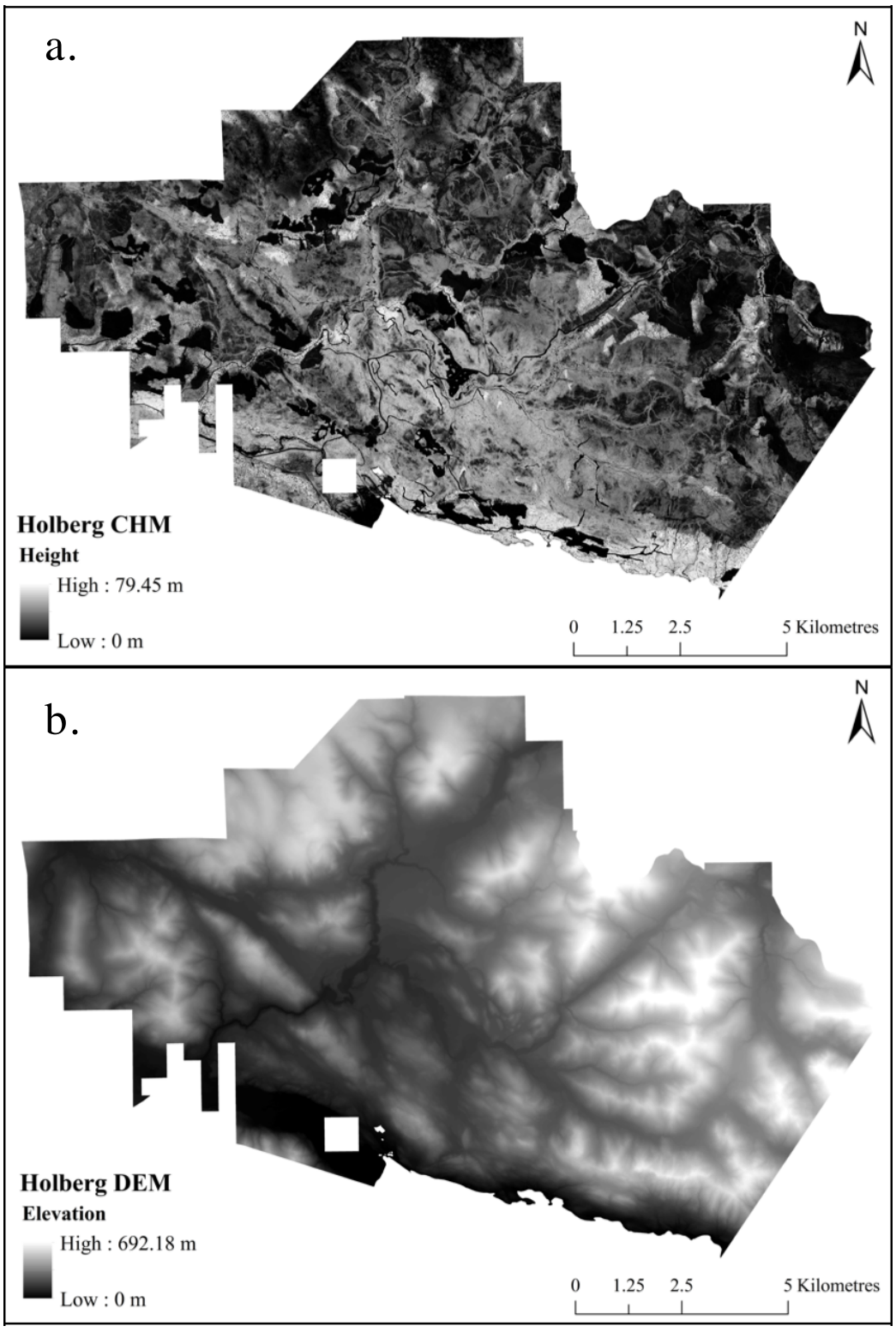

Figure 3.5. Example of the CHM surfaces (a) and DEM surfaces (b) generated from the lidar data for the Holberg study site.

3.3.3 Individual tree object extraction

In order to move from the raster-based CHM surfaces, representing top of canopy height, to a vector-based dataset representing individual trees and their associated heights, a treetop detection algorithm was used. The detection method employed here was initially developed by Niemann (2009), however there are a variety of techniques that have been developed for the detection of individual tree objects from lidar data (Eysn et al., 2015). There is currently no best-practice approach, as the detection method is highly data and parameter dependent. Before the detection algorithm was applied, the CHM surfaces were smoothed to reduce within crown variation, present due to the high spatial resolution of the CHMs and high point density of the original point cloud. Ideally, the detection algorithm would identify only a single local maxima (treetop) per logical tree crown, yet candelabra branches and other deformities can present what appear to be additional local maxima within a single logical tree crown. By smoothing the CHMs first, this multi-maximum variation is reduced, while maintaining the true maxima. Several different smoothing strategies were evaluated, including a mean, median and low-pass Gaussian filter, using a variety of filter kernel sizes. Based on visually assessed omission and commission errors, a low-pass Gaussian filter using a 5x5 pixel kernel window was determined to be the optimal smoothing strategy. The kernel used a weights matrix with a variance of 0.5. Variances of 1.0 and 2.0 were evaluated, but found to result in over smoothing and high omission errors, with a 20 – 25% reduction in the total number of treetops objects detected. Regardless of the smoothing strategy, a small number of omission errors persisted. However, the majority of these errors were comprised of smaller understory trees or by trees in wells between two larger trees. As the focus of this

research was to detect large mature and old-growth trees, these errors were considered to be acceptable. Additionally, while the smoothing filter reduced the within crown variation, some instances of multiple treetop detection within a single logical crown (commission errors) also remained, due to the high-density nature of the point cloud and the geometrical and physical structure of large flat top or broken trees.

Once the CHMs had been smoothed they were passed through the treetop detection algorithm executed in a proprietary software package. The algorithm used a local maxima filter to identify the pixel with the highest height value (local maxima) within a 3x3 pixel kernel window. Selecting the appropriate kernel size for the filter was an important consideration. If the kernel used is too large, logical treetops will be skipped over and omitted, but if the kernel used it too small, multiple treetops will be detected within a single logical crown. Through visual inspection of the identified treetops it was determined that a fixed 3x3 pixel kernel window was the most appropriate for the data. A minimum height threshold was applied during algorithm execution to exclude the detection of any treetops below 5 m, ensuring that small shrubs and woody debris were not detected as treetops. The algorithm worked by passing the 3x3 pixel kernel window across the CHMs from left to right, identifying the pixel within the 3x3 kernel window with the highest height value (the local maxima). It then generated a spatial point centered on the pixel identified as the local maxima, and attributed the point with height value from the associated local maxima pixel. The resulting spatial points were then written out to a shape file that could be manipulated in a geospatial environment.

Quinn et al. (2016), evaluated this method for an installation of low productivity, relatively high density (500 – 2500 stems/ha.), and even aged, 65-year-old Douglas fir trees in the CWH BEC zone, with all trees ranging from 20 – 40 m in height. A 0.5 m resolution CHM was used and smoothed with three different filtering strategies (mean, median, and Gaussian) and varying kernel window sizes ranging from 3 – 7 pixels wide. Detection accuracy was assessed against an infield stem survey. Results indicated that the algorithm had a 75 – 85% user's accuracy (i.e. of all treetops detected, how many detections were correct). Detection accuracy was highly variable and dependent on algorithm parameters (smoothing filter and kernel size). Omission errors were determined to be a function of stem density and the height differential for the given tree and its six nearest neighbors, with high stem densities and low height differentials resulting in the highest omission errors. Based on these findings, this treetop detection method likely produced highly accurate detections due to the low stem densities and high height differentials present in the forests evaluated by this research.

Each spatial point generated by the detection algorithm is assumed to represent the location and the height of an individual treetop, and thus the height and location of an individual tree. These individual tree point-based data were used as the spatial modelling and mapping unit for this research. The final dataset was clipped to the spatial extent of the LLAS polygon coverage and quality checked by manually comparing the identified treetops to the point cloud. Where multiple treetops were detected within a single logical crown, the lower of the two treetops was removed from the dataset, under the assumption that the highest point represented the true treetop. Trees detected on the steep slopes in

the Jeune Landing region that were affected by the normalization process (3.3.1) were also removed, as their heights may have been unreliable. Overall, the number of treetops removed represented a proportionally small number of the total dataset (< 1%), which was made up of approximately 2.5 million individual tree objects.

3.4 Training Data Selection

The rankings of the LLAS waypoint data were pseudo-replicated to individual trees that were spatially adjacent the waypoints and representative of the ranking assigned to each waypoint. To compensate for the spatial variability intrinsic to the waypoint data (+/- 15 m), each waypoint was buffered using a 20 m radius buffer. Several different buffer distances were evaluated by plotting the heights of all trees identified within the given buffer distance versus the associated waypoint rankings. A buffer distance of 20 m was selected as is optimized separability between rankings, accounted for the maximum spatial variability of the GPS points, and approximated the spatial resolution of gridded habitat descriptors (3.5). All tree objects falling within the buffered area were selected and sorted by height. For each buffer, the median tree height was calculated, and only trees above the median height were retained. Each tree was then attributed with the habitat suitability ranking of its associated waypoint. The buffering process ensured that more than one tree was associated with each LLAS waypoint and the median height filtering process removed any misrepresentative trees from the sample (Figure 3.6). For example, an understory tree (< 15 m) could have been located within the buffer area of Rank 1 waypoint, and would therefore have been selected and identified as Rank 1 habitat. This tree would then strongly misrepresent the biophysical characteristics

typically associated with Rank 1 habitat (trees > 28.5 m tall) (Burger, 2004). By removing all trees below the median height, the retained trees were more likely to be the trees that the habitat suitability rankings were originally meant to represent. The final training dataset contained 6197 individual trees each with a height value and a pseudo-replicated habitat suitability ranking derived from their associated LLAS waypoint. These data were used to train the predictive classification model.

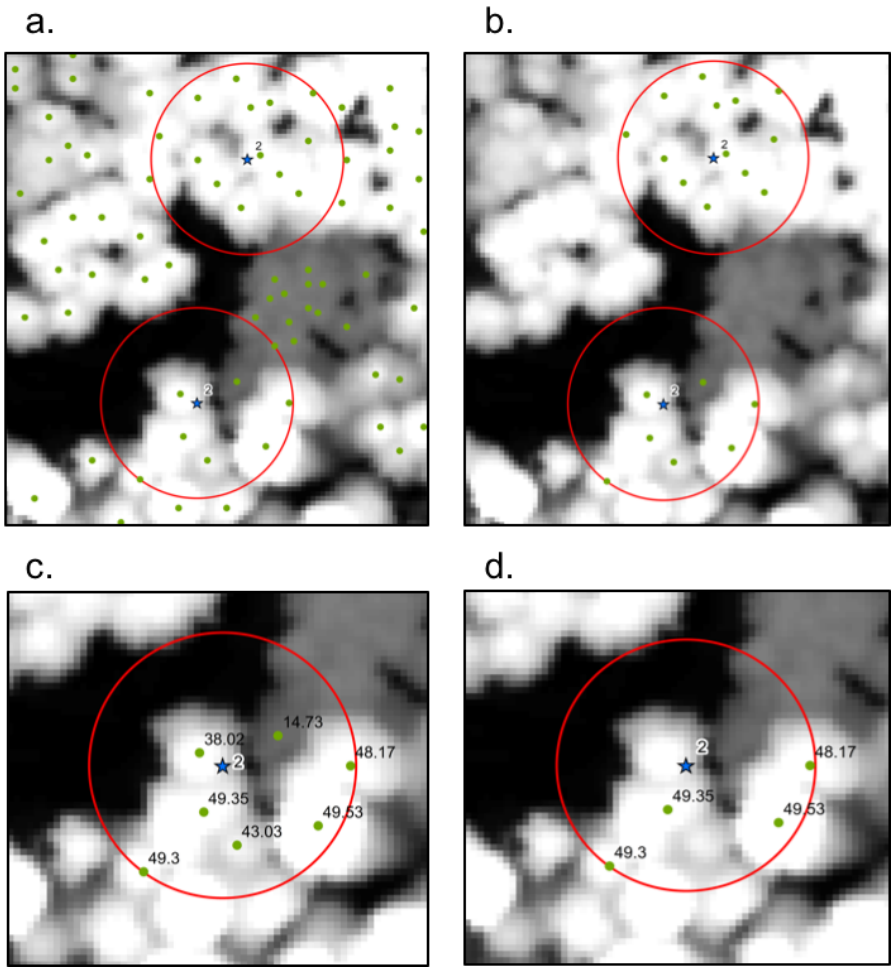

Figure 3.6. An example of the buffering and median height filtering process used for the selection of individual trees for the training dataset assigned a pseudo-replicated habitat suitability ranking from their associated LLAS waypoint: (a) Rank 3 waypoint buffered at 20-m radius (c and d) sorting of selected tree by height and removal of all trees below the median height. Remaining trees in (d) assigned a pseudo-replicated ranking for their associated waypoint.

3.5 Habitat Descriptors

A series of raster-based structural habitat descriptors were generated from the normalized lidar point cloud and the DEMs. All descriptors were calculated using an area-based approach at a spatial resolution of 20 m. The canopy descriptors were calculated using a proprietary software package following methods outlined in Niemann (2009). They included: mean canopy height, coefficient of variation, skewness, kurtosis, canopy closure, the height of 21 lidar height quantiles (from 0 to the 100th percentile at 5% increments), the height of the 85th lidar percentile, the average height above the 85th lidar percentile, and canopy rugosity. Terrain-based descriptors were calculated using QGIS (Version 2.14.3) and included: elevation, slope gradient, terrain aspect, topographic wetness index (TWI), topographic ruggedness index (TRI), topographic relief and distance to saltwater. A polygon-based dataset representing BEC zones was acquired from the provincial database (DataBC, 2016), and a point-based dataset representing spatial autocorrelation was derived using the individual tree dataset and the local Moran's I (LMI) spatial statistic (Moran, 1948).

Four criteria were used to determine which descriptors were retained as model predictors: (1) their ability to separate the training data by their assigned habitat suitability rank, (2) their comparability to the attributes used to assessed the LLAS waypoints, creating continuity with existing habitat mapping methods, (3) expert knowledge regarding characteristics known to influence marbled murrelet nesting habitat, and (4) recent literature utilizing lidar-based predictors for bird-habitat modelling (Ackers et al., 2015; Bae et al., 2014; Farrell et al., 2013; Hagar et al., 2014; Zellweger et al., 2013). Based on

these criteria, 12 descriptors were selected as model predictors: individual tree height, canopy rugosity, canopy closure, the height of the 85th lidar percentile, the average height above the 85th lidar percentile, elevation, slope gradient, terrain aspect, TRI, distance to saltwater, BEC zone and the LMI spatial statistic (Table 3.4).

3.5.1 Individual tree height

Individual tree heights (*Height*) were derived from the individual tree dataset extracted from the CHMs (4.4). Height was measured in metres and was accurate to the nearest centimeter. Generally, Suitable habitat is defined by trees that are > 28.5 m tall (Burger, 2002), and while not all tall trees will provide suitable nesting habitat, taller trees are more likely to contain the large branches and deformities that provide suitable nesting platforms (Burger et al., 2010). Furthermore, this predictor was determined to be directly comparable to the gridded *EL_p99_max* attribute evaluated in the lidar-based murrelet occupancy model developed by Hagar et al. (2014), used to represent the height of the tallest trees within the gridded canopy area.

3.5.2 Canopy rugosity

Canopy rugosity *(Rugosity)* is a measure of the height variations in the upper surface of the canopy, i.e. surface roughness. It was defined for this research as the standard deviation (σ) of all vegetation return heights from the mean vegetation height within a given pixel. Lower values of canopy rugosity indicate smoother more uniform canopies, while higher values indicate rougher more vertically complex canopies. Higher vertical canopy complexities may potentially improve access to nesting platforms for the birds

(Burger, 2004). More vertically complex canopies may also indicate the presence of trees extending up and above the surrounding canopy, a possible indicator of a suitable nest trees (Silvgergieter & Lank, 2011a). Additionally, canopy rugosity is directly comparable to the *Vertical Canopy Complexity* attribute that was assessed during LLAS (Burger, 2004), and the *FRSTCVABVMD_std* attribute evaluated by Hagar et al. (2014), used to represent vertical canopy complexity.

3.5.3 Canopy closure

Canopy closure (*Canopy Closure*) was calculated as the ratio of the total number of returns within a given pixel compared to the total number of returns at the user defined ground threshold (5 m). The resulting metric ranges from 0 to 1.0, where 0 indicates no closure, all gap, and 1.0 indicates full closure, no gap. As discussed, canopy closure is known to relate to habitat suitability, with the most suitable habitat having a canopy closure of 40 – 60% (Burger, 2004). Furthermore, this predictor was directly comparable to the *Canopy Cover* attribute assessed during LLAS (Burger, 2004), and the *ALLCVABVMN_max* attribute evaluated by Hagar et al., (2014), used to represent canopy cover in the upper portion of the canopy.

3.5.4 Height of the 85th lidar percentile

As mentioned, twenty-one lidar height quantiles were calculated for each pixel, one at every 5th height percentile. Each lidar height quantile reports the height at which the corresponding percent of all returns fall below. For example, at the 10th quantile (the 50th percentile) the output value represents the height at which 50% of all the returns in a

given pixel fall below. Quantiles are not set height increments, but are dependent on the distribution of returns within each pixel. Height of the 85th lidar percentile (*Height_85P*) is therefore the height at which 85% of all returns fall below for a given pixel. This metric represents the height of the co-dominant canopy and is measured in metres (Niemann, 2009).

3.5.5 Average height above the 85th lidar percentile

Following the same percentile stratification as noted above, the average height above the 85th percentile (*AHA_85P*) was calculated by averaging the heights of all lidar returns falling above the height defined by the 85th percentile for each pixel. This metric represents the height of the dominant canopy and is measured in metres (Niemann, 2009). Both the Height_85P and AHA_85P metric can be related the *% of Large Trees* attribute assessed during the original LLAS (Burger, 2004), and also to the *EL_99p_max* attribute evaluated by Hagar et al. (2014). Higher values of Height_85P and AHA_85P are indicative of canopies with a high percentage of large trees, which would thus be more likely to provide suitable nesting habitat.

3.5.6 Elevation

An elevation predictor (*Elevation*) was generated by resampling the DEMs from a 2 m resolution to a 20 m resolution using nearest neighbor interpolation (Grohmann, 2015). The metric is a representation of surface terrain heights in m AMSL and was included as a predictor due to its known relationship with the distribution of suitable nesting habitat on Vancouver Island (Burger et al., 2010).

3.5.7 Slope gradient

The DEMs also were used to generate a slope surface at a 2 m spatial resolution, which was then resampled to a 20 m resolution (*Slope*) (Grohmann, 2016). Slope was calculated in degrees, and represents the maximum rate of change between a given pixel and its adjacent pixels defined by a 3x3 pixel kernel. Slope was included as a predictor based on its comparability to the *Slope Grade* attribute assessed during the original LLAS (Burger, 204), its ability to separate the training data by habitat suitability rank, and its known relationships with habitat suitability (Burger & Bahn, 2004; Burger et al., 2010; Wilk et al., 2014).

3.5.8 Terrain aspect

Like slope, the DEMs were used to generate an aspect surface at a 2 m spatial resolution, which was then resampled to a 20 m spatial resolution (*Aspect*) (Grohmann, 2016). Aspect in this instance was determined by the direction of the pixel with the steepest downslope gradient from the center pixel to its neighbors defined by a 3x3 pixel kernel window. Aspect was calculated in degrees and not categorized into cardinal directions in order to maintain data precision. Aspect is not an attribute evaluated during LLAS habitat assessments, and has not consistently been considering in predictive habitat models for the marbled murrelet. However, as discussed, aspect may influence suitable nesting habitat, with increased moss growth on wetter north facing slopes when compared to drier south facing slopes. It was therefore predominantly included in this analysis for exploratory purposes.

3.5.9 Topographic ruggedness

A habitat descriptor representing topographic ruggedness (*TRI*) was calculated from the DEMs at a 20 m spatial resolution using methods from Riley et al. (1999). The metric characterized terrain heterogeneity by evaluating the total change in elevation from a given center pixel to its eight neighboring pixels defined by a 3x3 pixel kernel window (Riley et al., 1999). This predictor was comparable to the *Topographic Complexity* attribute assessed during the original LLAS, and as mentioned, it is thought that topographic complexity may influence the vertical complexity of the canopy above, ultimately influencing the suitability of the habitat.

3.5.10 Distance to saltwater

Distance to saltwater (*DIST_SW*) was calculated using the PostGIS spatial extension for a PostgreSQL database. Frist, a spatial point was generated on the center of every pixel in an empty 20 m spatial resolution raster. Using the "ST_Distance" function in the geodatabase, the shortest distance from each point to the Pacific Ocean coastline, defined by a provincial land boundary, was calculated. The points and their associated distances were then rasterized at a 20 m resolution and distance values were converted to kilometres and rounded to the nearest tenth of a metre. Distance inland was included as predictor as it is an attribute known to influence habitat suitability (CMMRT, 2003; Hagar et al., 2014).

3.5.11 BEC zone

Polygon data representing the dominant BEC zone, subzone and variant (*BEC*) for the study sites were acquired from the provincial database. All habitat in the study sites fell within the CWH zone or the WH zone, which were further separated in to a four subzones and variants: (1) CWH submontane very wet maritime subzone (vm 1); CWH montane very wet maritime subzone (vm 2); CWH southern very wet hypermaritime subzone (vh 1); and the MH windward moist maritime subzone (mm 1). As mentioned, BEC zone has been generally related to suitable nesting habitat, with some zones such as the Coastal Douglas fir (CDF), CWH and MH zones being more likely to contain forests with variable canopy structures and therefore more likely to provide suitable nesting habitat (Burger et al., 2010). However, this relationship occurs at a fairly broad scale and may not be a contributing factor at the scale of an individual tree. The use of BEC zone as a model predictor was therefore predominantly for exploratory purposes.

3.5.12 LMI spatial statistic

LMI is a statistical measure of spatial autocorrelation, the simple phenomena that data from locations nearer one another in space are more likely to be similar than data from locations further away from each other (O'Sullivan & Unwin, 2010). The LMI evaluates if the associated attribute value for a given data point differs when compared to the local mean of the attribute value at a statistically significant level. For this research, the local spatial neighborhood was defined by a fixed distance band of 100 m. The statistic generates an index value, a z-score, a p-value, and COType field. An index value of 0 indicates no spatial autocorrelation, i.e. complete spatial randomness, a positive index

value indicates positive spatial autocorrelation, i.e. spatial clustering, and a negative index value indicates negative spatial autocorrelation, i.e. a spatial outlier (O'Sullivan & Unwin, 2010). The z-score and p-value are used to determine the statistical significance of the index value, by comparing it to a completely randomized distribution of the data computed during the algorithm execution (O'Sullivan & Unwin, 2010). For this research, the COType field was selected to represent spatial autocorrelation as it indicated if the data point exhibited statistically significant spatial autocorrelation when compared to its neighboring points, but also the type of spatial autocorrelation. Possible classifications of the COType were: (HH) indicating positive spatial autocorrelation, identifying spatially correlated clusters of points with a high attribute value (i.e. clusters of tall trees); (LL) indicating positive spatial autocorrelation, identifying spatially correlated clusters of points with a low attribute value (i.e. clusters of short trees); (HL) indicating negative spatial autocorrelation, identifying spatial outliers with attribute values that are higher than the values of their surrounding points (i.e. a taller tree surrounded by shorter trees); (LH) indicating negative spatial autocorrelation, identifying spatial outliers with attribute values that are lower than the values of their surrounding points (i.e. a shorter tree surrounded by taller trees); or (NS) indicating that there is no statistically significant difference between the attribute value of the given point and its surround points. The input dataset for the LMI statistic was the point-based individual tree dataset and the attribute value evaluated was tree height. As discussed, vertical complexity can be described in part by the relative vertical isolation of a given tree from its neighbors, creating complexity in the top of the canopy surface and improving access to platforms (Silvergieter & Lank, 2011). This relative vertical isolation can be detected by the LMI

spatial statistics, as indicated by trees with a HL COType value. As murrelet habitat modelling has not been conducted at the spatial scale of the individual tree, the LMI spatial statistic has never been evaluate as a model predictor. It was therefore included in this research as an exploratory predictor.

Table 3.4. Summary of the 12 habitat descriptors included as predictors in the BRF classification model.

Predictor	Summary	Resolution	Rationale
Height	Individual tree height (m) derived from the CHMs	Point data	Suitable habitat is known to be associated with taller trees, specifically those > 28.5 m tall (Burger, 2002).
Rugosity	Measure of canopy surface roughness (m) derived from normalized point cloud	20 m	Suitable habitat is associated with canopies with higher vertical complexities (Burger, 2002).
Canopy Closure	Measure of canopy closure (0.0 – 0.1), derived from normalized point cloud	20 m	Suitability nesting habitat is associated with a canopy closure of 40 – 60% (Burger, 2002).
Height_85P	Height (m) of the 85th lidar percentile, representing height of the co-dominant canopy; derived from the normalized point cloud	20 m	Suitable habitat is associated with forests with a higher percentage of large trees (Burger, 2002), indicated by higher co-dominant canopy heights.
AHA_85P	Average height (m) of all returns above the 85th percentile, representing height of the dominant canopy; derived from the normalized point cloud	20 m	Suitable habitat is associated with forests that have a higher percentage of large trees (Burger, 2002), also indicated by higher dominant canopy heights.
Elevation	Elevation (m AMSL) derived from the DEMs	20 m	Suitable habitat is typically found from 0 – 900 m AMSL on Vancouver Island (Burger, 2002).
Slope	Slope (degrees) of the terrain surface derived from the DEMs	20 m	Suitable habitat has been associated with steeper slopes (Burger et al., 2010) and flat valley bottoms (Burger & Bahn, 2004).
Aspect	Aspect (degrees) of the dominant slope gradient of terrain surface	20 m	Aspect has not been definitively associated with habitat suitability; included as an exploratory predictor.
TRI	Topographic ruggedness index (m) indicating terrain roughness, derived from the DEMs	20 m	Topographic variability potentially increases canopy variability, improving habitat suitability and access to platforms (CMMRT, 2003).
DIST_SW	The distance (km) to the nearest body of saltwater, derived from the DEMs and a provincial land boundary	20 m	Habitat that is located from 0.5 – 30 km inland from saltwater is most likely to provide suitable nesting habitat (CMMRT, 2003).
BEC	The dominant BEC zone, subzone, and variant for the given polygon area	Polygon data	Most nests in B.C. are associated with the CWH BEC zone (Burger, 2002). However, may not be influential at an individual tree based scale; included as an exploratory predictor.
LMI	The COType field from the LMI spatial statistic, identifying spatial autocorrelation and spatial outliers, calculated for each individual tree	Point data	Nest trees have been found to be 15 – 20% taller than surrounding trees (Silvergieter & Lank, 2011). The HL COType can be used to indicate these spatial outliers.

3.6 Data Attribution

All trees in the training dataset (3.4) were attributed with an associated attribute value from each of the 12 habitat predictors. This produced the final dataset used to train the predictive classification model. This attribution process was then repeated for all tree objects detected across the study sites (excluding those in the training dataset), creating the unranked dataset to be assigned a predicted habitat suitability ranking by the BRF classification model.

3.7 BRF Classification Model

The random forest classifier builds hundreds to thousands of individual classification trees to maximum depth, with no pruning, by drawing out a bootstrapped sample from the training dataset and recursively partitioning it into smaller subsets using the values of randomly selected predictors (Breiman, 2001). Each split optimizes for homogeneity of the target variable, resulting in mutually exclusive subsets that become increasingly homogenous within, and increasingly heterogeneous between. This process continues iteratively until the subsets cannot be made any more homogenous (Williams, 2011). Each tree in the forest is effectively an independent model built with two levels of randomness, the random selection of observations through “bagging” (bootstrapped aggregation), and the random selection of predictors used for splitting. Because of this, the effects of correlations between classification trees are significantly reduced (Prasad et al., 2006).

Model accuracy was assessed internally using out-of-bag (OOB) observations instead of external in order to preserve as include as many observations from minority classes as possible in the building of the classification model. Once a given tree is complete, it is used to predict the target variable of the observations that were not used to build the tree, i.e. the out-of-bag observations. Once all trees have been built and OOB error estimates calculated for each, the algorithm uses the majority rule to determine the overall predicted class of the target variable for each observation (Cutler et al., 2007). The overall predicted class is then compared to the known class for each observation, producing the overall OOB error rate for the model (Williams, 2011). OOB evaluation provides unbiased estimates of error that can be considered cross-validated error estimates (Cutler et al., 2007). While an individual classification tree may overfit the data, the combination of trees reduces, if not removes, the potential for overfitting as each tree was fit using a different combination of predictors and observations (Breiman, 2001).

Results from random forests can be complicated to decipher, due to the sheer number of classification trees included and the somewhat of a "black box" approach (Williams, 2011). Variable importance measurements can therefore be used to aid in understanding model outputs, providing insight in to how the ecological phenomenon under study is related to each of the model predictors (Williams, 2011). Random forests can evaluate variable importance using two different metrics: (1) the mean decrease in predictive accuracy, and (2) the mean decrease in the Gini Index. The mean decrease in predictive accuracy is measured by calculating a new synthetic OOB dataset, whereby the values for a given predictor have been randomly permutated. These synthetic OOB data are then

passed through to each tree to receive a new synthetic prediction and generate a synthetic OOB error rate. The average difference between the original OOB error rate and the new synthetic OOB error rate is then calculated. The higher the difference, the more important the predictor was to the model (Williams, 2011). The Gini Index is measured by evaluating the total decrease in impurity at each node (as one subsample is split into two) using a given predictor. The index reports the mean decrease across all trees in the forest, the higher the decrease the more important the predictor was for making splits, i.e. resulted in more homogenous subgroups and thus was a better predictor. The mean decrease in predictive accuracy was selected as the appropriate metric to measure variable importance for this research as it offers less biased measurements when models include both numeric and categorical predictors (Strobl et al., 2007).

Partial dependence plots can then be generate to evaluate the probability that a given class of the target variable would be predicted by the model based on the values of a given predictor (Cutler et al., 2007). The calculated difference between the logarithm of the individual class probability and the logarithm of the average class probability is depicted along the y-axis, while the x-axis displays the associated values for the given predictor being evaluated (Berk, 2008). The probabilities are determined by calculating the total number of observations that were predicted as the given class, for each possible value of the predictor, divided by the total number of observations, while holding the values of all other predictors constant (Branion-Calles et al., 2015).

The BRF classification model was built using the *randomForest* statistical package in R (Version 3.3.1). The model included 795 individual classification trees, determined to be the optimal number by evaluating the minimum overall OOB error rate over 1000 model iterations, using 1 to 1000 trees (Figure 3.7) (Chen et al., 2004). Four randomly selected predictors were considered in each tree, determined to be the optimal number by evaluating the overall OOB error rate through iterative model run alternating the number of predictors (Williams, 2011). Lastly, the model was balanced by down sampling the majority classes. Down-sampling the majority classes has been shown to a more effective balancing approach than over-sampling the minority classes (Chen et al., 2004), and was thus the selected approach for this methodology. This was done by setting a maximum number of samples that could be drawn each time a bootstrapped sample was collected. The maximum number of samples was determined by multiplying the total number of observations in the minority class (Rank 1, with 99 observations) by the total number of target classes (five). Variable importance measurements were then calculated based on the mean decrease in predictive accuracy and partial dependence plots were generated. Finally, the BRF classification model was used to predict a habitat suitability ranking for all unranked trees. All trees were then mapped and visually displayed by their predicted habitat suitability rankings, producing the final object-based predictive habitat suitability maps.

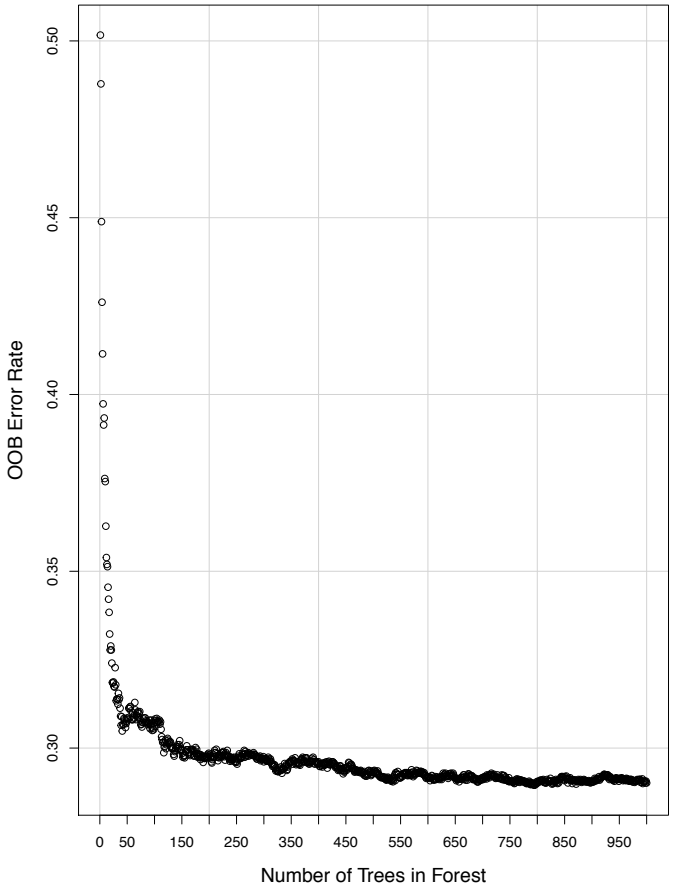

Figure 3.7. The overall OOB error rate calculated for successive model iterations from 1 to 1000 trees.

3.8 Ranking Comparisons

To quantitatively compare the predicted habitat suitability rankings of the individual trees to those of the original LLAS polygons, two different approaches were used: (1) for each LLAS polygon, the average predicted ranking was calculated based on all trees falling within a given polygon, and (2) for each LLAS polygon, the highest predicted ranking within each polygon was determined, based on all trees falling with the polygon. Two new sets of polygon-based habitat maps were then created using the boundary definitions of the original LLAS polygons, but attributed with the average and highest object-based habitat suitability rankings. These new polygon-based maps were compared to the

original LLAS polygon habitat maps to evaluate if the original habitat maps were potentially overgeneralizing habitat suitability and thus underestimating the total amount of suitable habitat. Additionally, by comparing the average lidar predicted ranking per polygon to the original polygon ranking, substantial within polygon variability could be detected, which would be indicted by a polygon having an average object-based predicting ranking that differed from its original LLAS polygon ranking. Finally, the predicted habitat suitability maps were qualitatively assessed, to visually evaluate if smaller patches of suitably ranked trees (Rank 1, Rank 2 or Rank 3) could be identified within LLAS polygons previously designated as unsuitable (Rank 4 or Rank 5).

3.9 Methods Summary

This chapter presented the key components of the new methodological framework developed by this research. The LLAS waypoint data were re-assessed to determine their reliability. Individual tree objects were detected from the lidar-derived CHMs using a local maxima filter, and a series of habitat descriptors were generated from the lidar data. Ultimately twelve habitat descriptors were selected as model predictors. The LLAS waypoint data were then used to derive the model training dataset by selecting individual trees that were representative of their habitat suitability rankings, which were then attributed with values from each of the twelve habitat predictors. Using this dataset, a BRF classification model was built and used to predict a habitat suitability ranking for all tree objects detected across the study sites. The object-based predicted rankings were then compared to those of existing LLAS habitat polygons. The following chapter presents the key findings from these methodological steps

Chapter 4: Results

4.1 LLAS Waypoint Reliability

Overall, the habitat suitability rankings of the LLAS waypoint data were moderately consistent between survey methods (48%) (Table 4.1). Waypoints from Rank 1 and Rank 5 were the most consistent, reporting the lowest proportional errors, 33% and 14%, respectively. Rank 3 and Rank 4 were less consistent with proportional errors of 59% and 54%, respectively. Rank 2 was the least reliable ranking, reporting a proportional error of 73%, with eight of eleven Rank 2 waypoints reporting a different habitat suitability rank between surveys. Results also suggest that when inconsistent, the original waypoint were more likely to underestimate habitat suitability than overestimate, with 68% of all rank changes represented by an increased habitat rank after re-assessment (Table 4.1).

While habitat rankings were only moderately consistent, the majority of all waypoints that experienced a rank change transitioned from one operationally suitable rank (Rank 1, Rank 2, or Rank 3) to another, or from one operationally unsuitable rank (Rank 4 or Rank 5) to another. For example, a waypoint originally designated as Rank 3 was re-assessed and determined to actually represent Rank 2 habitat. While the rankings are different, they both fall within the broader operational classification of suitable habitat. Only 15% of the waypoints changed from one operational ranking to another; three from a suitable ranking to an unsuitable ranking, and five from an unsuitable ranking to a suitable ranking. When considering the overall agreement of habitat rankings in this operational context, the waypoint rankings were consistent (85%) (Table 4.2).

The novel assessment of the Best Tree attribute indicated that 70% of the waypoint locations re-assessed contained some degree of habitat variability even within their small (~3 ha) plot areas (Table 4.3). Waypoints designated as Rank 3 and Rank 4 by the re-assessment survey had the highest occurrence of within plot variability. The assessment of the Surrounding Area attribute indicated that 17% the waypoint plot areas were discrete patches (~3 ha) of suitably ranked habitat surrounded by unsuitable habitat (Table 4.3).

Table 4.1. Overall consistency of waypoint rankings between surveys and the proportional error associated with waypoints from each habitat suitability ranking.

Habitat suitability ranking	Number of waypoints					Proportional error
	Original surveys	Refined survey	Rank changed	Rank increased	Rank decreased	
Rank 1	6	10	2	0	2	**33.33%**
Rank 2	11	13	8	6	2	**72.73%**
Rank 3	17	13	10	7	3	**58.83%**
Rank 4	13	10	7	5	2	**53.84%**
Rank 5	7	8	1	1	0	**14.29%**
Total	54	54	28	19	9	
Overall Consistency						**48.15%**

Table 4.2. Overall consistency of habitat suitability rankings between surveys after pooling the data by their operational habitat suitability rankings; Suitable and Unsuitable.

Habitat suitability ranking	Number of waypoints	
	Rank changed	Rank same
Suitable (Rank 1, 2 & 3)	3	31
Unsuitable (Rank 4 & 5)	5	15
Overall consistency		**85.19%**

Table 4.3. Comparison of the overall waypoint rankings assigned during refined reassessment survey to the rankings assigned to the Best Tree attribute and the Surrounding Area attribute.

Waypoint habitat suitability ranking	Best Tree rank		Surrounding Area rank	
	Same	Higher	Same	Lower
Rank 1	10	0	6	4
Rank 2	3	10	9	4
Rank 3	1	12	12	1
Rank 4	0	10	10	0
Rank 5	2	6	8	0
Total	**16**	**38**	**45**	**9**

4.2 Training Data

The object-based dataset used for model training contained 6197 observations, each representing an individual tree. Due to the natural distribution of habitat across the study sites, observations representing moderate (Rank 3) and low (Rank 4) suitability habitats dominated the dataset with (Figure 4.1). Observations from Rank 1, indicating the most suitable habitat, made up the smallest proportion of the study sites and thus the training dataset, with only 99 observations. This unequal distribution of observations in the training dataset is what required the use of a *balanced* random forest classifier.

The distribution of the training data related to each of the ten numeric habtiat predictors is presented in Figure 4.2. Considering the landscape and topographic – based predictors, Plot 1 shows a clear relationship between habitat suitability and elevation, with low elevation areas providing the most suitable habitat. Plot 2 generally shows that less steep slopes were associated with the most suitable habitat when compared to steeper slopes.

Plot 3 shows that the majority of trees in the training dataset occurred on southeast and southwest - facing slopes (90 – 270°). Plot 4 indicates that topographic ruggedness was fairly low for all trees in the training dataset, with Rank 4 habitat occuring in the most topographicially ruggedd regions. Plot 5 indicates that the majority of trees selected for model trainining were located 2 – 8 km inland from saltwater, with habitat of the lowest quality (Rank 5) being on avergage the furthest inland. Plot 2 and Plot 4, representing Slope and TRI contain a small number of extreme outliers. These values can be explained by trees that were located directly adjacent to, but not on, steep slopes. Therefore, they reported very high values for both Slope and TRI because of the larger 20x20 m grid sizes used to calculate the habitat metrics, which were influenced by the values of adjacent steep slopes.

Considering the canopy based predictors, Plot 6 indicates a clear relationship between tree height and habitat suitability, with trees identified as Rank 1 reporting the highest heights on average and Rank 5 reporting the lowest heights on average. A similar relationships can be seen in Plot 7, indicating that increasing canopy rugosity was related to increasing habitat suitability, with canopies exhibiting the highest vertical complexities being associated with highest habitat suitability rankings. In Plot 8 it can be seen that the majority of all trees in the training dataset had high canopy closure values, approaching full closure (1.0). The low-valued outliers in Plot 8 can again be explained by the influence of the larger 20x20 m grid size used to calculare the canopy closure metrics. Whereby these extreme observations were adjacent to large forest gaps, i.e. harvested blocks or streams, and were therefore assigned a lower canopy closure value than what

was present at, and truly representative of, the given trees. A well defined relationship between increaseing height of the canopy above the 85th lidar percentile and increasing habitat suitability can be seen in Plot 9, particularly for Rank 5 observations, strongly related to low values of Height_85P. Two outliers with uncharacteristically low height values can be seen in this plot for Rank 1 and Rank 3 trees. These data points were visually investigated and determined to again be consequences of the grid size used to calculate the habitat metrics, whereby small pockets of Rank 1 and Rank 3 habtiat were identified directly adjecent to habitats of a much lower suitability. The trees were therefor assigned uncharacteristicially low canopy height values for habtiats of their qualty. Plot 10 depicts a similar relationship to Plot 9, with habitat suitability increasing as the average height of the canopy above the 85th lidar percentile increased. It should be noted that in all plots, observations from Rank 4 contain the most variation in values for all habitat predictors.

When evaluating the distribution of the training data in relation to the categorical predictors, it can be seen that the training dataset was dominated by tall trees that were positively spatially autocorreleated, indicated by the HH COType (Figure 4.3). Trees attributed with the LL COType were exclusivly associated with Rank 4 and Rank 5 habitat, as were trees attributed with the LH COType. Trees attributed with the HL COType, indicating tall spatial outliers, were less prevalent, making up a smaller prorotion of the total sample, but were associated with observations from all five habitat sutiability rankings. Lastly, trees attibuted with a NS COType were associate with all habitat suitability rankings. Trees associated with the CWH BEC zone dominated the

training dataset (Figure 4.4), specifically those associated with the vm 1 and vm 2 subzone variants. Rank 1 trees were only associated with the vm 1 subzone variant of the CWH BEC zone, while the mm 1 subzone variant of the MH BEC zone was the least common of all zones, and was only associated with trees identified as Rank 4 habitat.

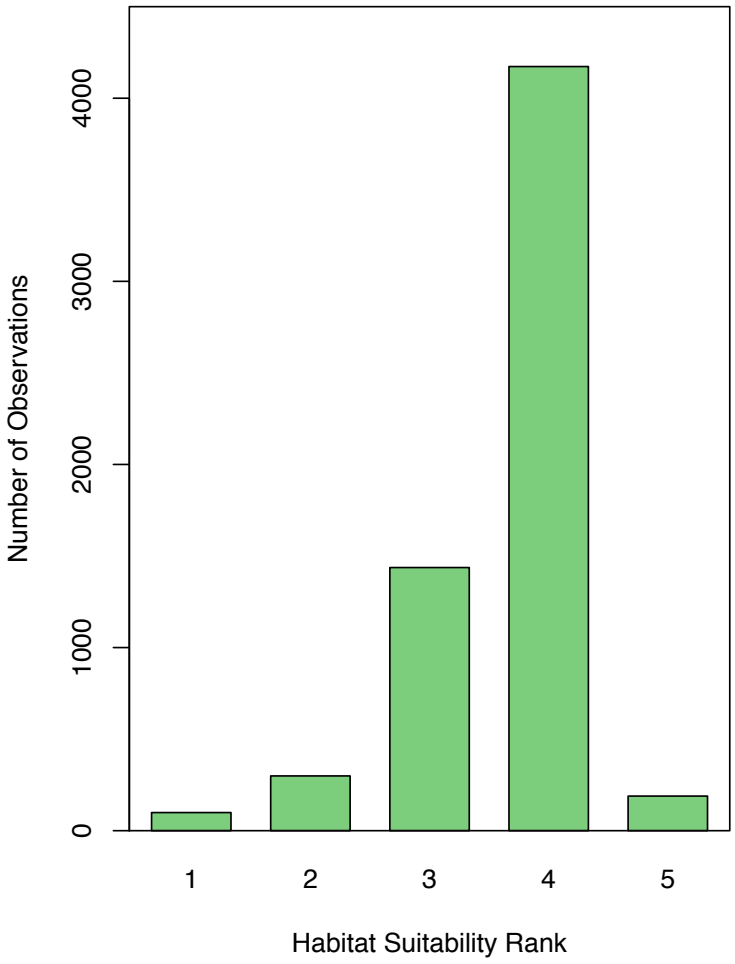

Figure 4.1. Distribution of the data used for model training, interpreted as the number of individual tree objects from each habitat suitability ranking.

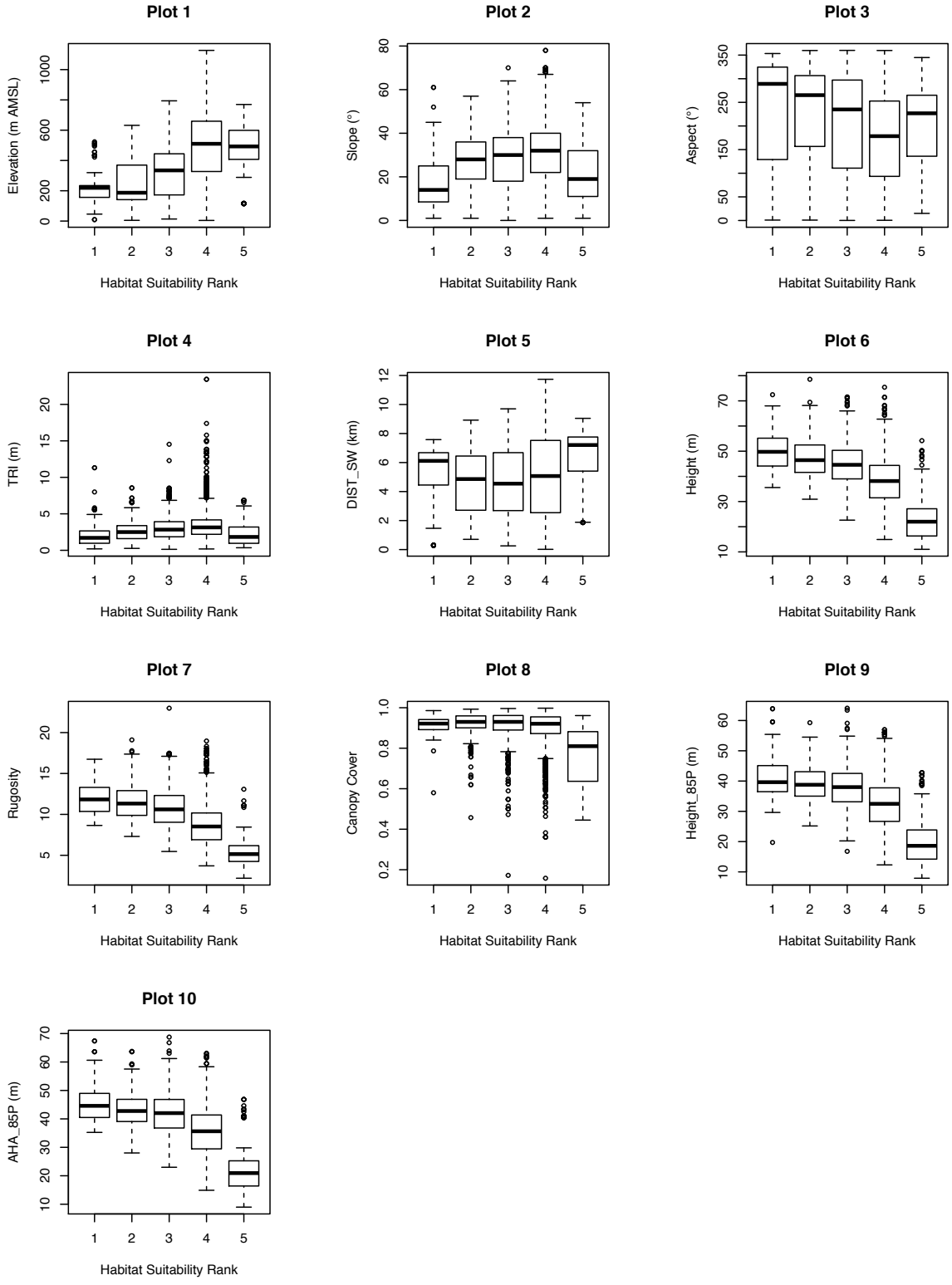

Figure 4.2. Distribution of data used for model training related to the values of each of the ten numeric habitat predictors.

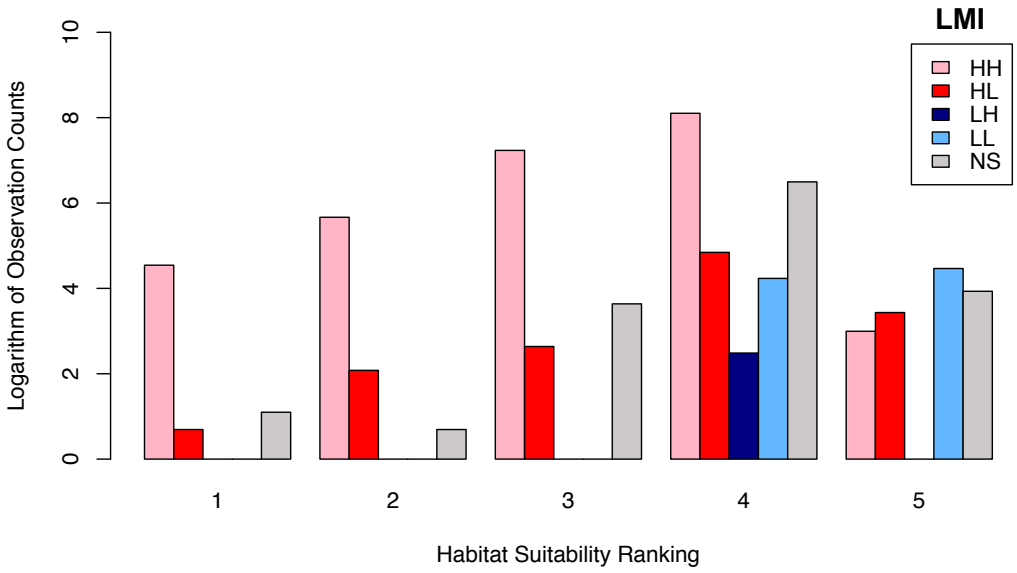

Figure 4.3. Distribution of the data used for model training related to the categories of the Local Moran's I predictor. Abbreviations include: high high (HH), low low (LL), low high (LH), high low (HL) and not significant (NS).

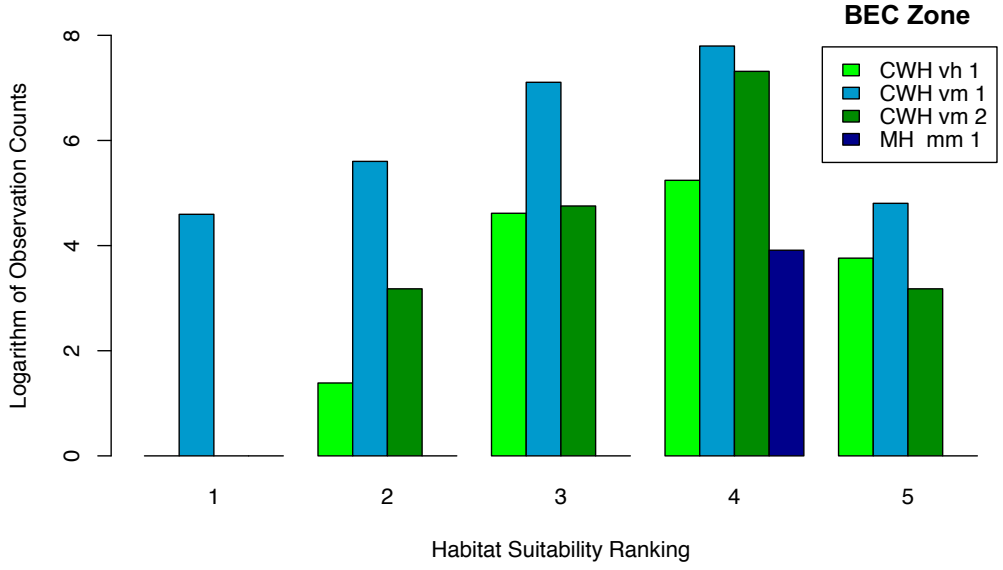

Figure 4.4. Distribution of the data used for model training related to the categories of the Biogeoclimatic Ecological Classification zone predictor. Abbreviations include: Biogeoclimatic Ecological Classification (BEC), Coastal Western Hemlock (CWH), Mountain Hemlock (MH), submontane very wet maritime (vm 1), montane very wet maritime (vm 2), southern very wet hypermaritime (vh 1), and windward moist maritime (mm 1).

4.3 Model Performance

The overall predictive accuracy of the BRF model was 71% (Table 5.3). Classification accuracies of individual habitat ranks varied. Rank 5 and Rank 1 reported the highest classification accuracies, with 98% and 90% respectively. Followed by Rank 2 and Rank 3 with 86% and 74%, respectively. Rank 4 reported the lowest classification accuracy, with 67%. A Kappa statistic of 0.51 indicated that the model performed 51% better than a random classifier. Of the 29% of all trees that were misclassified, 74% were caused by an overestimation of habitat suitability.

Table 4.4. Confusion matrix for the BRF classification model, based on OOB predictions. Reporting the overall classification accuracy, the Kappa statistic and the individual class accuracies for each habitat suitability rank.

		Predicted class					Class accuracy
		Rank 1	Rank 2	Rank 3	Rank 4	Rank 5	
Actual class	Rank 1	**89**	2	8	0	0	**0.90**
	Rank 2	9	**257**	26	7	0	**0.86**
	Rank 3	41	160	**1066**	170	0	**0.74**
	Rank 4	24	201	890	**2806**	252	**0.67**
	Rank 5	0	0	2	2	**185**	**0.98**
Overall Predictive Accuracy = 71.05% Kappa statistic = 51.24%							

4.3.1 Evaluating model predictors

Variable importance measured by the mean decrease in predictive accuracy indicted that the five most important predictors were: (1) Elevation, (2) DIST_SW, (3) Aspect, (4) Slope, and (5) TRI, in descending order (Figure 4.5). Followed by Rugosity, AHA_85P,

BEC, Height_85P, Height, Canopy Closure, and LMI, in descending order. A clear scale-based stratification of variable importance is visible, where the large-scale landscape and terrain-based predictors reported the highest variable importance, followed by the forest-scale canopy-based predictors and the individual tree - based predictors. It can also be seen that there is a clear distinction between all predictors and the least important predictor, LMI, reporting an overall mean decrease in predictive accuracy of - 4.47. However, by evaluating the importance of each variable relative to the classification of each habitat suitability rank individually (Table 4.5), it can be seen that the LMI predictor was an important variable for the classification of all habitat suitability rankings except for Rank 4. Table 4.5 shows that LMI reported a mean decrease in predictive accuracy of – 16.65 for Rank 4. This highly negative importance measurement skews the overall variable importance ranking for the LMI predictor, causing it to report a somewhat misleading overall negative importance measurement.

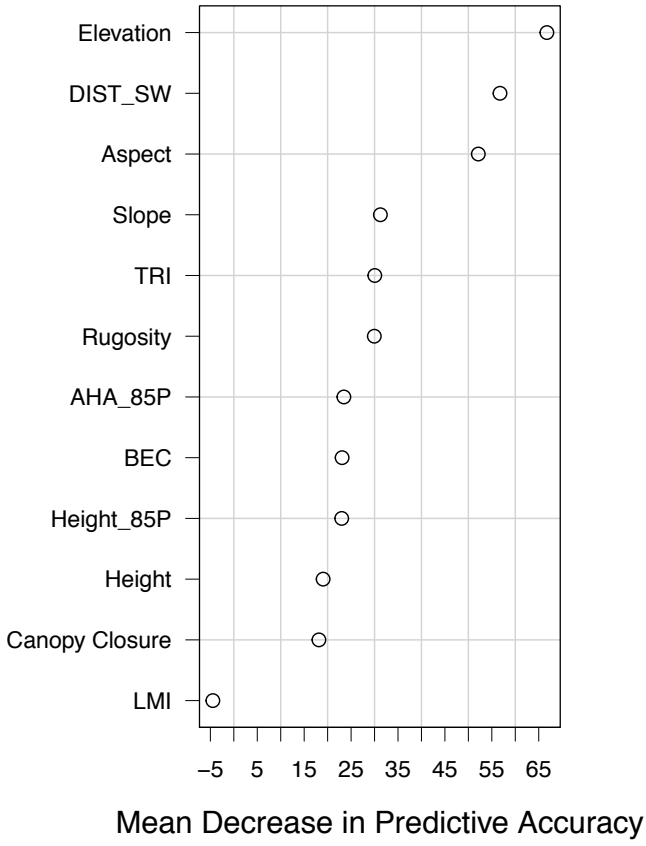

Figure 4.5. Variable importance as measured by the mean decrease in predictive accuracy from the BRF classification model.

Table 4.5. Measured values of variable importance for each predictor as determined by the mean decrease in predictive accuracy for the classification of each habitat suitability rank individually, and overall.

	Mean decrease in predictive accuracy					
Predictor	Rank 1	Rank 2	Rank 3	Rank 4	Rank 5	Overall
Elevation	77.03	74.93	42.50	44.09	37.44	66.74
DIST_SW	55.30	42.78	41.54	31.05	32.42	56.75
Aspect	22.42	41.48	27.83	42.67	34.17	52.12
Slope	37.43	24.66	23.95	19.09	17.41	31.24
TRI	21.32	31.50	20.90	18.17	17.38	30.05
Rugosity	37.48	40.22	28.73	10.32	40.85	29.95
AHA_85P	30.83	29.88	16.75	8.79	25.47	23.46
BEC	12.59	18.74	17.33	16.48	16.38	23.08
Height_85P	23.90	22.61	17.46	10.86	20.77	23.00
Height	27.36	17.62	10.49	9.29	23.28	19.04
Canopy Closure	26.17	25.58	16.99	0.15	24.54	18.14
LMI	8.02	10.90	9.53	-16.65	28.97	-4.47

4.3.2 Variable associations

The likelihood of a tree being classified as Rank 1 or Rank 2 increased as elevation decreased (Figure 4.6ab). The likelihood of being classified as Rank 3 generally increased as elevation decreased, with the exception of a large drop in likelihood at ~ 250 m AMSL (4.6c). The likelihood of being classified as Rank 4 or Rank 5 was strongly related to increasing elevation values (4.6de).

The likelihood of being classified as Rank 1 habitat increased as distance from saltwater increased, peaking ~ 6 km inland (4.6f). Ranks 2 – 5 showed an inverse relationship with

distance from saltwater, whereby the likelihood of being classified as any of the given ranks increased as the distance from saltwater decreased, with likelihood peaking around 2 km inland and dropping around 5 – 6 km (4.6g – j).

Aspect had a less defined relationship with habitat suitability. However, trees were more likely to be classified as Rank 1 or Rank 2 when located on northwest facing slopes (270 – 360°) (4.7ab). The likelihood of being classified as Rank 3 habitat was highest when trees were located on northeast and northwest facing slopes (0 – 90° and 270 – 360°) (4.7c). The classification of Rank 4 was not strongly associated with any specific aspect values, but was least likely to be classified when trees were located on northwest facing slopes (270 – 360°) (4.10d). Rank 5 was most likely to be classified when trees were located on southwest facing slopes (~250°) (4.7e).

Values of slope were strongly related to the likelihood of being classified as each of the habitat suitability rankings. Rank 1 was most likely to be classified when trees were located on slopes < 30° (4.7f). Ranks 2, 3 and 4 were most likely to be classified when trees were located on moderately steep slopes, between 10 – 50°, and peaking around 30° (4.7g – i), while Rank 5 was most likely to be classified when slopes were > 50° (4.7j).

All observations had relatively low TRI values, however Rank 1 was most likely to be classified when TRI was lowest (4.8a). Generally, low topographic ruggedness values (≤ 5 m) were associated with a high likelihood of being classified as Rank 2, Rank 3 or

Rank 4 (4.8b – d), while the likelihood of being classified as Rank 5 increased as topographic ruggedness increased, peaking around a TRI value of 5 m (4.8e).

The likelihood of being classified as Rank 1 or Rank 2 increased as canopy rugosity increased, particularly when rugosity values were > 10 m (4.8fg), while low rugosity values (< 10 m) were associated with an increased likelihood of being classified as Rank 3, Rank 4 or Rank 5, peaking around a rugosity value of 6 m (4.8h – j).

Rank 1 and Rank 2 were most likely to be classified when the height of the dominant canopy (AHA_85P) was between 30 – 40 m (4.9ab). Rank 1 was also highly likely to be classified when the height of the dominant canopy was >= 50 m (4.9a). Rank 3 was most likely to be classified when the height of the dominant canopy was between 25 – 35 m, with likelihood peaking at 25 m (4.9c). The likelihood of being classified as Rank 4 and Rank 5 increased as the height of the dominant canopy decreased, and was highest when the height of the dominant canopy was < 25 m (4.9de).

The likelihood of being classified as Rank 1 or Rank 2 increased as the height of co-dominant canopy (Height_85P) increased (4.9fg). Rank 1 was most likely to be classified when values were > 45 m (4.9f), while Rank 2 was most likely to be classified when values were ~ 30 m (4.9g). Rank 3 was most likely to be classified when values were between 20 – 40 m (4.9h). The likelihood of being classified as Rank 4 or Rank 5 increased as the height of the co-dominant canopy decreased, peaking at ~ 20 m (4.9ij).

Individual tree height was strongly related to habitat suitability, with the likelihood of being classified as Rank 1 or Rank 2 increasing as tree height increased (4.10ab). Rank 1 was most likely to be classified when tree height was > 50 m (4.10a), while Rank 2 was most likely to be classified when tree height was between 30 – 50 m (4.10b). The likelihoods of being classified as Rank 3, Rank 4, or Rank 5 all increased as tree height decreased (4.10c – e). Rank 3 was most likely to be classified when tree height was between 25 – 35 m, while Rank 4 and Rank 5 were most likely to be classified when tree height was < 25 m.

No observations were associated with a canopy closure value of < 0.5 (50%), indicated by the levelling in the partial dependence plots in Figure 4.10f – j. Rank 1 had a less defined relationship with canopy closure, but was most likely to be classified when canopy closure was 60 – 70%, and again when canopy closure was ~ 85% (4.10f). Rank 2 was most likely to be classified when canopy closure was > 90% (4.10g). Rank 3 was most likely to be classified when canopy closure was ~75% and ~ 85% (4.10h), Rank 4 was most likely to be classified when canopy closure was > 70%, peaking at ~ 90% (4.10i), and Rank 5 was likely to be classified when canopy closure was 70 – 80% (4.10j).

For both the categorical predictors LMI and BEC zone, the partial dependence plots showed relatively few clear relationships between the likelihood of a given habitat suitability rank being classified by the model and the categories of either predictor, however some minor relationships were observed (Figure 4.11a – j). The likelihood of

being assigned a classification of Rank 1 was not associated to any of the LMI and BEC zone categories (4.11a and f). The likelihood of an observation being classified as Rank 2 was highest when an observation was attributed with a HH COType (4.11b) and the CWH vm 2 or MH mm BEC zone (4.11g). The likelihood of an observation being classified as Rank 3 was highest when the LMI COType was HH, LH or NS in descending order (4.11c), and when the BEC zone was CWH vm 2 (4.11h). The likelihood of a Rank 4 classification was relatively equally associated with all of the LMI COType categories, with a slightly lower likelihood when the observation had a LL COType value (4.11d). Slightly higher likelihoods of a Rank 4 classification were also associated with the CWH vm 2 or MH mm 1 BEC zones (4.11i). The likelihood of an observation being classified as Rank 5 was highest when it had a HL or LL LMI COType (4.11e), and was from the CWH vh1 or CWH vm 1 BEC zone (4.11j).

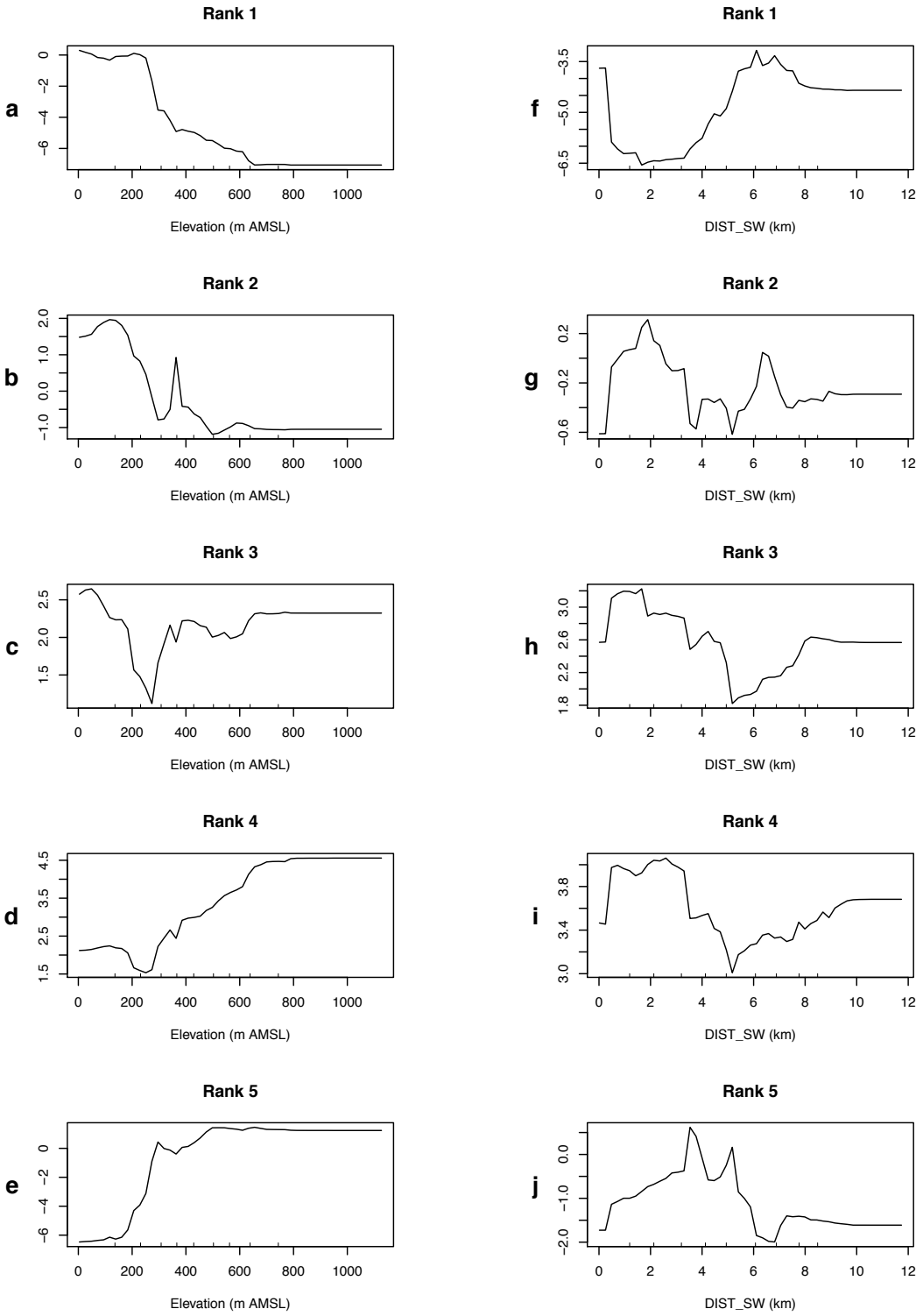

Figure 4.6. Partial dependence plots for the Elevation (a – e) and DIST_SW (f – j) predictors. The plots can be interpreted as the increasing or decreasing probability that the given habitat suitability rank would be classified based on the values of the given predictor, while holding all other predictors constant. For example, in (a), the probability of a Rank 1 classification being assigned to a given tree was low when elevation was > 600 m AMSL, but rapidly increased as elevation decreased, with probability peaking at ~ 200 m AMSL.

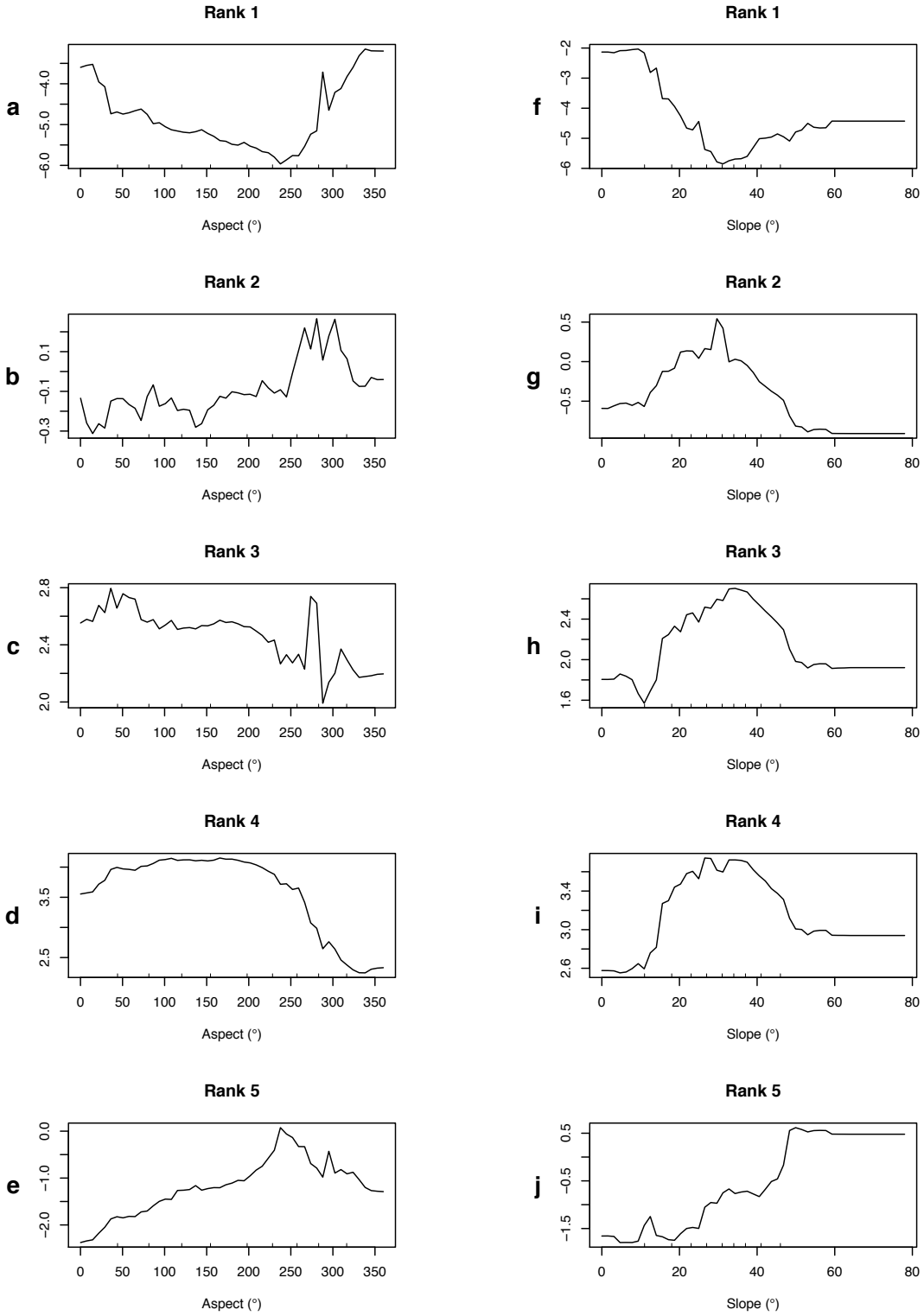

Figure 4.7. Partial dependence plots for the Aspect (a – e) and Slope (f – j) predictors. The plots can be interpreted as the increasing or decreasing probability that the given habitat suitability rank would be classified based on the values of the given predictor, while holding all other predictors constant. For example, in (a), the probability of a Rank 1 classification being assigned to a given tree was lowest when aspect was southwest facing, but increased as aspect transitioned to northwest facing.

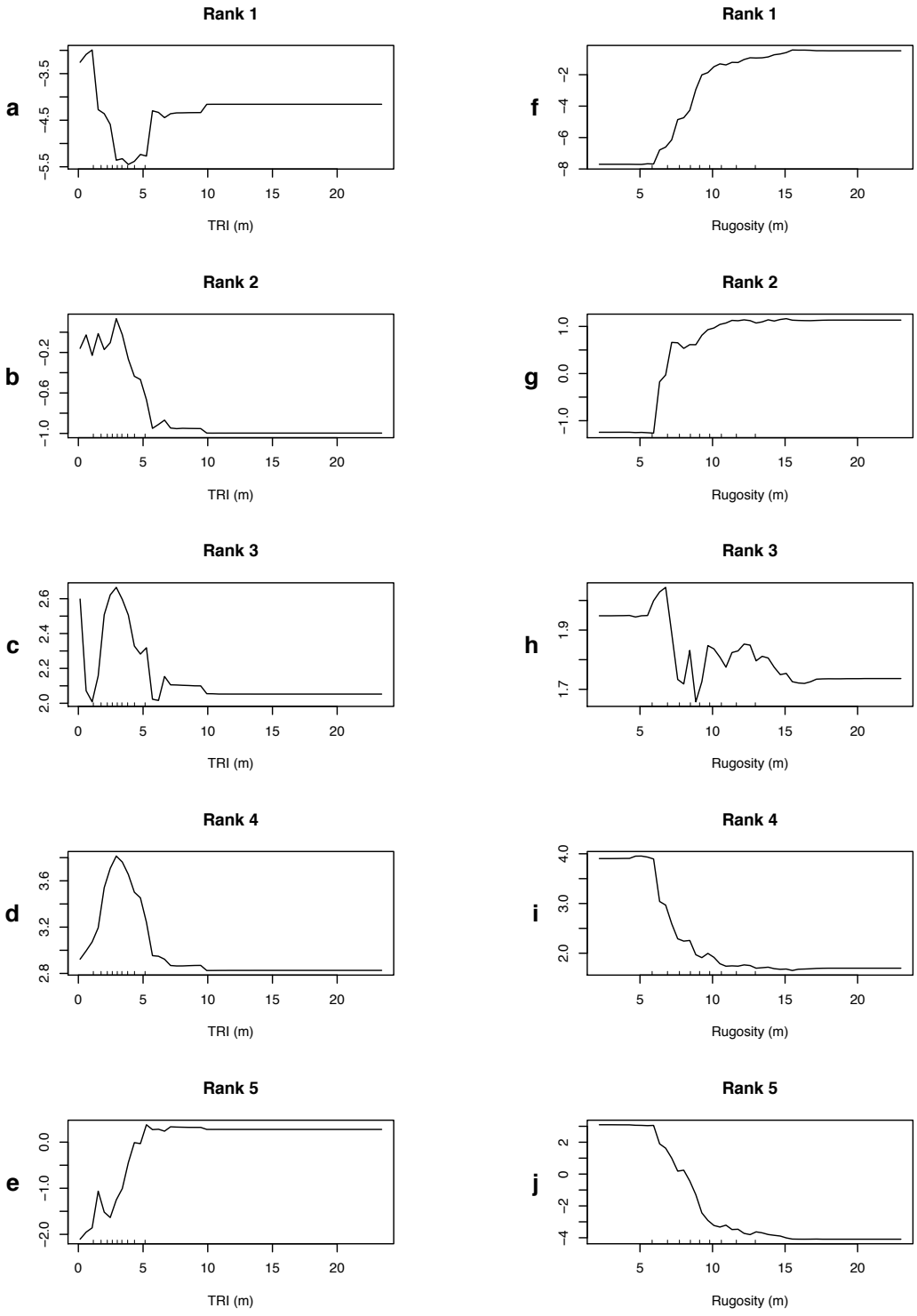

Figure 4.8. Partial dependence plots for the TRI (a – e) and Rugosity (f – j) predictors. The plots can be interpreted as the increasing or decreasing probability that the given habitat suitability rank would be classified based on the values of the given predictor, while holding all other predictors constant. For example, in (a), the probability of a Rank 1 classification being assigned to a given tree was lowest when topographic ruggedness was 2 – 5 m, but increased as the index values decreased towards 0 m and increased towards 20 m.

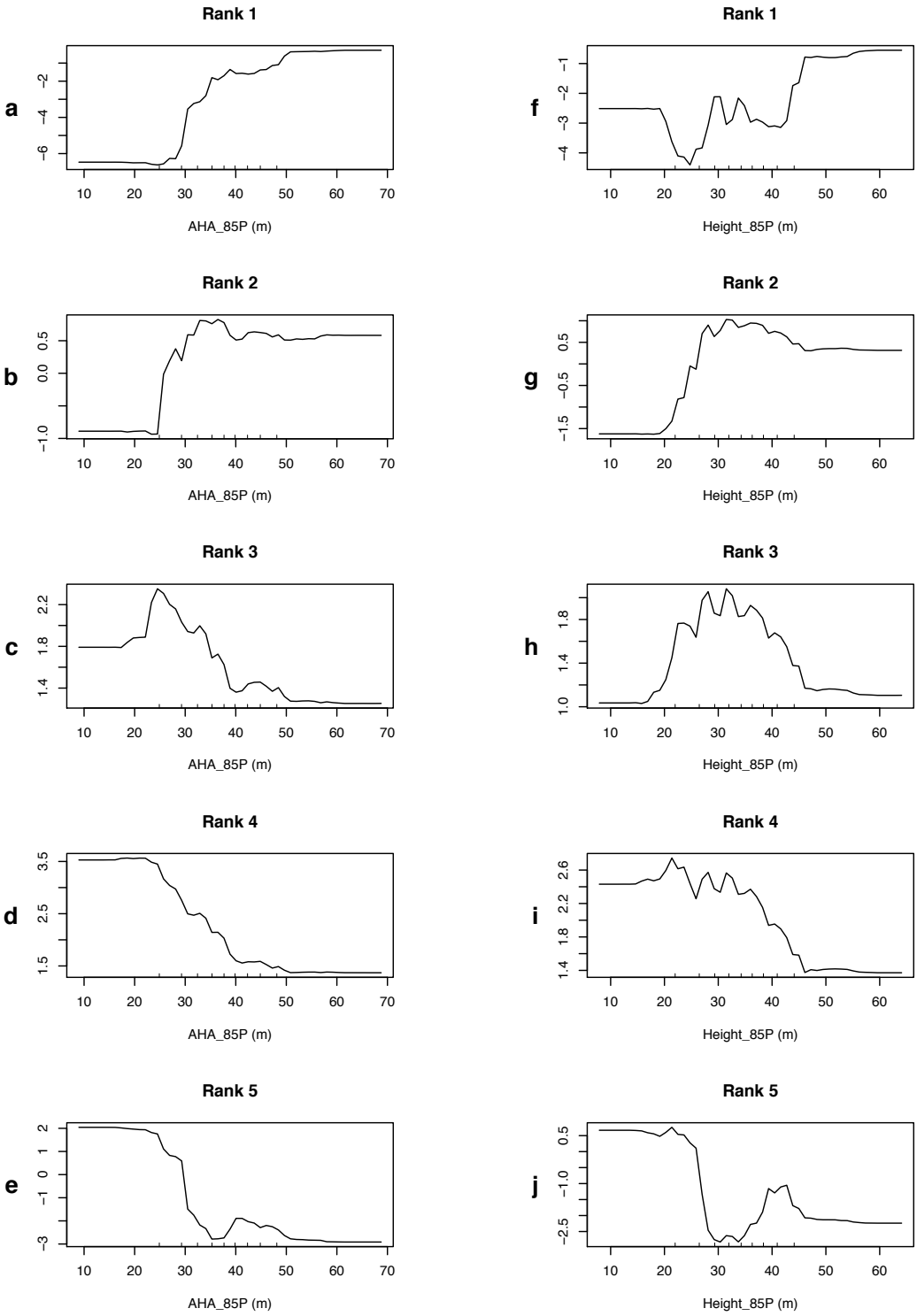

Figure 4.9. Partial dependence plots for the AHA_85P (a – e) and Height_85P (f – j) predictors. The plots can be interpreted as the increasing or decreasing probability that the given habitat suitability rank would be classified based on the values of the given predictor, while holding all other predictors constant. For example, in (a), the probability of a Rank 1 classification being assigned to a given tree was low when the average height above the 85th lidar percentile was < 25 m, but increased as height increased, with probability peaking at ~50 m.

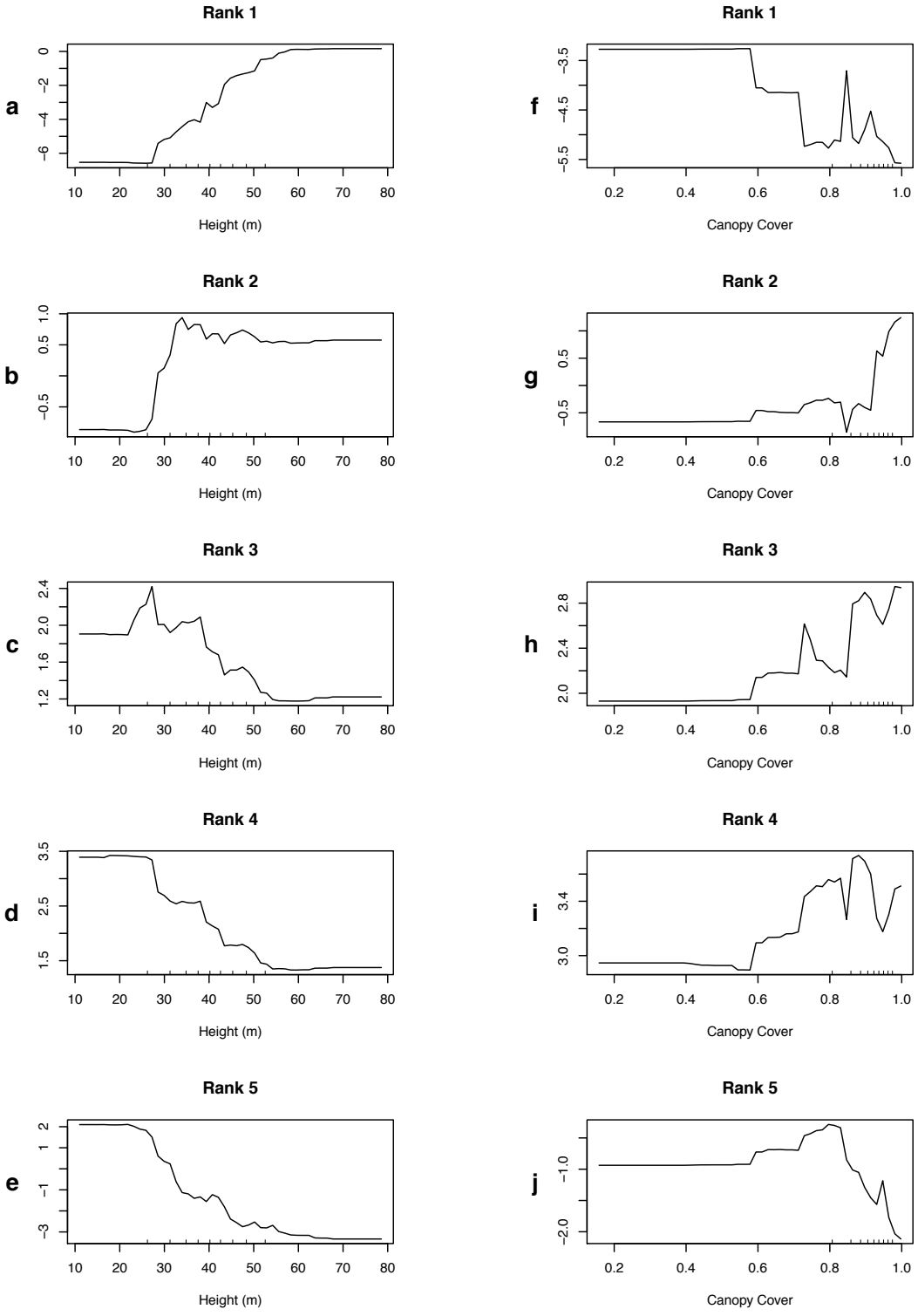

Figure 4.10. Partial dependence plots for the Height (a – e) and Canopy Closure (f – j) predictors. The plots can be interpreted as the increasing or decreasing probability that the given habitat suitability rank would be classified based on the values of the given predictor, while holding all other predictors constant. For example, in (a), the probability of a Rank 1 classification being assigned to a given tree increased as tree height increased, with probability peaking at ~ 60 m.

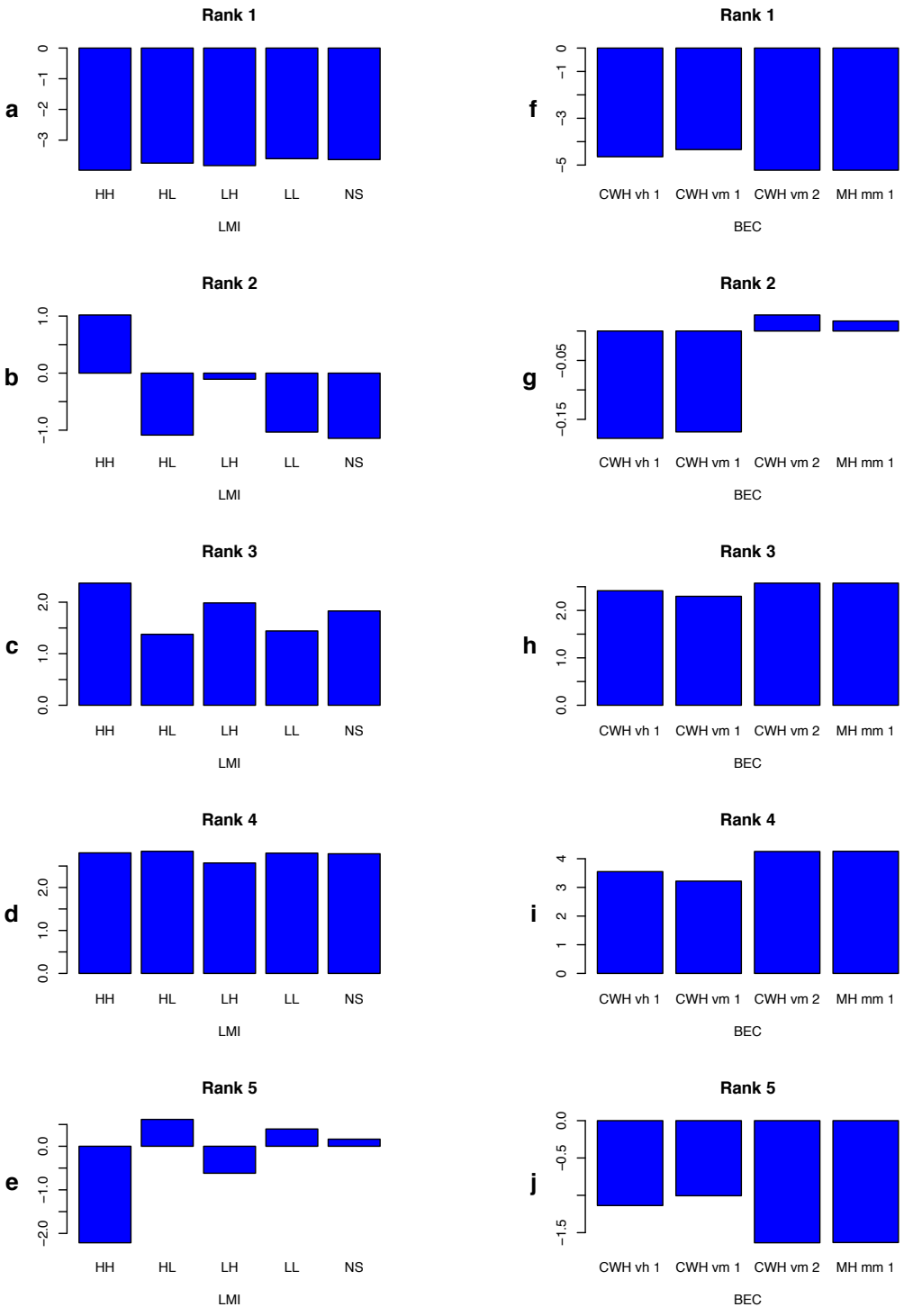

Figure 4.11. Partial dependence plots for the categorical LMI (a – e) and BEC (f – j) predictors. Bars extended upwards from zero indicate the highest likelihood of classification for the given habitat suitability ranking and the associated predictor category, while bars extended the furthest below zero indicate the least likelihood of being associated with the given habitat suitability ranking for the given predictor category. For example, in (b) it can be seen that a Rank 2 classification was most likely to be predicted when the LMI category was HH.

4.4 Distribution of Predicted Habitat

In the Holberg region, suitable habitat was predicted in small clusters that were often linearly distributed along riparian areas, particularly Rank 1 and Rank 2 habitat found predominantly along the Goodspeed River (Figure 4.12). Unsuitable habitat was distributed in much larger contiguous areas at higher elevations, particularly in the northwest corner of the study region towards Mount Waddington. Rank 1 and Rank 2 made up the smallest proportion of habitat with 1% and 5% respectively, while Rank 5 made up the largest proportion of habitat, with 46%. Overall, the Holberg region contained the second largest component of Suitable habitat (Table 4.6).

In the Koprino region, suitable habitat was predominantly found on the eastern side of the Koprino River Valley and the northern end of Hathaway Creek (Figure 4.13). Rank 1 made up the smallest proportion of habitat (1%), and was almost exclusively located in the Koprino River Valley. Unsuitable habitat was clustered more centrally on the higher elevation slopes of Mount Byng and was dominated by Rank 4 habitat (50%). Overall, the Holberg region contained the smallest proportion of Suitable habitat (Table 4.6).

The Jeune Landing region was the largest of the three regions and was dominated by Rank 4 habitat (77%) (Figure 4.14). Rank 1 and Rank 2 habitats were clustered on the northwest facing slopes of the valleys following Teeta and Cayuse creek along the southeastern side Neroutsos Inlet, the north and northwest facing mountain slopes near Yreka at the mouth of Neroutsos Inlet, and on the eastern side of central Victoria Lake. Rank 3 habitats were distributed in smaller more discontinuous clusters, often located on

the higher elevation peripheries of Rank 1 and Rank 2 habitats. Unsuitable habitat was typically predicted in high elevation areas, including the slopes of Mount Wolfenden, Mount Clark, Comstock Mountain, Kashutl Peak, and the mountains south and east of Victoria Lake. Overall, the Jeune Landing region contained the largest proportion of Suitable habitat (Table 4.6).

Table 4.6. Distribution of predicted habitat by number of trees per habitat suitability ranking.

Predicted habitat suitability ranking	Number of trees per study site		
	Holberg	Koprino	Jeune Landing
Rank 1	4,916	3,457	7,246
Rank 2	21,027	39,794	60,361
Rank 3	61,911	107, 373	122,130
Suitable habitat	87,854	150,624	189,737
Rank 4	133,508	166,794	1,257,164
Rank 5	185,735	16,102	185,540
Unsuitable habitat	319,243	182,896	1,442,704

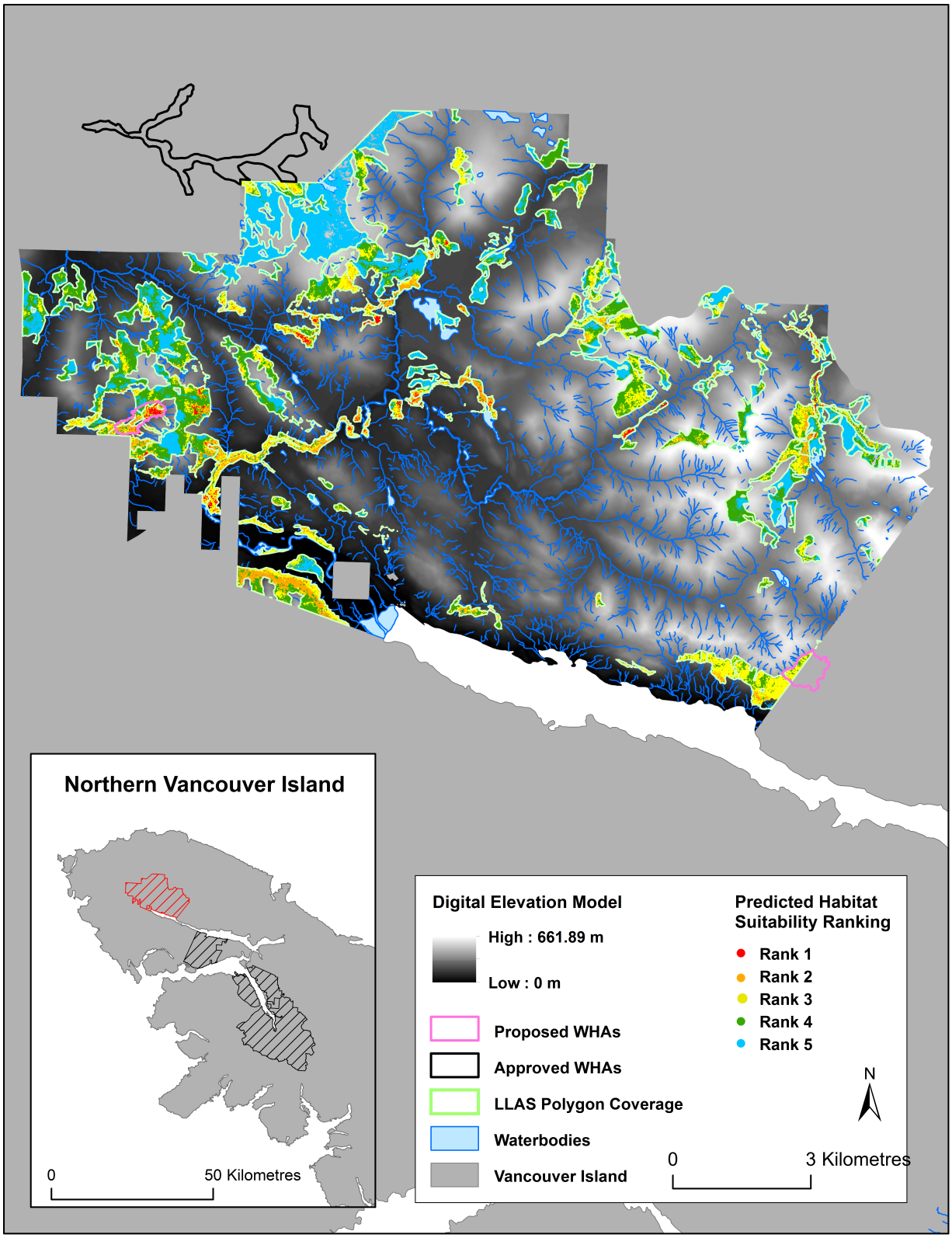

Figure 4.12. Object-based predictive nesting habitat suitability map for the Holberg study site.

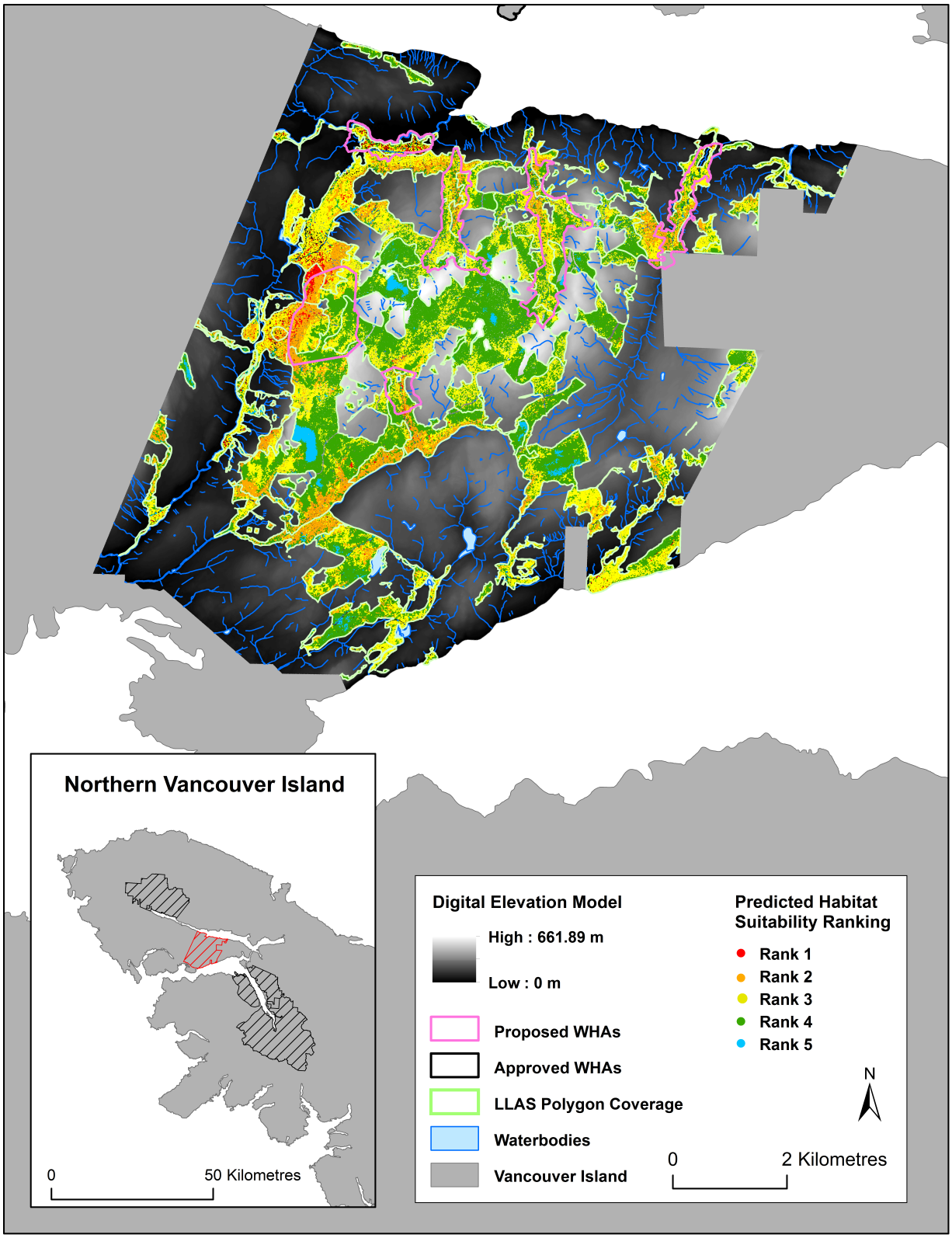

Figure 4.13. Object-based predictive nesting habitat suitability map for the Koprino study site.

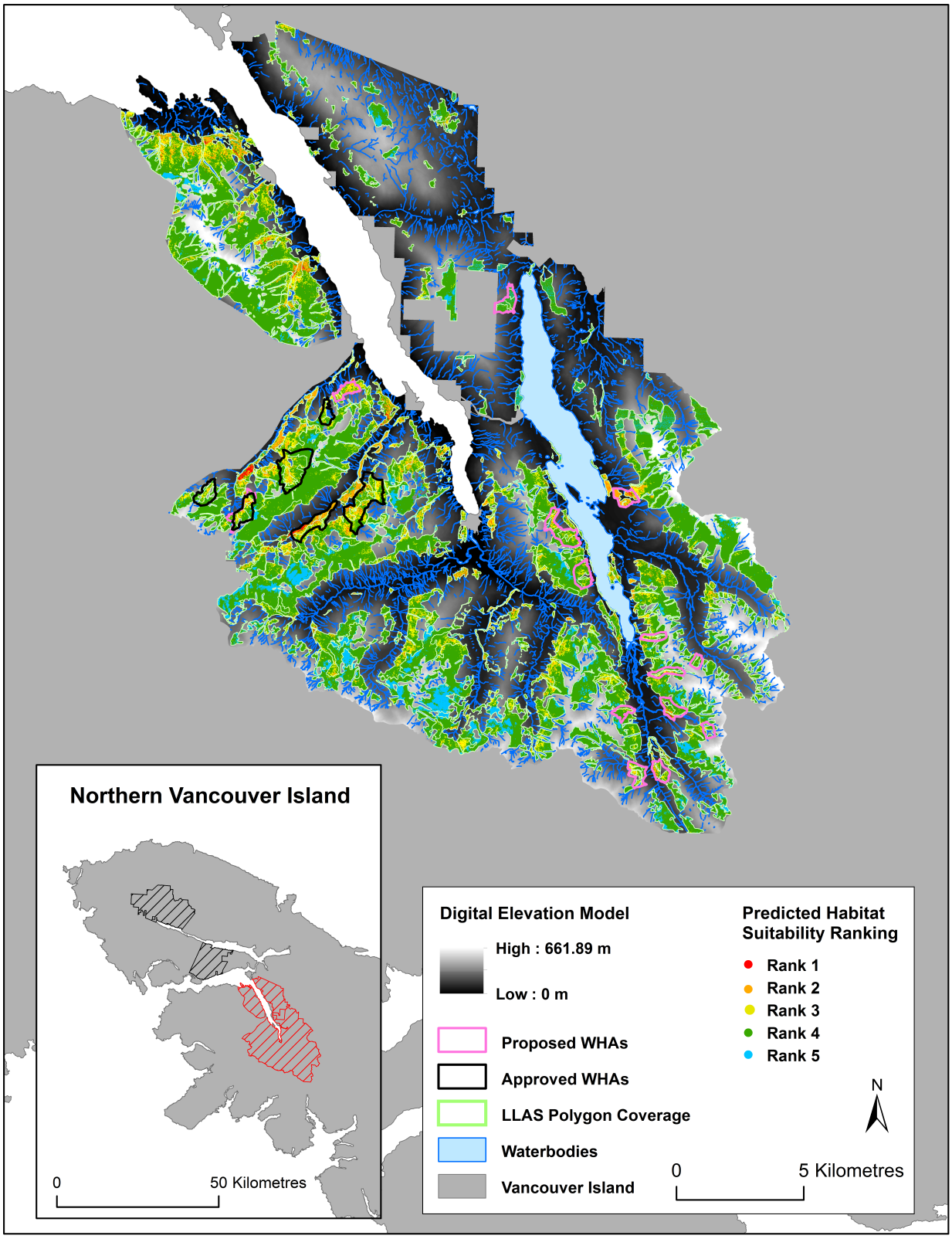

Figure 4.14. Object-based predictive nesting habitat suitability map for the Jeune Landing study site.

4.5 Ranking Comparisons

Overall, the average object-based predicted rankings per polygon were fairly similar to the original polygon rankings (65%) (Figure 4.15) (Table 4.7). LLAS polygons representing Rank 4 and Rank 5 habitat were the most stable, with 81% and 67% of polygons being assigned an equivalent average object-based predicted ranking, respectively. However, LLAS polygons representing Rank 1, Rank 2 or Rank 3 habitat were unstable, with all Rank 1 LLAS polygons reporting a lower average object-based predicted ranking, and only 25% of Rank 2 polygons and 41% of Rank 3 polygons being assigned an equivalent average object-based predicted ranking. When different, the average object-based predicted rankings were predominantly lower than the original LLAS polygon rankings. The highest predicting object-based rankings per polygon showed little consistency with the original LLAS polygon habitat rankings (15%) (Figure 4.15) (Table 4.8). With the obvious exception of Rank 1 LLAS polygons, almost all other LLAS polygons were assigned an increased habitat suitability ranking based on the highest object-based predicted ranking per polygon, and the habitat maps based on the highest object-based predicted rankings per polygon indicating almost exclusively suitable habitat.

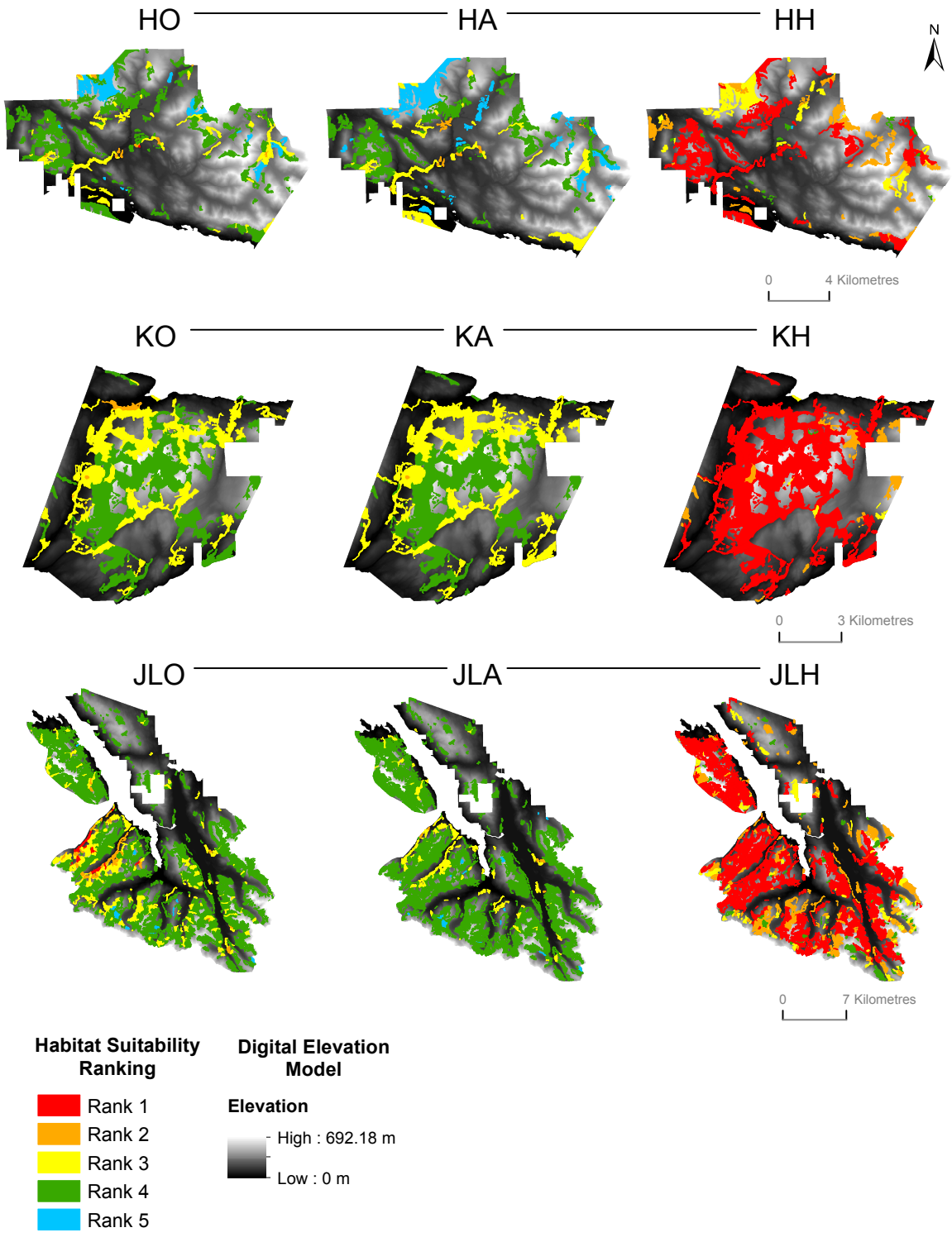

Figure 4.15. Comparison of the original habitat suitability rankings assigned to the LLAS polygons (right) to the average object-based habitat suitability ranking per polygon (center), and the highest object-based habitat suitability ranking per polygon (left). Abbreviations include: Holberg (H), Koprino (K), Jeune Landing (JL, Original (O), Average (A), and Highest (H).

Table 4.7. Confusion matrix comparing the habitat suitability rankings of the original LLAS polygons to those of the polygons generated from the average object-based predictions per polygon; for all study areas combined.

		Rank of polygon based on average predicted rankings					Class accuracy
		Rank 1	Rank 2	Rank 3	Rank 4	Rank 5	
LLAS polygon habitat suitability ranking	Rank 1	**0**	1	7	2	1	**0.00**
	Rank 2	0	**11**	20	13	0	**0.25**
	Rank 3	0	4	**79**	106	3	**0.41**
	Rank 4	0	0	49	**348**	34	**0.81**
	Rank 5	0	0	0	9	**18**	**0.67**
Overall agreement = 64.68%							

Table 4.8. Confusion matrix comparing the habitat suitability rankings of the original LLAS polygons to those of the polygons generated from the highest object-based predictions per polygon; for all study areas combined.

		Rank of polygon based on highest predicted ranking					Class accuracy
		Rank 1	Rank 2	Rank 3	Rank 4	Rank 5	
LLAS polygon habitat suitability ranking	Rank 1	**7**	2	1	1	0	**0.64**
	Rank 2	34	**8**	1	1	0	**0.18**
	Rank 3	100	73	**13**	6	0	**0.07**
	Rank 4	127	137	87	**78**	2	**0.18**
	Rank 5	1	5	8	13	**0**	**0.00**
Overall agreement = 15.04%							

4.6 Within Polygon Variability

While no quantitative spatial analysis was conducted, the new object-based predictive habitat suitability maps were qualitatively analyzed. Visually identifying areas where patches of trees had been predicted a higher habitat suitability ranking than that of the LLAS polygon they fell within. Figure 4.16 provides an example of one of these patches from the Jeune Landing region. The majority of predicted rankings within the polygon can be seen to coincide with the original ranking of the LLAS polygon (Rank 4). This polygon was also assigned an average object-based predicted ranking of Rank 4. However, it can be seen that within polygon variability was detected. Denoted by the

presence of several clusters of Rank 3 and Rank 2 trees throughout. The most notable feature is the cluster of Rank 1 and Rank 2 trees at the northern end of the polygon. Figure 4.17 provides a similar example from the Holberg region showing a LLAS polygon original designated as Rank 4, also assigned an average object-based predicted ranking of Rank 4, but again contains a small patch of potentially very suitable habitat, indicated by the cluster of Rank 1 trees. Small clusters of habitat such as those identified in these two figures, were common throughout many of the LLAS polygons, and were estimated to have been present in at least 30% of all LLAS polygons.

4.7 Results Summary

This chapter presented the key findings from this research. Overall, the LLAS waypoint data were determined to be reliable for model training. The BRF model produced high classification accuracies, particularity for the most suitable habitat ranks (Rank 1 & Rank 2). Lastly, the object-based predictive habitat maps facilitated the detection of small patches suitable habitat within larger areas previously designated as unsuitable, with an estimated 30% of polygons containing these suitable patches. Additionally, 85% of all LLAS polygons contained some component of habitat that was more suitable than the polygon ranking represented based on the object-based rankings. The following chapter will discuss these findings and their relevance for strategic species and resource management.

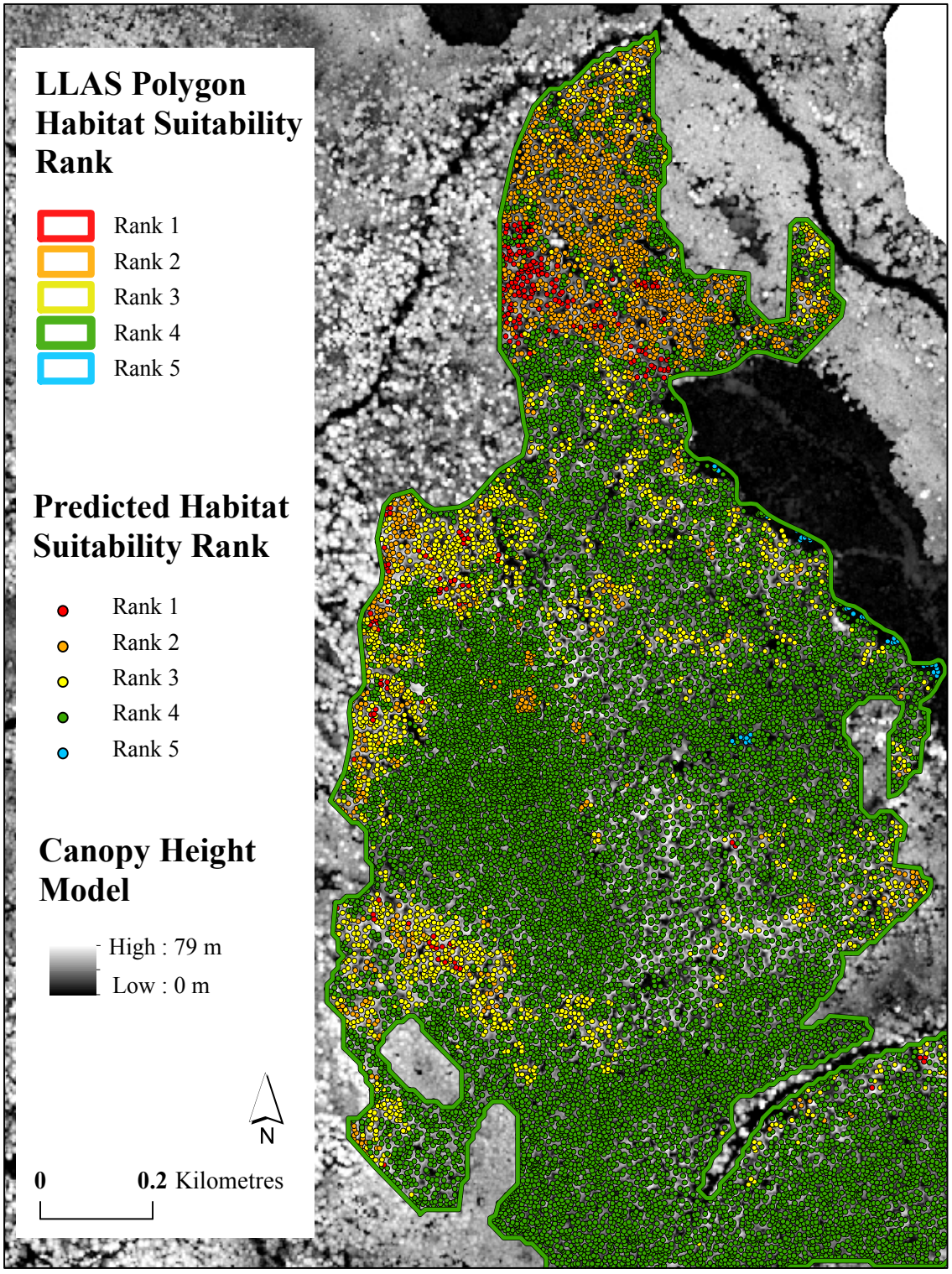

Figure 4.16. An example of visually identified patches of suitably ranked trees (indicated by the yellow, orange, and red points) encompassed within an unsuitably ranked LLAS polygon (defined by the hollow green polygon boundary) from the Jeune Landing study site.

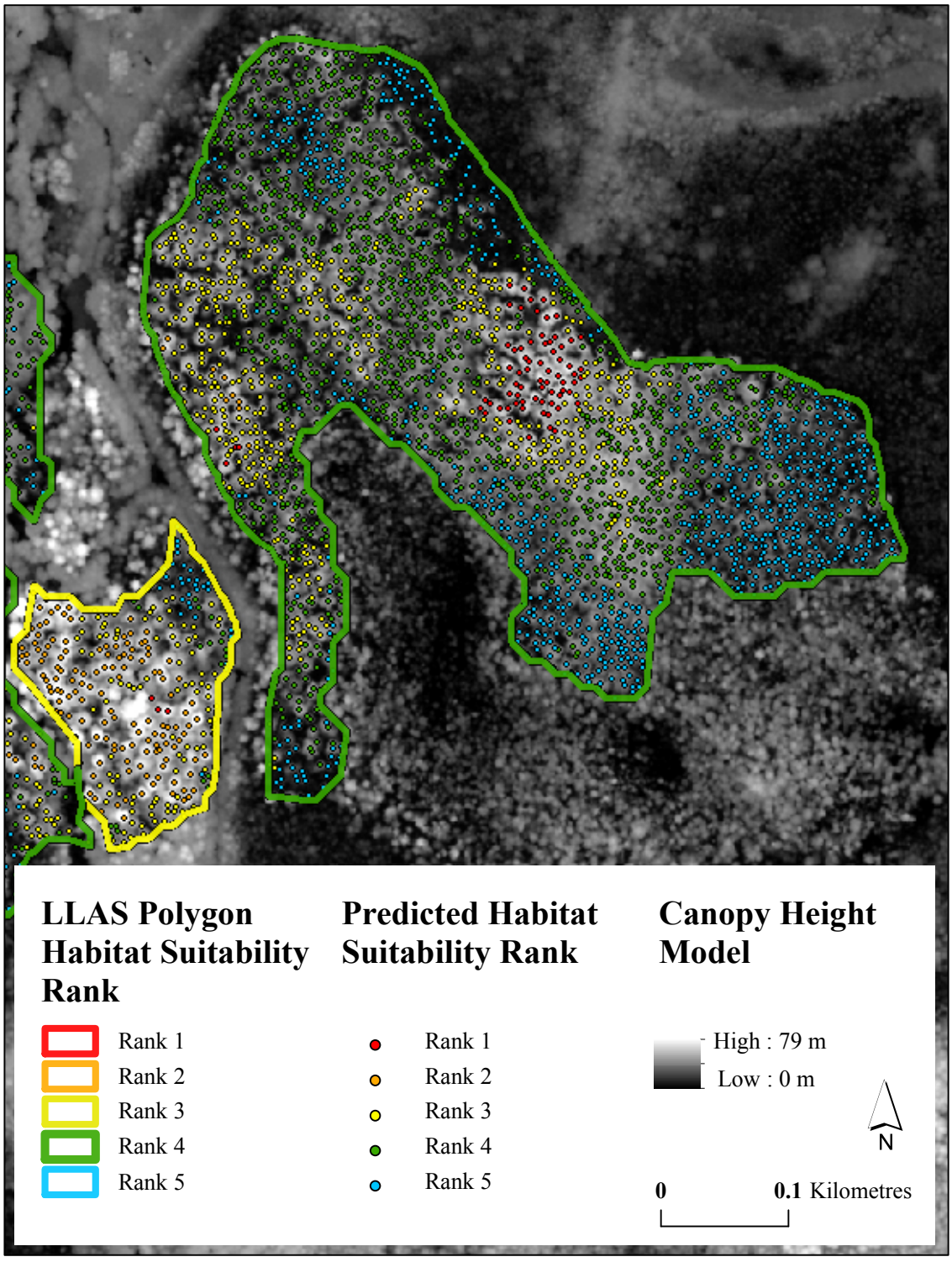

Figure 4.17. Example of a visually identified patch of suitably ranked trees (indicated by the red points) encompassed within an unsuitably ranked LLAS polygon (defined by the hollow green polygon boundary) from the Holberg study site.

Chapter 5: Discussion

This research made the ecological assumption that the biophysical characteristics indicative of suitable nesting habitat were consistent across the study sites evaluated, and further, that marbled murrelets will select these suitable areas over unsuitable areas for nesting. Therefore, habitat with suitable structural characteristics represents habitat the species may use for nesting. By successfully modelling this suitable nesting habitat, reliable habitat data can be produced and used to facilitate the effective spatial management of remaining habitats. In order to advance the spatial quantification of habitat, this research developed a practical habitat mapping methodology capable of quantitatively mapping habitat suitability at the scale of the individual tree. Significantly improving upon the stand-based scale and qualitative assessment of habitat suitability used by current methods. In order to address the first research question – *Can lidar-derived structural habitat metrics be used to predict habitat suitability at the scale of an individual tree using habitat data derived from ranked LLAS waypoints?* – the reliability of the waypoint rankings, the overall and individual model classification accuracies, the variable importance measurements and relationships, and the object-based predictive habitat suitability maps were evaluated.

5.1 LLAS Waypoint Reliability

Before using the LLAS waypoint data to identify and rank individual tree observations, to later be used for model training, the data were re-assessed using a high-intensity, plot-based, LLAS method. By doing so, increased confidence could be placed in accuracy of the training data and thus model results. Furthermore, recommendations could be made

for future studies wishing to utilize the existing network of LLAS waypoint data across the province. Overall, the habitat suitability rankings of the LLAS waypoint data were moderately reliable (48%) (Table 4.1). Results from the re-assessment surveys suggested that when inconsistent, the original LLAS waypoint data were more likely to underestimate habitat suitability than overestimate, with 68% of all rank changes represented by an increased habitat rank after re-assessment. These results coincide with expectations of using a LLAS method with an increased-intensity (Burger, 2004). Allowing observers to more accurately assess the presence on nesting platforms and moss, both key distinguishers of habitat suitability, which were likely not as visible at the less intense scale used in the original surveys. Because the presence of platforms and moss were more easily identified during the high-intensity surveys, it makes sense that many of the waypoints received a higher habitat suitability ranking during the re-assessment surveys. While the overall reliability of the habitat rankings was only moderate, results indicated that the rankings were decidedly more reliable (85%) when considered within the broader operational ranking designations used for strategic habitat management: Suitable (Rank 1, Rank 2 and Rank 3) and Unsuitable (Rank 4, Rank 5 and Rank 6) (Table 4.2). Because these operational ranking divisions are used when making species and habitat management decisions, the implications of the ranking inconsistencies and the potential underestimation of habitat suitability were determined to be limited, and the LLAS waypoint data were determined to be reliable for modelling.

While it is suggested that a lidar-based habitat mapping approach be used for future habitat studies, it is recognized that LLAS are a well-established and integral method for

large-scale cost effective identification or confirmation of suitable nesting habitat for the marbled murrelet in B.C. They can directly evaluate the presence of both platforms and moss, not possible solely through API, forest cover mapping, or even airborne lidar - based modelling (Burger, 2004; Donald et al., 2010; Waterhouse et al., 2007). However, this research suggests they may be most valuable for the collection of data that can then be used to inform lidar-based predictive habitat models. Many habitat studies are repeatedly constrained by data quality and availability, and are often compelled to use spatially sparse or imperfect data, particularly for elusive and endangered species (Quayle & Westereng, 2000). Therefore, the wide distribution of the existing LLAS data across much of B.C., make the data a highly valuable data resource for researchers, ideal for future spatial habitat modelling applications, particularly in regions with limited nest site or occupancy data. Yet, the reliability of the waypoint data will depend on both the scale and intensity of the surveys used to acquire the data. It is thus recommended that LLAS waypoint data collected with a low or medium – intensity survey method be verified with a high-intensity method, such as the one developed for this research, before inclusion in future marbled murrelet habitat suitability models.

Lastly, if using this methodology, and feasible to collect entirely new LLAS waypoint data, it is suggested that the size of the plot area assessed during the surveys be decreased, in order to be more comparable with the size of the buffer area used when selecting individual trees for the training dataset. While the use of a 100 m radius plot area (~3 ha) greatly improved upon the larger polygon-based scale used in previous habitat assessments, a 20 – 50-m radius plot area (< 1 ha) would help to ensure that the

individual trees selected for model training were representative of habitat suitability rankings assigned with waypoint location.

5.2 Model Accuracy

Model results suggest that lidar-derived habitat descriptors can accurately predict the suitability of nesting habitat within mature and old-growth forests for the marbled murrelet on Northern Vancouver Island, with the model reporting a high overall classification accuracy of 71.95% (Table 4.4). This conclusion is further supported by a Kappa statistic of 0.51, which is a robust indicator of model performance when using imbalanced datasets (Fatourechi et al., 2008). This suggests that the model performed 51% better than a random statistical classifier. Of the 29% of observations that were misclassified by the model, 74% were caused by an overestimation of habitat suitability. As the maintenance of suitable habitat is the most important objective for species recovery, this potential overestimation of habitat suitability was considered to be more preferable than underestimation. Furthermore, this overestimation may unintentionally combat the trend of underestimation of habitat suitability discovered in the LLAS waypoint data, potentially producing more accurate predictions overall. Yet the accurate classification of each habitat suitability ranking is not equally important in the context of habitat and species management. Recent work by Wilk et al. (2016) suggests that murrelets will select the most suitable habitat within areas of all potentially suitable habitats. Therefore, the accurate classification of the most suitable habitat (Rank 1 and Rank 2) is most critical to species and habitat management. The modelling approach developed here thus provides a highly effective tool for management, with Rank 1 and

Rank 2 reporting individual classification accuracies of 90% and 86%, respectively. The accurate classification of the least suitable habitat is also important for habitat management in mixed-use landscapes, immediately ruling out areas that can then be considered for other activities such as timber harvesting, and allowing managers to focus their efforts on the further characterization of suitable habitat. The lowest quality habitat considered in this research was Rank 5, which reported an individual classification accuracy of 98%. This further solidifies the conclusion that lidar-based predictors can be used to successfully predict nesting habitat suitability for the marbled murrelet at the scale of an individual tree using LLAS waypoint data.

Rank 3 and Rank 4 reported the poorest classification accuracies, with 74% and 67% respectively. These results are consistent with the known challenges of identifying and distinguishing between habitats of these two suitability ranks (Burger, Waterhouse, et al., 2009; Hagar et al., 2014). Additionally, Donald et al. (2010) found that Rank 3 and Rank 4 habitat classifications were also the least reliable classifications based on existing habitat mapping methods (LLAS and API). In the context of this research, these lower accuracies can be explained by two factors. First, the larger number of samples from each of these rankings in the training dataset when compared to all others. Rank 3 made up 23% of all observations, while Rank 4 made up 67% of all observations. These larger sample sizes created more within class variance, which may have introduced more noise into the dataset, confusing model predictions. Second, there are a variety of habitat structures that can be associated with Rank 3 and Rank 4 habitats. For example, Rank 3 habitat can be comprised of trees with suitable structural characteristics (appropriate tree

height, canopy closure etc.), but have little moss presence, or it can be comprised of trees with less desirable structural attributes (smaller trees, less canopy cover), but have sufficient moss presence. As the model relied purely on structural characteristics, distinctions that rely on non-structural attributes, such as the presence of moss, are likely not possible. In these scenarios, the model may have produced a misclassification, explaining the lower classification accuracies.

Overall model performace, but particularily the classification of Rank 3 and Rank 4 habitat, could be improved by removing observations from the training dataset with extreme values (Figure 4.2). As discussed in section 4.2, these observations were retained as they represented exteme data values that were not errors. Their skewed values were due to the use of grid-based metrics to represent characteristics of individual trees. Following this approach, a given pixel can fall between two structurally heterogeneous environments, such as the edge of a harvested block. The pixel would then report a much lower value for canopy closure than was truly present at the location of the individual tree for which the canopy closure value was assigned to. These occurrences were relatively few, and thus likely did not greatly impact model performance. However, removing them from the dataset could yield improved separability of Rank 3 and Rank 4 habitats, which were the most affected by these extreme values, and produce higher overall classification accuracies.

5.3 Variable Importance

Based on expert opinion, literature, and their ability to distinguish between habitat suitability rankings, 12 habitat descriptors were selected as model predictors: individual tree height (*Height*), canopy rugosity (*Rusosity*), canopy closure (*Canopy Closure*), height of the dominant canopy (*AHA_85P*), height of the co-dominant canopy (*Height_85P*), elevation (*Elevation*), distance to saltwater (*DIST_SW*), topographic ruggedness (*TRI*), slope gradient (*Slope*), topographic aspect (*Aspect*), BEC zone (*BEC*), and the COType of the LMI spatial statistic (*LMI*).

Based on the mean decrease in predictive accuracy (Figure 4.5), a clear scale-based stratification was detected in predictor importance. The landscape-scale predictors, Elevation, DIST_SW, and Aspect reported the highest variable importance, in decreasing order. All reporting a > 50% mean decrease in overall model predictive accuracy when values were randomly permutated for each predictor. Followed by the large-scale topographic predictors of Slope and TRI, both reporting a > 30% mean decrease in predictive accuracy. The classification of habitat suitability was then influenced by structural characteristics of the canopy and the individual tree, with Rugosity, AHA_85P, Height_85P, Height, and Canopy Closure all reporting an 18 – 30% mean decrease in predictive accuracy, in decreasing order. This scale-based stratification of predictor importance aligns with existing research, whereby nesting habitat suitability is thought to be first dictated by large-scale geographic and topographic characteristics, and then by the biophysical attributes of the forests and individual trees within the geographically and topographically suitable regions.

BEC zone was determined to have a lower variable importance than all other landscape-scale predictors, with a mean decrease in predictive accuracy of 23%. While BEC zones can be generally associated with habitat suitability, as they relate to regional productivity and growth patterns (Burger et al., 2010), habitat of any suitability (Rank 1 – Rank 6) could be found within any BEC zone. While BEC zone is likely correlated to habitat suitability at the broader landscape scale, results suggest that it is not likely a strong predictor of habitat suitability at the scale of the individual tree. It is therefore suggested that future habitat studies working at a fine spatial scale do not include BEC zone as a model predictor.

As previously noted, LMI was the lowest ranked predictor, actually reporting a negative overall mean decrease in predictive accuracy (- 4.47%). This suggests that the model would have performed better without its inclusion. However, because LMI was an important predictor for the classification of all habitat suitability rankings except Rank 4, the model actually performed worse overall without the predictor and reported only a slight improvement (~ 2%) in the individual classification accuracy of Rank 4. As such, the predictor was maintained. Yet the predictor still reported the lowest variable importance overall. Because of this, it is suggested that the LMI statistical measure may have more potential as a stand-alone tool for statistical analysis, rather than as a model predictor. It is a user friendly tool with highly flexible parameter settings, and is a well-established tool for detecting patterns in spatial ecological phenomena (Fortin et al., 2002). Specifically, it is suggested that future marbled murrelet habitat studies evaluate the use of the LMI spatial statistic to identify the presence of vertically isolated trees (HL

CoType) and or clusters of tall trees (HH COType) within LLAS polygons, both of which may be indicative of smaller pockets of suitable habitat located within unsuitably ranked LLAS polygons (Stachura-Skierczynska & Kosinski, 2014). This application could offer a primitive tool for the identification of smaller patches of suitable habitat within larger less suitable habitat areas, and would only require the point-based individual tree dataset derived from the CHM surfaces.

5.4 Variable Associations

Based on the partial dependence plots (Figure 4.6 – 4.11), the classification of suitable nesting habitat (Rank 1, Rank 2 and Rank 3) was generally associated with lower elevations (< 600 m AMSL), areas located further inland (> 6 km), southwest and northwest facing slopes (250 – 325°), flat and moderately steep slopes (0 – 50°), and regions with relatively low topographic complexity (TRI < 5 m). This relationship between elevation and habitat suitability corresponds with the existing notion that suitable habitat on Vancouver Island (with the exception of the eastern coast) is most likely to occur at elevations ranging from 0 – 600 m AMSL (Burger, 2002). The increasing likelihood of a suitable habitat classification as distance inland increases loosely corresponds with findings from Hagar et al. (2014), who found that murrelet occupied stands were located further inland than unoccupied stands. While aspect has been found to have a relatively inconsistent relationship with habitat suitability (Burger et al., 2010), results from this study indicate that fine scale topographic aspect is related to habitat suitability. The relationships observed between slope and habitat suitability also correspond with results from existing studies that have found suitable nesting habitat

(Burger et al., 2010), and occupied stands (Waterhouse et al., 2007; Wilk et al., 2014), are associated with moderately steep and steep slopes. Furthermore, Burger & Bahn (2004) found that suitable nesting habitat was also associated with flat slopes in valley bottoms, where small isolated pockets of suitable old-growth were located on gravel bars or flood plains. While the high likelihood of a Rank 1 classification being associated with very low TRI values (< 5 m) may be explained by the aforementioned patches of highly suitable habitat located on flat gravel bars and flood plains, the relationship between decreasing topographic complexity and increasing habitat suitability does not align with the previously stated hypothesis that increased topographic complexity may increase vertical complexity of the canopy above, and thus the potential suitability of the habitat. It is possible this theorized relationship may not exist, however it may also be possible that the influence of topographic complexity on canopy complexity may not be present at the fine 20 m spatial scale used to model terrain and canopy structure. Future studies could evaluate the use of a larger grid size to represent topographic variability, which may be able to better capture this hypothesized relationship.

The likelihood of receiving a suitable habitat classification (Rank 1, Rank 2 or Rank 3) was also associated with more vertically complex canopies, indicated by higher rugosity values (> 10), higher dominant and co-dominant canopy heights (30 – 70 m), taller individual trees (25 – 80 m), and moderate (60%) to high (> 80%) canopy closure. The relationship of increased habitat suitability with increasing canopy rugosity is consistent with findings from Hagar et al. (2014), who found that murrelet occupied stands had higher vertical canopy complexities when compared to unoccupied stands. The

relationship of increased habitat suitability with increasing individual tree and canopy heights also coincides with known habitat associations for the species, where suitable habitat is dominantly comprised of trees that are > 28.5 m tall and stands that are > 141 years old (Burger, 2002). Furthermore, Hagar et al. (2014) found that the maximum height of the canopy was as strong indicator of occupied stands, being on average 77.5 m in occupied stands. Canopy closure had a somewhat unexpected relationship with the likelihood of an observation being assigned a suitable habitat classification by the model. Typically, suitable habitat is associated with a canopy closure of 30 – 70%, with the most suitable habitat having a canopy closure of 40 – 60% (Burger, 2002). While the likelihood of being assigned a suitable classification by the model was associated with this moderate canopy closure (~ 60%), it was also associated with uncharacteristically high values of canopy closure (> 80%), which are typically indicative of unsuitable habitat (Burger, 2002). This discrepancy may be due to the difference between the qualitative estimations of canopy closure used in prior studies (Burger, 2002) and the quantitative measurements used here, where closure was directly measured from the lidar point cloud. Lastly, based on the indistinctive partial dependence plots, there were no clear associations between the likelihood of a being assigned a suitable habitat ranking by the BRF model and any categories of the LMI or BEC zone predictors.

5.5 Object-Based Mapping Scale

The use of lidar data for quantifying the biophysical characteristics of forests is now common practice, taking hold as a key component of forest management (Eysn et al., 2015; White et al., 2013) and wildlife habitat studies (Ackers et al., 2015; Bae et al.,

2014; Farrell et al., 2013; Garabedian et al., 2014; Goetz et al., 2010; Holbrook et al., 2015; Müller et al., 2009; Vogeler et al., 2013; Zellweger et al., 2013). Area-based methods for generating habitat descriptors, such as the ones used here, provide important information at the stand-based scale for forest inventorying and management. However, the ability to quantify forests at the scale of the individual tree provides a significant advancement for forest science, and is particularly advantageous when the ecological phenomena under investigation is influenced by characteristics at the sub-stand level. This research developed a methodology that utilizes a hybrid-scale quantification approach, where individual tree objects were attributed with values derived from area-based habitat metrics.

By mapping nesting habitat at the scale of the individual tree, this methodology provided spatial habitat data at the finest possible scale, which can either be utilized in its existing fine-scale form, or up-scaled based on user preferred clustering methods and parameter settings. As single occurrences of suitable trees are less likely to provide suitable nesting habitat that occurrences of multiple suitable trees, this ability to up-scale the data using any user defined areal spatial criteria is highly advantageous. There is still debate about the exact size of the minimum habitat area required for nesting (Burger et al., 2004; Silvergieter & Lank, 2011b). However, as more definitive data are acquired, the method developed here will allow the used to map habitat at the most meaningful and representative spatial scale for the species.

5.6 Ranking Comparisons

To address the second research question – *can this object-based mapping methodology be used to identify smaller patches of suitably ranked habitat within larger areas previously identified as less suitable by existing methods?* – the object-based habitat suitability maps were compared to the existing, LLAS polygon-based habitat maps. Specifically, the average and highest object-based rankings per polygon were compared to the LLAS polygon rankings, and the object-based habitat suitability maps were visually evaluated to identify if discrete patches of suitable habitat had been identified within larger less suitable LLAS polygons.

The polygon-based habitat maps generated from the average and highest object-based predicted rankings were not intended to truly represent the habitat suitability for the given polygon areas (Figure 4.15). Instead, they were meant to highlight the potential overgeneralization of habitat suitability caused by the spatial scale of current habitat mapping methods. The classification of habitat based on the averaged object-based predicted ranking per polygon was fairly similar to the existing classification of habitat in the region (65%). This indicates that existing methods are likely correctly representing the dominant or overall suitability of the habitat within the larger LLAS polygons. However, LLAS polygons that were assigned an average object-based predicted ranking that differed from their original ranking, likely contained larger patches of habitat that were of a higher or lower habitat suitability than the majority of the polygon area, i.e. there were enough trees of a different ranking within the polygon to results in a different average object-based predicted ranking. Using the new object-based rankings, these

LLAS polygons could be divided up into a number of smaller habitat polygons that were more homogeneous in habitat suitability.

As expected, the highest predicted rankings were almost exclusively higher than the original LLAS polygon rankings, particularly for LLAS polygons originally attributed with an unsuitable habitat ranking (Rank 4 or Rank 5). Based on the highest object-based predicted ranking per polygon, results suggested that 85% of all LLAS polygons contained some component of habitat that was more suitable than the overall ranking of LLAS polygon indicated. While many of these more suitable habitat components were likely comprised of only a few trees, and would thus be unlikely to support nesting, other components were comprised of larger clusters of these more suitable trees. While no qualitative spatial analysis was conducted to cluster and quantify these encapsulated patches, it was estimated that at least 30% of all LLAS polygons contained components of more suitable habitat that could be considered large enough to constitute a "patch" of habitat. Figures 4.16 and 4.17 provide visually confirmed examples of some of these encapsulated patches. These results provide evidence that the methodology developed here was able to successfully detect and spatially identify habitat variability at a sub-stand level, a superior level of habitat quantification and differentiation unattainable at the scale of current habitat mapping methods. Because Waterhouse et al. (2007) found that the habitat patches (~3ha) being used for nesting by marbled murrelets were often of higher suitability than the LLAS or API polygons they fell within, this new methodology and its improved habitat quantification is likely to be highly beneficial for the strategic management of the species and their associated habitat.

Overall, the rankings comparison results provide further support for the use of an object-based habitat mapping methodology for future habitat mapping initiatives. More refined spatial habitat data will allow for improved quantification of the total amount of available suitable nesting habitat in the province, and aid in the establishment of legally protected habitat areas such as WHAs. The establishment of WHAs and other protected areas such as parks, conservancies, and ecological reserves, is critical. As only an estimated 1,392,351 ha of suitable nesting habitat remained in B.C. by 2011, just 352,703 ha above the minimum habitat retention levels required for the species to recovery (Environment Canada, 2014). Further, as of 2009, only 515,411 ha (35%) of suitable nesting habitat in B.C. was legally protected (B.C. Ministry of Environment, 2004; Mather et al., 2010).

While resource constraints prohibited this study from doing so, it is suggested that future habitat studies verify the object-based habitat maps produced by this methodology, particularly the clusters of more suitable habitat identified within less suitable LLAS polygons. This could be done using a high-intensity LLAS method, such as the one developed here, or through in field plot assessments, where individual trees can be spatially identified and measured. Although the verification of training data offered meaningful insight into the operational accuracy of model predictions, verification of the direct model predictions will allow for more definitive conclusions about results, and thus more effective management decisions moving forward.

5.7 Future Applications

Based on the high classification accuracy demonstrated by this new methodology and its ability to produce spatially refined habitat data, it is suggested that a lidar-based modeling approach be used for future habitat mapping initiatives for the marbled murrelet in B.C. where the required data are available. This addresses the third and final research question: *can a lidar-based modelling approach be recommended for future marbled murrelet habitat mapping initiatives for the marbled murrelet in B.C.?* Three specific applications are recommended for future research applications.

First, as a network of LLAS waypoint data already exist across much of B.C., and nest site and occupancy data are limited, it is suggested that existing and newly acquired LLAS waypoint data be used to produce standardized, object-based predictive habitat suitability maps for the marbled murrelet across B.C. as more lidar data are collected. While this would not improve the qualitative nature of the habitat classifications assigned to the LLAS waypoint data, it would provide a consistent network of habitat data across the province at a refined spatial scale. These data could then be scaled up to a minimum patch size, once determined, to produce an updated province-wide baseline of available suitable nesting habitat.

The second recommended application is to test the use of this methodology for building a habitat selectivity model using occupancy or known nest site data instead of LLAS waypoint habitat suitability data. It is acknowledged that this application is currently limited by the availability of overlapping lidar and nest site and or occupancy data.

However, several lidar acquisition campaigns are currently underway for regions with existing nest site and occupancy data (S. McDonald, personal communication, January 2017). A successful occupancy model at the scale of the individual tree would provide more definitive and impactful data for species and habitat management.

The third and final recommendation is to utilize the method developed here to create a new independent quantitative lidar-based habitat classification scheme, ultimately replacing the need for LLAS and or API to classify and map habitat. This new quantitative classification scheme would be based on defined thresholds for a set of standard lidar-derived habitat characteristics (i.e. tree height, canopy closure, canopy and topographic complexity etc.) that could be used to definitively distinguish habitat suitability at both the stand-based and individual tree – based scale. The threshold values used to distinguish between habitat suitability rankings would be based on empirical relationships derived by testing the habitat characteristics of occupied stands and individual nest trees against those from unoccupied stands and trees. A reliable quantitative classification scheme would significantly decrease the costs currently associated with the helicopter surveys and air photo collection campaigns used to classify habitat, and remove the inconsistencies that are often introduced to the data due to the qualitative nature of the assessments.

5.8 Additional Model Predictors

While this methodology considered 19 different habitat descriptors, there are additional several additional predictors that could be considered in future modelling applications

that may improve the classification of habitat suitability. The maximum height of the 10th lidar percentile can be used to indicate of the height of the bottom of the forest canopy (Hagar et al., 2014), which may be an indicator of adequate space for the birds' jump-off takeoffs below the canopy. This metric was evaluated in the occupancy model built by Hagar et al (2014), and was found to be an indicator of occupied stands, with an average value of 48.0 m.

The kurtosis of the vertical canopy height distribution (Niemann, 2009) could also be considered. This metric can be used to describe the vertical distribution of canopy layers, with lower values of kurtosis indicating more structurally complex canopies, potentially indicating more suitable habitat (Hamer et al., 2008). The minimum kurtosis of the canopy was evaluated by Hagar et al. (2014) and found to be an indicator of occupied stands.

The density of trees has also recently been found to be related to habitat suitability, with Wilk et al. (2016) finding that nest sites had a lower density of trees, but of a larger size, when compared to random sites. The calculation of stem density and density of large trees (user defined threshold) would be straightforward, only requiring the individual tree objects derived from the CHM and their associated height attributes (Maltamo et al., 2004), and may help to distinguish between the most suitable habitat classes.

Diameter at breast height (DBH) could be evaluated as a model predictor. DBH is known to be a critical indicator of suitable nesting habitat as it is strongly correlated to the

presence of suitable nesting platforms, which are the most definitive indicator of suitable nesting habitat (Burger et al., 2010). While DBH is not reliably directly measurable from airborne lidar data, it can be estimated using tree height (Parker & Evans, 2004). The relationship between tree height and DBH is dependent on number factors including tree species and site conditions (Zhao et al., 2012). Because these data were not available to this study, DBH was not included as a model predictor. However, future studies with the required data could evaluate the use of lidar-estimated DBH as a model predictor. As the presence of platforms is the most significant indicator of suitable habitat at the scale of an individual tree, the inclusion of this predictor would likely yield improved classification accuracies.

Lastly, the incorporation of remotely sensed data that may allow for the detection of moss presence within the canopy could be evaluated. Structure-from-Motion (SfM) is an emergent, low-cost, highly accurate, photogrammetric technique for obtaining high-resolution, three-dimensional information about topographic surfaces (Westoby et al., 2012). The technique follows the traditional stereoscopic photogrammetric principal, where three-dimensional positions can be determined for an object using multiple overlapping images of the given feature from offset angles (Wallace et al., 2016). Based on this principal, a computer vision algorithm can then be used to generate a three-dimensional point cloud from the high-resolution orthophotography. While point clouds derived from SfM technologies can provide information about canopy structure in low canopy density environments, they are typically outperformed by lidar derived point clouds when assessing canopy structure in denser forests with higher canopy closure

(Leberl et al., 2010; Wallace et al., 2016). This is because there is no penetration into the canopy using the SfM methods, whereas airborne laser scanners can penetrate into the canopy to produce more comprehensive point clouds (Wallace et al., 2016). It is therefore suggested that SfM point clouds not be used to replace lidar-derived point clouds, but instead are used independently to evaluate the presence of moss within the canopy. This can be done by directly rectifying the imagery originally used to derive the SfM point cloud, on to the point clouds itself, essentially producing three-dimensional imagery. Tree crowns derived from the lidar point cloud (Popescu et al., 2003; Strîmbu & Strîmbu, 2015) could then be intersected with this colorized SfM point cloud, and the spectral characteristics of the individual crowns could be evaluated to determine if moss presence can be reliably detected within the individual tree crowns using in-field survey data of known presence or absence. Like DBH, this predictor could provide highly valuable information and yield higher classification accuracies, as it could begin to characterize the suitability of micro-habitat characteristics within individual trees. The incorporation of a reliable moss detection predictor would also likely improve the classification of Rank 3 and Rank 4 habitats that are, as discussed, often only differentiable by the presence or absence of suitable platforms and or moss or duff coverage.

5.9 Lidar-Specific Challenges and Recommendations

Finally, lidar data allow for the quantitative measurement of structural attributes and the ability to refine the spatial scale of habitat data, it presents its own challenges. Several lidar-specific recommendations are made for future studies. While the high financial costs associated with the acquisition and processing of lidar data have been significantly

reduced over the past decade due to the expansion of commercially available sensors and data to the public and academic sectors (Bradbury et al., 2005), costs can still be quite high. However, by deriving multiuse products from the data, such as volume estimates for inventorying, terrain data for road building and block planning, and area-based canopy descriptors for wildlife modelling, these higher financial costs can be shared across departments or corporations. By deriving these multi-use products and distributing costs, the acquisition of lidar data can become a more realistic and attainable option for a wider range of users.

For future studies collecting lidar data specifically for marbled murrelet habitat assessment, it is recommended that data with a point density of at least ~10 pts/m^2 be acquired. This point density would ensure adequate representation of the canopy and the ground surface below, as well as the accurate detection of individual tree objects and calculation of habitat descriptors from the point cloud. Because suitable nesting habitat is dominantly provided by coniferous trees and not deciduous, the time of year is not a critical consideration for data collection. Further, it is recommended that CHMs derived from lidar data be gridded at a minimum of a 1 m spatial resolution, with the ideal resolution being sub-metre. Individual tree objects should be detected from CHMs that have been filtered to remove noise in the upper canopy. To select the appropriate filter, multiple filters should be evaluated (mean, Gaussian, median etc.), using varying kernel size windows, by testing the resultant treetop data against the point cloud to evaluate the rates of omission and commission. Specific height-based kernel sizes can also be evaluated when detecting individual tree objects from the smoothed CHMs, again by

testing the resultant treetop data against the point cloud to evaluate the rates of omission and commission. Lastly, canopy descriptors should ideally be calculated at a spatial resolution between 10 and 30 m, dependent on the structural characteristics of the forests being assessed (i.e. larger trees typically have larger crowns and thus require larger grid spacing to accurately capture canopy structure).

Chapter 6: Conclusion

6.1 Summary and Conclusions

This research utilized lidar data to derive both the structural habitat descriptors used as model predictors and the individual tree objects used as the spatial modelling units. A data driven methodology was developed to predict the habitat suitability (Rank 1 – Rank 5) of individual trees within mature and old-growth forests (> 141 years) on Northern Vancouver Island. The methodology utilized a BRF ensemble classifier and 12 habitat predictors (10 lidar-derived) to predict habitat suitability derived from LLAS waypoint data.

The LLAS waypoint data were re-assessed with a high-intensity, plot-based LLAS method to evaluate the reliability of their assigned habitat suitability rankings. Overall, results indicated the waypoint data were moderately reliable (48%), with the data being more likely to underestimate habitat suitability than overestimate it. Yet, when considered within the context of the broader operational habitat rankings used for strategic management (Suitable: Rank 1, Rank 2, and Rank 3 or Unsuitable: Rank 4, Rank 5, and Rank 6), the habitat rankings were reliable (85%). The data were therefore determined to be accurate indictors of habitat suitability and were used to inform the selection of model training data.

Individual tree objects were extracted from lidar-derived CHMs, and 19 habitat descriptors were extracted from the normalized lidar point cloud and the lidar-derived DEMs. Ultimately, 12 descriptors were selected as model predictors based on expertise,

literature, and separability: individual tree height (*Height*), canopy rugosity (*Rugosity*), height of the dominant canopy (*AHA_85P*), height of the co-dominant canopy (*Height_85P*), canopy closure (*Canopy Closure*), elevation (*Elevation*), distance to saltwater (*DIST_SW*), topographic aspect (*Aspect*), slope gradient (*Slope*), topographic ruggedness index (*TRI*), BEC zone (*BEC*) and the COType of the LMI spatial statistic (*LMI*).

The BRF classification model reporting an overall classification accuracy of 71.05% and individual classification accuracies of 90%, 86%, 74%, 67% and 98% for Rank 1, Rank 2, Rank 3, Rank 4 and Rank 5, respectively. Variable importance measurements indicated there was a clear scale-based stratification of variable importance, where nesting habitat suitability was most influence by landscape-scale predictors (elevation, distance to saltwater, aspect, slope, and topographic ruggedness, in decreasing order), and then by canopy-based predictors (canopy rugosity, height of the dominant and co-dominant canopy, height of the individual tree, and canopy closure, in decreasing order). Based on low variable importance, the predictors representing BEC zone and LMI were determined to be more valuable as pre-stratification or clustering tools, rather than as model predictors. The BRF classification model was then used to predict the habitat suitability of all unranked trees in the study area, producing the final object-based predictive habitat suitability maps.

These object-based habitat suitability maps were then compared to stand-based LLAS polygon habitat maps, representing the current habitat maps used for strategic

management within the study sites. Comparisons demonstrated that the refined spatial scale utilized by the methodology developed here does facilitate the detection of smaller patches of suitable habitat within larger unsuitable habitat areas. Lastly, this research made recommendations for future lidar-based marbled murrelet habitat studies. Specifically, for the extension of object-based habitat suitability map coverage across the province utilizing this methodology, the development of a lidar-based occupancy model, and the eventual establishment of a quantitative, lidar-based habitat classification scheme.

The two main limitations of this research surrounded the reliability of the LLAS waypoint data, and the absence of a validation campaign to evaluate the accuracy of the object-based model predictions. However, this research provides a preliminary method that can be further refined through continued research that has access to more reliable habitat data and the required resources to conduct a validation campaign.

6.2 Research Contributions

The recovery of the marbled murrelet in B.C. is dependent on the preservation of suitable nesting habitat. As their preferred nesting habitats, large old-growth trees, are often prime candidates for harvesting due to their high timber value, the efficient management of resources in these mixed-use landscapes is critical. In order to adequately manage these landscapes, reliable spatial habitat data are required. While there is consensus about the biophysical and geographical characteristics that comprise suitable nesting habitat, there has been continued uncertainty about the large stand-based spatial scale and qualitative classification of habitat used by current habitat mapping methods.

This research attempted to fill these methodological gaps by developing a repeatable methodological framework capable of quantitatively mapping habitat at a sub-stand, individual tree – based scale. While lidar data have long offered proven methods for the direct characterization of structural forest components (Maltamo et al., 2014; White et al., 2013), this research demonstrates its added utility for wildlife applications. This thesis contributes to the literature regarding the classification and mapping of marbled murrelet nesting habitat, as well as other structurally-dependent forest dwelling species. The methodology developed here facilitates improved habitat quantification through the use of a refined spatial scale. These refined spatial data can be used to help inform the establishment of protected areas, not only helping to facilitate species recovery, but also protecting habitat for other old-growth dependent species. Additionally, the method developed here provides a repeatable framework that can be used to expand the network of improved habitat data across the province, which will help to improve the quantification of nesting habitat in all seven conservation regions. Lastly, this new methodology provides habitat data a spatial scale that facilitates up-scaling, which will become increasingly valuable as more definitive data regarding the most appropriate spatial scale for mapping marbled murrelet nesting habitat (i.e. minimum patch size) become available.

Lidar-based predictive modelling for marbled murrelet nesting habitat has been explored in the U.S. (Hagar et al., 2014), however its application here in B.C., and the utilization of an object-based scale was novel. This research provided further evidence that lidar-derived habitat descriptors can be used to improve the prediction of suitable nesting

habitat for the marbled murrelet, and demonstrates, that by utilizing lidar data, the spatial scale of habitat data can be refined from a stand-based scale to an individual tree – based scale. As the total amount of suitable nesting habitat in B.C. is expected to continue to decline, this improved quantification of habitat is a critical advancement for strategic managers that will facilitate improved forest resource management, ultimately aiding in the recovery of the marbled murrelet.

References

Ackers, S. H., Davis, R. J., Olsen, K. A., & Dugger, K. M. (2015). The evolution of mapping habitat for northern spotted owls (*Strix occidentalis caurina*): A comparison of photo-interpreted, Landsat-based, and lidar-based habitat maps. *Remote Sensing of Environment*, *156*, 361–373. https://doi.org/10.1016/j.rse.2014.09.025

Bahn, V., & Newsom, D. (2002). Habitat suitability mapping for Marbled Murrelets in Clayoquot Sound. In *Multi-Scale Studies of Populations, Distribution and Habitat Associations of Marbled Murrelets in Clayoquot Sound, British Columbia (*Burger, A.E. & Chatwin, T., Eds.) (101-120).

Binford, L. C., Elliott, B. G., & Singer, S. W. (1975). Discovery of a nest and the downy young of the Marbled Murrelet. *Wilson Bulletin* 87:303- 319.

Bloxton, T. D., & Raphael, M. G. Jr. (2009). *Breeding ecology of marbled murrelet in Washington State – Five year project summary* (2004 – 2008). USDA Forest Service. Pacific Northwest Research Station. Olympia Washington.

B.C. Conservation Data Center (2016). B.C. Species and Ecosystems Explorer – MarbledMurrelet. Retrieved from http://a100.gov.B.C..ca/pub/eswp

B.C. Ministry of Environment. (2004). *Indentified Wilflide Managment Strategy: Marbled Murrelet*. Accounts and Measures for Managing Identified Wildlife (Vol. 1).

B.C. Ministry of Forests Lands and Natural Resource Operations. (2016). Biogeoclimatic Ecological Classification (BEC) Zone Map of B.C. Forest Analysis and Inventory. Retrieved from https://catalogue.data.gov.B.C..ca/dataset/biogeoclimatic-ecosystem-classification-bec-map

Bae, S., Reineking, B., & Ewald, M. (2014). Comparison of airborne lidar, aerial photography, and field surveys to model the habitat suitability of a cryptic forest species – the hazel grouse. *International Journal of Remote Sensing*, 35(17), 37–41. https://doi.org/10.1080/01431161.2014.955145

Berk, R. A. (2008). Statistical Learning from a Regression Perspective, New York, NY Springer New York. https://doi.org/10.1007/978-0-387-98135-2

Bertram, D. F., Drever, M. C., McAllister, M. K., Schroeder, B. K., Lindsay, D. J., & Faust, D. A. (2015). Estimation of coast-wide population trends of marbled murrelets in Canada using a Bayesian hierarchical model. *PLoS ONE*, *10*(8), 1–21. https://doi.org/10.1371/journal.pone.0134891

Bradbury, R. B., Hill, R. A., Aason, D. C., Hinsley, S. A., Wilson, J. D., Balzter, H., … Bellamy, P. E. (2005). Modelling relationships between birds and vegetation structure using airborne LiDAR data: a review with case studies from agricultural and woodland environments. *International Journal of Avian Science*, *147*, 443–452.

Bradley, R. W., & Cooke, F. (2001). Cliff and deciduous tree nests of marbled murrelets in Southwestern British Columbia. *Northwestern Naturalist*, *82*(2), 52–57. http://www.jstor.org/stable/3536786.

Branion-calles, M. C. (2015). *Modelling and Mapping Regional Indoor Radon Risk in British Columbia, Canada* (Master's thesis). Retrieved from UVicSpace ETD.

Branion-Calles, M. C., Nelson, T. A., & Henderson, S. B. (2015). A geospatial approach to the prediction of indoor radon vulnerability in British Columbia, Canada. *Journal of Exposure Science and Environmental Epidemiology*, 1–12. https://doi.org/10.1038/jes.2015.20

Breidenbach, J., Koch, B., Kändler, G., & Kleusberg, A. (2008). Quantifying the influence of slope, aspect, crown shape and stem density on the estimation of tree height at plot level using lidar and InSAR data. *International Journal of Remote Sensing*, 29(5), 1511–1536.https://doi.org/10.1080/01431160701736364

Breiman, L. (2001). Random Forrest. *Machine Learning*, 45(1), 5–32. https://doi.org/10.1023/A:1010933404324

Burger, A. E. (1997). Behavior and Numbers of Marbled Murrelets Measured with Radar. *Journal of Field Ornithology*, *68*(2), 208–223.

Burger, A. E. (2001). Using radar to estimate populations and assess habitat associations of Marbled Murrelets. *The Journal of Wildlife Management*, *65*(4), 696–715. Retrieved from http://www.jstor.org/stable/3803021

Burger, A. E. (2002). Marbled Murrelet Conservation Assessment, Part A: Conservation assessment of Marbled Murrelets in British Columbia: a review of the biology, populations, habitat associations and conservation. *Technical Report Series No. 387*, Canadian Wildlife Service, Delta, B.C. Retrieved form http://www.sfu.ca/biology/wildberg/bertram/mamurt/links.htm

Burger, A. E. (ed.) (2004). Standard Methods for Identifying and Ranking Nesting Habitat of Marbled Murrelets (*Brachyramphus marmoratus*) in British Columbia using Air Photo Interpretation and Low-Level Aerial Surveys. Ministry of Water, Land and Air Protection, Victoria B.C. and Ministry of Forests Nanaimo, B.C. Retrieved from http://www.env.gov.bc.ca/wld/documents/fia_docs/mamu_standard.pdf

Burger, A. E. (unpublished). Effects of human landscape modification on nesting Marbled Murrelets – a review (Draft). Canadian Wildlife Services, Environment Canada, Delta, B.C.

Burger, A. E., & Bahn, V. (2004). Inland habitat associations of Marbled Murrelets on southwest Vancouver Island, British Columbia. *Journal of Field Ornithology*, *75*(1), 53–66.

Burger, A. E., & Chatwin, T. A. (eds.) (2002). Multi-Scale Studies of Populations, Distribution and Habitat Associations of Marbled Murrelets in Clayoquot Sound, British Columbia. Ministry of Water, Land and Air Protection, Victoria, B.C.

Burger, A. E., Manley, I. A., Silvergieter, M. P., Lank, D. B., Jordan, K. M., Bloxton, T. D., & Raphael, M. G. (2009). Re-use of nest sites by Marbled Murrelets (*Brachyramphus marmoratus*) in British Columbia. *Northwestern Naturalist*, *90*(3), 217–226. https://doi.org/10.1898/NWN08-50.1

Burger, A. E., Masselink, M. M., Tillmanns, A. R. M., Szabo, A. R., Farnholtz, M., & Krkosek, M. J. (2004). Effects of habitat fragmentation and forest edges on predators of Marbled Murrelets and other forest birds on Southwest Vancouver Island. Proceedings of the Species at Risk 2004 Pathways to Recovery Conference, Victoria, B.C., 1–19.

Burger, A. E., Ronconi, R. A., Silvergieter, M. P., Conroy, C., Bahn, V., Manley, I. A., … Lank, D. B. (2010). Factors affecting the availability of thick epiphyte mats and other potential nest platforms for Marbled Murrelets in British Columbia. *Canadian Journal of Forest Research*, *40*(4), 727–746. https://doi.org/10.1139/X10-034

Burger, A. E., & Waterhouse, F. L. (2009). Relationships between habitat area, habitat quality, and populations of nesting Marbled Murrelets. *BC Journal of Ecosystems and Management*, *10*(1), 101–112.

Burger, A. E., Waterhouse, F. L., Donaldson, A., Lank, D. B., & Whittaker, C. (2009). New methods for assessing Marbled Murrelet nesting habitat: Air photo interpretation and low-level aerial surveys. *BC Journal of Ecosystems and Management*, *10*(1), 4–14. 14. www.forrex.org/publications/jem/ISS50/vol10_no1_art2.pdf

Casas, Á., García, M., Siegel, R. B., Koltunov, A., Ramírez, C., & Ustin, S. (2016). Burned forest characterization at single-tree level with airborne laser scanning for assessing wildlife habitat. *Remote Sensing of Environment*, 175(2016), 231-241. https://doi.org/10.1016/j.rse.2015.12.044

Chen, C., Liaw, A., & Breiman, L. (2004). Using random forest to learn imbalanced data. University of California, Berkeley, 1–12.

CMMRT (Canadian Marbled Murrelet Recovery Team). (2003). Marbled Murrelet Conservation Assessment 2003, Part B: Marbled Murrelet Recovery Team Advisory Document on Conservation and Management. Canadian Wildlife Service, Delta, B.C. http://www.sfu.ca/biology/wildberg/bertram/mamurt/links.htm

Conroy, C. J., Bahn, V., Rodway, M.S., Ainsworth, L., & Newsom, D. (2002). Estimating nest densities for Marbled Murrelets in three habitat suitability categories in the Ursus Valley, Clayoquot Sound. Pages 121-137 in Multi-scale studies of populations, distribution and habitat associations of Marbled Murrelets in Clayoquot Sound, British Columbia. A. E. Burger and T. A. Chatwin (eds.). Ministry of Water, Land and Air Protection, Victoria, B.C.

COSEWIC. (2012). COSEWIC assessment and status report on the Marbled Murrelet *Brachyramphus marmoratus* in Canada. Committee on the Status of Endangered Wildlife in Canada. Ottawa. 1-82.www.registrelep-sararegistry.gc.ca/default_e.cfm, last accessed January 1, 2017

Cutler, D. R., Edwards, T. C., Beard, K. H., Cutler, A., Hess, K. T., Gibson, J., & Lawler, J. J. (2007). Random forests for classification in ecology. *Ecology*, *88*(11), 2783–2792. https://doi.org/10.1890/07-0539.1

Donald, D. S., Waterhouse, F. L., & Ott, P. K. (2010). Verification of a Marbled Murrelet habitat inventory on the British Columbian Central Coast. B.C. Ministry of Forests & Range Science Progress and Ministry of Environment Stewardship Division, Victoria, B.C. *Technical Report No. 060*. http://www.for.gov.bc.ca/hfd/pubs/Docs/Tr/Tr060.htm

Environment Canada. (2014). Recovery Strategy for the Marbled Murrelet (*Brachyramphus marmoratus*) in Canada. *Species at Risk Act* Recovery Strategy Series. Environment Canada, Ottawa. 1-49.

Evans, J. S., & Hudak, A. T. (2007). A multiscale curvature algorithm for classifying discrete return LiDAR in forested environments. *IEEE Transactions on Geoscience and Remote Sensing*, *45*(4), 1029–1038. https://doi.org/10.1109/TGRS.2006.890412

Eysn, L., Hollaus, M., Lindberg, E., Berger, F., Monnet, J. M., Dalponte, M., … Pfeifer, N. (2015). A benchmark of lidar-based single tree detection methods using heterogeneous forest data from the Alpine Space. *Forests*, *6*(5), 1721–1747. https://doi.org/10.3390/f6051721

Falxa, G. A., Raphael, M. G., Baldwin, J., Lynch, D., Miller, S. L., Nelson, S. K., … Young, R. D. (2013). Marbled murrelet effectiveness monitoring, Northwest Forest Plan: 2011 and 2012 summary report. U.S. Fist and Wildlife Service, Arcata, CA.

Farrell, S. L., Collier, B. A., Skow, K. L., Long, A. M., Campomizzi, A. J., Morrison, M. L., … Wilkins, R. N. (2013). Using LiDAR-derived vegetation metrics for high resolution, species distribution models for conservation planning. *Ecosphere*, *4*(3), 1–18. https://doi.org/10.1890/ES12-000352.1

Fatourechi, M., Ward, R. K., Mason, S. G., Huggins, J., Schlögl, A., & Birch, G. E. (2008). Comparison of evaluation metrics in classification applications with imbalanced datasets. *Proceedings - 7th International Conference on Machine Learning and Applications, ICMLA 2008*, 777–782. https://doi.org/10.1109/ICMLA.2008.34

Fortin, M. J., Dale, M. R. T., & Hoef, J. (2002). Spatial analysis in ecology. *Encyclopedia of Environmetrics*, *4*, 2051–2058. https://doi.org/10.1002/9780470057339.vas039

Gabriel, P. O., & Golightly, R. T. (2014). Aversive conditioning of Steller's Jays to improve marbled murrelet nest survival. *Journal of Wildlife Management*, *78*(5), 894–903. https://doi.org/10.1002/jwmg.725

Graf, R. F., Mathys, L., & Bollmann, K. (2009). Habitat assessment for forest dwelling species using LiDAR remote sensing: Capercaillie in the Alps. *Forest Ecology and Management*, *257*(1), 160–167. https://doi.org/10.1016/j.foreco.2008.08.021

Grohmann, C. H. (2015). Effects of spatial resolution on slope and aspect derivation for regional-scale analysis. *Computers and Geosciences*, *77*, 111–117. https://doi.org/10.1016/j.cageo.2015.02.003

Guisan, A., & Zimmermann, N. E. (2000). Predictive habitat distribution models in ecology. *Ecological Modelling*, *135*, 147–186. https://doi.org/10.1016/S0304-3800(00)00354-9

Hagar, J. C., Eskelson, B. N. I., Haggerty, P. K., Nelson, S. K., & Vesely, D. G. (2014). Modeling marbled murrelet (*Brachyramphus marmoratus*) habitat using LiDAR derived canopy data. *The Wildlife Society Bulletin*, 1–13.

Hamer, T. E., & Nelson, S. K. (1995). Characteristics of Marbled Murrelet nest trees and nesting stands. USDA *General Technical Report*, 69–82.

Hamer, T. E., Varland, D. E., McDonald, T. L., & Meekins, D. (2008). Predictive model of habitat suitability for the marbled murrelet in western Washington. *Journal of Wildlife Management*, *72*, 983–993. https://doi.org/10.2193/2006-565

Heurich, M., Persson, A., Holmgren, J., & Kennel, E. (2003). Detecting and measuring individual trees with laser scanning in mixed mountain forest of central Europe using an algorithm developed for Swedish boreal forest conditions. International Archives of Photogrammetry, *Remote Sensing and Spatial Information Sciences*, 36, 307–312.

Holmgren, J., & Soderman, U. (2002). Detecting and measuring individual trees using an airborne laser scanner. *Photogrammetric Engineering & Remote Sensing*, 68(9), 925–932.

Horn, H. L., Arcese, P., Brunt, K., Burger, A. E., Davis, H., Doyle, F., … Waterhouse, F. L. (2009). Part 3: Knowledge Base for Focal Species and their Habitats in Coastal B.C. Report 3 of the EBM Working Group Focal Species Project. Integrated Land Management Bureau, Nanaimo, B.C.

Isenburg, M. (2014). LAStools - Efficient LiDAR processing software (version 140322, unlicensed), obtained from http://rapidlasso.com/LAStools

Jakubowski, M. K., Li, W., Guo, Q., & Kelly, M. (2013). Delineating individual trees from lidar data: A comparison of vector- and raster-based segmentation approaches. *Remote Sensing*, *5*(9), 4163-4186. https://doi.org/10.3390/rs5094163

Jensen, R. J. (2000). Remote Sensing of the Environment: An Earth Resource Perspective (Keith C. Clarke, Eds.). Prentice Hall, Upper Saddle River, New Jersey.

Lawler, J. J., White, D., Neilson, R. P., & Blaustein, A. R. (2006). Predicting climate induced range shifts: Model differences and model reliability. *Global Change Biology*, *12*(8), 1568–1584. https://doi.org/10.1111/j.1365-2486.2006.01191

Leberl, F., Irschara, A., Pock, T., Meixner, P., Gruber, M., Scholz, S., & Wiechert, A. (2010). Point Clouds: Lidar versus 3D Vision. *Photogrammetric Engineering and Remote Sensing*, *76*(10), 1123–1134.

Lefsky, M. A., Cohen, W. B., Parker, G. G., & Harding, D. J. (2002). Lidar remote sensing for ecosystem studies. *BioScience*, *52*(1), 19-30. https://doi.org/10.1641/0006-3568(2002)052[0019:LRSFES]2.0.CO;2

Lim, K., Treitz, P., Wulder, M., St-Onge, B., & Flood, M. (2003). LiDAR remote sensing of forest structure. *Progress in Physical Geography*, *27*(1), 88–106. https://doi.org/10.1191/0309133303pp360ra

Liu, X. (2008). Airborne LiDAR for DEM generation: some critical issues. *Progress in Physical Geography*, *32*(1), 31–49. https://doi.org/10.1177/0309133308089496

Long, J., Hazlitt, S., Nelson, T., & Laberee, K. (2011). Estimating 30-year change in coastal old‐growth habitat for a forest-nesting seabird in British Columbia, Canada. *Endangered Species Research*, *14*(1), 49–59. https://doi.org/10.3354/esr00341

Lorenz, T. J., Raphael, M. G., Bloxton, T. D., & Cunningham, P. G. (2016). Low breeding propensity and wide-ranging movements by marbled murrelets in Washington. *The Journal of Wildlife Management*, 1–16. https://doi.org/10.1002/jwmg.21192

Mack, D. E., Ritchie, W. P., Nelson, S. K., Kuo-harrison, E., & Hamer, T. E. (2003). Methods for surveying marbled murrelets in forests: A revised protocol for land management and research. Pacific Seabird Group Technical Publication Number 2. Available from http://www.pacificseabirdgroup.org, last accessed January 2017.

Malt, J. M., & Lank, D. B. (2007). Temporal dynamics of edge effects on nest predation risk for the marbled murrelet. *Biological Conservation*, *140*(1–2), 160–173. https://doi.org/10.1016/j.biocon.2007.08.011

Malt, J. M., & Lank, D. B. (2009). Marbled Murrelet forest nest predation risk in managed landscapes: scales effects at multiple dynamic fragmentation. *Ecological Applications*, *19*(5), 1274–1287.

Maltamo, M., Eerikäinen, K., Pitkänen, J., Hyyppä, J., & Vehmas, M. (2004). Estimation of timber volume and stem density based on scanning laser altimetry and expected tree size distribution functions. *Remote Sensing of Environment*, *90*(3), 319–330. https://doi.org/10.1016/j.rse.2004.01.006

Maltamo, M., Naesset, E., & Vauhkonen, J. (2014). Forestry Applications of Airborne Laser Scanning: Concepts and Case Studies. Managing Forest Ecosystems (M. Maltamo, E. Naesset, & J. Vauhkonen, Eds.). Springer New York, NY.

Manley, I. A., Waterhouse, F. L., & Harestad, A. S. (1999). Nesting habitat of marbled murrelets on the Sunshine Coast. *Forest Research Extension Note*. Vancouver Forest Region. Nanaimo, B.C. EN-002, 1–7.

Mather, M., Chatwin, T., Cragg, J., Sinclair, L., & Bertram, D. (2010). Marbled Murrelet nesting habitat suitability model for the British Columbia coast. *BC Journal of Ecosystems and Management*, *11*(1 and 2), 91–102.

McDonald, S., & Leigh-Spencer, S. (2014). Summary of Marbled Murrelet Habitat Low-Level Aerial Survey and Mapping Techniques. *General Technical Report*. https://doi.org/10.1007/s13398-014-0173-7.2

McShane, C., Hamer, T. E., Carter, H. R., Swartzman, G., Friesen, V., Ainley, D., … Keany, J. (2004). Evaluation Report for the 5-Year Status Review of the Marbled Murrelet in Washington, Oregon, and California. U.S. Fish and Wildlife Service Region 1, Portland, OR.

Meidinger, D., & Pojar, J. (1991). *Ecosystems of British Columbia*. B.C. Ministry of Forests, Victoria, B.C. Special Report Series 6.

Meyer, D., Leisch, F., & Hornik, K. (2003). The support vector machine under test. *Neurocomputing*, *55*(1–2), 169–186. https://doi.org/10.1016/S0925-2312(03)00431-4

Miller, S. L., Raphael, M. G., Falxa, G. a., Strong, C., Baldwin, J., Bloxton, T., … Young, R. D. (2012). Recent population decline of the marbled murrelet in the Pacific Northwest. *The Condor*, *114*(4), 771–781. https://doi.org/10.1525/cond.2012.110084

Nelson, S. K. (1997). Marbled Murrelet (*Brachyramphus marmoratus*). In *The Birds of North America* (F. Poole, & A. Gill, Eds.). (pp. 118–119). Philadelphia: Academy of Natural Sciences.

Niemann, K. O. (2009). Evaluation of Emerging Remote Sensing Technologies for the assessment of forest Resources. UVic Hyperspectral and LIDAR Research Group Report, 1-97.

O'Sullivan, D., & Unwin, D. (2010). Area objects and spatial autocorrelation, In *Geographic information analysis* (2nd ed.) (187-214). John Wiley & Sons, Hoboken, NJ.

Parker, R. C., & Evans, D. L. (2004). An application of LiDAR in a double-sample forest inventory. *Western Journal of Applied Forestry,* 19, 95–101.

Peters, J., Baets, B. De, Verhoest, N. E. C., Samson, R., Degroeve, S., Becker, P. De, & Huybrechts, W. (2007). Random forests as a tool for ecohydrological distribution modelling. *Ecological Modelling*, *207*(2–4), 304–318. https://doi.org/10.1016/j.ecolmodel.2007.05.011

Piatt, J. F. (2007). Status Review of the Marbled Murrelet (*Brachyramphus marmoratus*) in Alaska and British Columbia. Open File Report 2006 – 1387. US Geological Society, US Fish and Wildlife Service.

Popescu, S. C., Wynne, R. H., & Nelson, R. F. (2003). Measuring individual tree crown diameter with lidar and assessing its influence on estimating forest volume and biomass. *Canadian Journal of Remote Sensing*, *29*(5), 564–577. https://doi.org/10.5589/m03-027

Prasad, A. M., Iverson, L. R., & Liaw, A. (2006). Newer classification and regression tree techniques: Bagging and random forests for ecological prediction. *Ecosystems*, *9*(2), 181–199. https://doi.org/10.1007/s10021-005-0054-1

Quayle, J. F., & Westereng, L. K. (2000). Methods or Madness? Developing Population Inventory Manuals for British Columbia' s Biodiversity. Proceedings of a Conference on the Biology and Management of Species and Habitats at Risk, Kamloops, B.C.

Quinn, G. S., Niemann, K. O., & Filipescu, C. (2016). Morphometric attribution of a 65-year-old Douglas-fir forest from an airborne and terrestrial integrated laser scanning dataset. Manuscript in preparation.

Ralph, C. J., Hunt, G. L. J., Raphael, M. G., & Piatt, J. F. (1995). Ecology and conservation of the Marbled Murrelet. *General Technical Report*, PSW-GTR-152. Albany, CA: Pacific Southwest Research Station, Forest Service, U.S. Department of Agriculture, 420 p.

Raphael, M. G. (2006). Conservation of the Marbled Murrelet under the Northwest Forest Plan. *Conservation Biology*, *20*(2), 297–305. https://doi.org/10.1111/j.1523-1739.2006.00382.x

Raphael, M. G., Falxa, G. A., Dugger, K. M., Galleher, B. M., Lynch, D., Miller, S. L., … Young, R. D. (2011). Northwest Forest Plan—the first 15 years (1994–2008): status and trend of nesting habitat for the Marbled Murrelet. *General Technical Report*, PNW-GTR-848. Forest Service, U.S. Department of Agriculture.

Raphael, M. G., Mack, D. E., & Cooper, B. A. (2002). Landscape-scale relationships between abundance of marbled murrelets and distribution of nesting habitat. *The Condor*, *104*(2), 331–342.

Riley, S. J., DeGloria, S. D., & Elliot, R. (1999). A terrain ruggedness index that quantifies topographic heterogeneity. *Intermountain Journal of Sciences*, 5(1-4), 23-27. https://doi.org/citeulike-article-id:8858430

Rodway, M. S., & H. M. Regehr. (2002). Inland activity and forest structural characteristics as indicators of Marbled Murrelet nesting habitat in Clayoquot Sound. In Multi- scale studies of populations, distribution and habitat associations of Marbled Murrelets in Clayoquot Sound, British Columbia (A. E. Burger and T. A. Chatwin, Eds.). (Pp. 57-87). Ministry of Water, Land and Air Protection, Victoria, B.C.

Ryder, G. R., Campbell, R. W., Carter, H. R., & Sealy, S. G. (2012). Earliest well-described tree nest of the Marbled Murrelet: Elk Creek , British Columbia , 1955. *Wildlife Afield*, *9*(1), 49–58.

Silvergieter, M. P., & Lank, D. B. (2011a). Marbled Murrelets select distinctive nest trees within old-growth forest patches. *Avian Conservation and Ecology*, *6*(2): 3. https://doi.org/10.5751/ACE-00462-060203

Silvergieter, M. P., & Lank, D. B. (2011b). Patch scale nest-site selection by marbled murrelets (*Brachyramphus marmoratus*). *Avian Conservation and Ecology*, *6*(2): 6. https://doi.org/10.5751/ACE-00483-060206

Stachura-Skierczynska, K., & Kosinski, Z. (2014). Evaluating habitat suitability for the middle spotted woodpecker using a predictive modelling approach. *Annales Zoologici Fennici*, *51*(4), 349–370. https://doi.org/10.5735/086.051.0402

Strachan, G., McAllister, M., & Ralph, C. J. (1995). Marbled Murrelet At-Sea and Foraging Behavior. *General Technical Report*, PWS-152. U.S. Department of Agriculture, Forest Service.

Strîmbu, V. F., & Strîmbu, B. M. (2015). A graph-based segmentation algorithm for tree crown extraction using airborne LiDAR data. *ISPRS Journal of Photogrammetry and Remote Sensing*, *104(2015)*, 30–43. https://doi.org/10.1016/j.isprsjprs.2015.01.018

Strobl, C., Boulesteix, A.-L., Zeileis, A., & Hothorn, T. (2007). Bias in random forest variable importance measures: illustrations, sources and a solution. *BMC Bioinformatics*, *8*(25), 1-21. https://doi.org/10.1186/1471-2105-8-25

Svetnik, V., Liaw, A., Tong, C., Culberson, C. J., Sheridan, R. P., & Feuston, B. P. (2003). Random forest: A classification and regression tool for compound classification and QSAR modeling. *Journal of Chemical Information and Computer Sciences*, *43*(6), 1947–1958. https://doi.org/10.1021/ci034160g

Turner, W., Spector, S., Gardiner, N., Fladeland, M., Sterling, E., & Steininger, M. (2003). Remote sensing for biodiversity science and conservation. *Trends in Ecology & Evolution*, *18*(6), 306–314. https://doi.org/10.1016/S0169-5347(03)00070-3

USFWS (U.S. Fish and Wildlife Service). (1997). Recovery plan for the threatened marbled murrelet (*Brachyramphus marmoratus*) in Washington, Oregon, and California. U.S. Fish and Wildlife Service, Region 1, Portland, OR.

Vierling, K. T., Vierling, L. A., Gould, W. A., Martinuzzi, S., & Clawges, R. M. (2008). Lidar: Shedding new light on habitat characterization and modeling. *Frontiers in Ecology and the Environment*, 6(2), 90-98. https://doi.org/10.1890/070001

Wallace, L., Lucieer, A., Malenovsky, Z., Turner, D., & Vopenka, P. (2016). Assessment of forest structure using two UAV techniques: A comparison of airborne laser scanning and structure from motion (SfM) point clouds. *Forests*, *7*(3), 1–16. https://doi.org/10.3390/f7030062

Waterhouse, F. L., Burger, A. E., Cober, A., Donaldson, A., & Ott, P. K. (2007). Assessing habitat quality of Marbled Murrelet nest sites on the Queen Charlotte Islands/Haida Gwaii, by algorithm, airphoto interpretation, and aerial survey methods. *Forest Research Technical Report,* TR-035. Nanaimo, B.C.

Waterhouse, F. L., Burger, A. E., Ott, P. K., Donaldson, A., & Lank, D. B. (2010). Does interpretation of Marbled Murrelet nesting habitat change with different classification methods? *BC Journal of Ecosystems and Management*, *10*(3), 20–34. www.forrex.org/publications/jem/ISS52/vol10_no3_art4.pdf

Waterhouse, L., Burger, A. E., Lank, D. B., Ott, P. K., Krebs, E. A., & Parker, N. (2009). Using the low-level aerial survey method to identify Marbled Murrelet nesting habitat. *Journal of Ecosystems and Management*, *10*(1), 80–96. www.forrex.org/publications/jem/ISS50/vol10_no1_art8.pdf

Wehr, A., & Lohr, U. (1999). Airborne laser scanning - an introduction and overview. *ISPRS Journal of Photogrammetry and Remote Sensing*, *54*(2), 68–82. https://doi.org/Doi 10.1016/S0924-2716(99)00011-8

Westoby, M. J., Brasington, J., Glasser, N. F., Hambrey, M. J., & Reynolds, J. M. (2012). 'Structure-from-Motion' photogrammetry: A low-cost, effective tool for geoscience applications. *Geomorphology*, 179(2012), 300–314. https://doi.org/10.1016/j.geomorph.2012.08.021

White, J. C., Wulder, M. A., Varhola, A., Vastaranta, M., Coops, N. C., Cook, B. D., … Woods, M. (2013). A best practices guide for generating forest inventory attributes from airborne laser scanning data using an area-based approach. Natural Resources Canada, Canadian Forest Service, Canadian Wood Fiber Centre. *Information Report*, F1-X-010.

Wilk, R. J., Raphael, M. G., & Bloxton, T. D. (2016). Nesting habitat characteristics of Marbled Murrelets occurring in near-shore waters of the Olympic Peninsula, Washington. *Journal of Field Ornithology*, *87*(2), 162–175. https://doi.org/10.1111/jofo.12150

Williams, G. (2011). Data Mining with Rattle and R: The Art of Excavating Data for Knowledge Discovery. (R. Gentleman, K. Hornik, & G. G. Parmigiani, Eds.). New York: Springer, NY.

Wong, S. N. P., Ronconi, R. A., Burger, A. E., & Hansen, B. (2008). Marine distribution and behavior of juvenile and adult marbled murrelets off Southwest Vancouver Island, British Columbia: Applications for monitoring. *The Condor*, *110*(2), 306–315. https://doi.org/10.1525/cond.2008.8377

Zellweger, F., Morsdorf, F., Purves, R. S., Braunisch, V., & Bollmann, K. (2013). Improved methods for measuring forest landscape structure: LiDAR complements field-based habitat assessment. *Biodiversity and Conservation*, *23*(2), 289–307. https://doi.org/10.1007/s10531-013-0600-7

Zhao, F., Guo, Q., & Kelly, M. (2012). Allometric equation choice impacts lidar-based forest biomass estimates: A case study from the Sierra National Forest, CA. *Agricultural and Forest Meteorology*, 165(2012), 64–72. https://doi.org/10.1016/j.agrformet.2012.05.019

Zharikov, Y., Lank, D. B., Huettmann, F., Bradley, R. W., Parker, N., Yen, … Cooke, F. (2006). Habitat selection and breeding success in a forest-nesting Alcid, the Marbled Murrelet, in two landscapes with different degrees of forest fragmentation. *Landscape Ecology*, *21*(1), 107–120. https://doi.org/10.1007/s10980-005-1438-5

Appendix A

The standard datasheet for aerial assessment of marbled murrelet nesting habitat suitability used at calibration sites during the original 2005/2006 LLAS that collected the LLAS waypoint data used for model training; from standard methods for API and LLAS for marbled murrelet habitat assessment (Burger, 2004).

Observers:				Date:			
Polygon or Air Photo #:				Still Photo #:			
Description:		UTM Zone:		Easting:			
				Northing:			
Rank (shaded parameters are most important)							
	6 Nil	5 Very low	4 Low	3 Moderate	2 High	1 Very High	
Large trees (% of canopy trees)	0	~1%	1-5%	6-25%	26-50%	51-100%	
% canopy & emergent trees with platforms	0	~1%	1-5%	6-25%	26-50%	51-100%	
Moss development (% canopy trees with obvious mossy pads)	0	~1%	1-5%	6-25%	26-50%	51-100%	
Canopy closure (circle nearest 10%)	-	<20% or >80%	20% or 80%	30% or 70%	40%, 50%, or 60%		
Vertical canopy complexity	Nil	Very low	Low	Moderate	High	Very High	
Topographic complexity	Nil	Very low	Low	Moderate	High	Very High	
Age class	<8 (<140 y)		8 (140-250 y)		9 (>250 y)		
Leading Tree Species: a) Slopes b) Valley Bottom	Western hemlock Hw	Amabilis fir Ba	Western redcedar Cw	Yellow cedar Yc	Sitka spruce Ss	Douglas fir Fd	Other:
Overall field ranking							
PATCH	6	5	4	3	2	1	
POLYGON	6	5	4	3	2	1	
(give % of polygon area in each class)							
Slope position	Valley bottom	Lower slope	Mid slope	Upper slope	Ridge top	Not included in ranking	
Slope grade	Flat	Gentle	Moderate	Steep			
Notes:							

Appendix B

Habitat characteristics and criteria used to assess habitat suitability during the high intensity plot-based LLAS used to re-asses the LLAS waypoint data; adapted from standard methods for API and LLAS for marbled murrelet habitat assessment (Burger, 2004).

1.0 The % of canopy trees that are large: the percentage of all trees that are large, i.e. height class ≥ 4 or > 28.4 m. This was classified as: Rank 1 (Very High) = 51-100% or at least 1 in every 2 trees, Rank 2 (High) = 26-50% or at least 1 in every 4 trees, Rank 3 (Moderate) = 6-25% or at least 1 in every 16 trees, Rank 4 (Low) = 1-5% or at least 1 in every 100 trees, Rank 5 (Very Low) = approximately 1% or less than 1 in every 100 trees), or Rank 6 (Nil) = 0% or no trees. It is impossible to judge exact tree height accurately from a helicopter, therefore the % of trees capable of providing a nest site for murrelets within the canopy or emergent layers is assessed.

2.0 The % of canopy and emergent trees with platforms: The percentage of canopy and emergent trees with one or more platforms (defined as limbs or deformities >15 cm in diameter providing a nest site and landing platform for murrelets). This was classified as: Rank 1 (Very High) = 51-100% or at least 1 in every 2 trees, Rank 2 (High) = 26-50% or at least 1 in every 4 trees, Rank 3 (Moderate) = 6-25% or at least 1 in every 16 trees, Rank 4 (Low) = 1-5% or at least 1 in every 100 trees, Rank 5 (Very Low) = approximately 1% or less than 1 in every 100 trees), or Rank 6 (Nil) = 0% or no trees. Assessments were focused on the limbs within the canopy, not on the outer or upper extremities as murrelets generally nest in the mid- to lower-third of the canopy. Mossy limbs on the upper canopy and emergent crowns are generally most obvious, while these might not be used by murrelets, they are often indicators of similar mossy platforms within the canopy itself. However, note that the absence of mossy platforms on the outer extremities does not mean they are absent within the canopy itself. It is easier to assess platforms within the canopy by looking horizontally into the canopy than by looking down from above. The helicopter was flown as close to the canopy along slopes and as low as possible over flat areas, taking into account all safety concerns. It is possible for the platform ranking to be higher than the moss ranking (3.0) but it is not possible for it to have a lower ranking than the moss variable.

3.0 The % of canopy trees with obvious mossy pads: Reported as the percentage of canopy and emergent trees with obvious mossy pads on the limbs. This was classified as: Rank 1 (Very High) = 51-100% or at least 1 in every 2 trees, Rank 2 (High) = 26-50% or at least 1 in every 4 trees, Rank 3 (Moderate) = 6-25% or at least 1 in every 16 trees, Rank 4 (Low) = 1-5% or at least 1 in every 100 trees, Rank 5 (Very Low) = approximately 1% or less than 1 in every 100 trees), or Rank 6 (Nil) = 0% or no trees. The majority of the plot locations were in moist habitats therefore mossy pads provided most of the platforms meaning this ranking was similar to the % of trees with platforms (2.0). However, as mentioned it is possible to have a plot

with platforms but with insufficient moss development, therefore the plot does not provide suitable habitat. It is also important to not confuse mossy pads on the limbs with obvious growths of lichen ("old man's beard") which are very common in some environments, but generally do not provide nest platforms.

4.0 Canopy Closure (to the nearest 10%): Canopy Closure is equal to the percentage of the ground that is covered by the canopy vegetation. This was classified as: Rank 1 (Very High) & Rank 2 (High) = 40, 50 or 60%, Rank 3 (Moderate) = 30% or 70%, Rank 4 (Low) = 20% or 80%, Rank 5 (Very Low) = < 20% or > 80%, or Rank 6 (Nil) = Harvested or Non-Vegetated. Note that both High and Very High share the same canopy closure values. Note also that the ranking is not linear: for example if a plot was identified as Rank 4 (Low) for Canopy Closure it could have been because the canopy was too sparse (circled < 20%) or that too dense (circled > 80%).

5.0 Vertical Canopy Complexity: Variation of the canopy, including an assessment of "gappiness". This was classified as: Rank 1 (Very High) = Very Non-Uniform (> 40% difference between leading trees and average canopy, very irregular canopy created by emergent trees, gaps, fallen trees), Rank 2 (High) = Non-Uniform (31-40% height difference, canopy gaps often visible due to past disturbance, irregular canopy created by emergent trees, gaps, fallen trees), Rank 3 (Moderate) = Moderately Uniform (21-30% height difference, some canopy gaps visible, evidence of past disturbance, a few emergent trees and obvious gaps), Rank 4 (Low) = Uniform (11-20% height difference, few canopy gaps visible, little or no evidence of disturbance, no emergent trees), and Rank 5 (Very Low) = Very Uniform (<11% height difference between leading trees and average canopy, no evidence of canopy gaps or recent disturbance, no emergent trees). Rank 6 (Nil) was not considered here.

6.0 Topographic Complexity: Topographic complexity is assessed based on the effect of stand-level topography in creating small gaps and creating a complex canopy structure. Stand-level complexity can be created by slope, small rocky outcrops, avalanche chutes, large boulders, etc. This was classified as: Rank 1 (Very High) = Very High Topographic Complexity, Rank 2 (High) = High Topographic Complexity, Rank 3 (Moderate) = Moderate Topographic Complexity, Rank 4 (Low) = Low Topographic Complexity, Rank 5 (Very Low) = Very Low Topographic Complexity, or Rank 6 (Nil) = No Topographic Complexity. Contributing topographic elements were noted if complexity was not low.

7.0 Age Class: The estimated age of the forest stand. This was classified as: Age Class < 8 (<140 y), Age Class 8 (141-250 y), or Age Class 9 (>250 y). It was noted if the plot Age Class was not consistent throughout. For example: Plot was Age Class < 8 but contained a few large veterans trees Age Class 9.

8.0 Leading Tree Species: The identification and ranking of the tree species in the plot. This was classified as: Rank 1 = Dominant, Rank 2 = Secondary, or Rank 3 = Tertiary. Note that more than one species can be included in each ranking (e.g., both

western hemlock and western red-cedar can be rated 1 if they are co-dominants). If less common species not listed on the data sheet, such as alders, are identified note their name and ranking in the additional notes section (12.0). Rare species which do not contribute significantly to the canopy and emergent layers were ignored.

9.0 Overall Plot Rank: After all of the above elements are assessed their rankings are used to determine an overall habitat suitability rank for the plot. This was classified as: Rank 1 = Very High Suitability, Rank 2 = High Suitability, Rank 3 = Moderate Suitability, Rank 4 = Low Suitability, Rank 5 = Very Low Suitability, or Rank 6 = Nil Suitability. If the habitat was not consistent throughout the plot it was noted during 10.0, 11.0 and or 12.0.

10.0 Best Tree Rank: After the Overall Plot Rank is decided, observers assess if there is a single tree, or small number of trees, within the plot that would constitute a higher habitat rank than the Overall Plot Rank. More specifically: if a high proportion of trees (51-100% or 1 in every 2 trees) in the plot had the characteristics of the identified tree(s), what Overall Plot Rank would you assign? This was classified as: Rank 1 = Very High Suitability, Rank 2 = High Suitability, Rank 3 = Moderate Suitability, Rank 4 = Low Suitability, Rank 5 = Very Low Suitability, or Rank 6 = Nil Suitability. This element was added to the LLAS methodology as a way of identifying within plot variability and habitat patches. If the Best Tree Rank differs from Overall Plot Rank, it is an indication that there is patch of habitat within the plot that may support marbled murrelet nesting even if the plot likely would not.

11.0 Surrounding Area Rank: This ranking was based on the general assessment of habitat surrounding a plot. More specifically: up to a distance of 250 m in all directions outside the plot, how does the habitat quality compare to that of the plot? This was classified as 1 = Very High, 2 = High, 3 = Moderate, 4 = Low, 5 = Very Low, or 6 = Nil. This element was added to the LLAS methodology as another way of identifying habitat patches and provide insight about the appropriate scale for modelling. If the Surrounding Area Rank differs from Overall Plot Rank, it is an indication that the plot itself is a patch of habitat within a larger area of habitat that may not support marbled murrelet nesting itself.

12.0 Additional Notes or Comments: Space was provided for brief notes such as but not limited to (1) Evidence of recent disturbance events, harvesting, avalanches, landslides, fires, wind-throw, etc. or other disturbance which might alter the amount of habitat, (2) How many trees are indicated by the Best Tree Rank – single, multiple etc., (3) Factors that might have limited the ability to accurately assess the plot such as weather (4) Additional tree species that were present but not listed on the data sheet or (5) Where observers disagreed on an assessment and how they came to agree.

Appendix C

The updated datasheet used during the 2015 LLAS conducted to re-assess LLAS waypoint data; adapted standard datasheet from standard methods for API and LLAS for marbled murrelet habitat assessment (Burger, 2004).

Observer:			Date:			
Point ID:		OziExplorer ID:		Photo ID:		
Habitat Suitability Rank	**6 Nil**	**5 Very low**	**4 Low**	**3 Moderate**	**2 High**	**1 Very High**
The % of canopy trees that are Large	**0**	**~1%**	**1-5%**	**6-25%**	**26-50%**	**51-100%**
The % of canopy & emergent trees with platforms	**0**	**~1%**	**1-5%**	**6-25%**	**26-50%**	**51-100%**
The % of canopy trees with obvious mossy pads	**0**	**~1%**	**1-5%**	**6-25%**	**26-50%**	**51-100%**
Canopy closure (circle nearest 10%)	-	<20% or >80%	20% or 80%	30% or 70%	40%, 50%, or 60%	
Vertical canopy complexity	**Nil**	**Very low**	**Low**	**Moderate**	**High**	**Very High**
Topographic complexity	Nil	Very low	Low	Moderate	High	Very High
Age class	**<8 (<140 y)**		**8 (140-250 y)**		**9 (>250 y)**	
Leading tree species *1 = Dominant* *2 = Secondary* *3 = Tertiary*	Western hemlock **Hw**	Amabilis fir **Ba**	Western red cedar **Cw**	Yellow cedar **Yc**	Sitka spruce **Ss**	Douglas fir **Fd**
Overall Plot Rank: Based on ~3 ha plot	**6**	**5**	**4**	**3**	**2**	**1**
Best Tree Rank: Within plot area	**6**	**5**	**4**	**3**	**2**	**1**
Surrounding Area Rank: Based on ~ 20 ha surrounding area	**6**	**5**	**4**	**3**	**2**	**1**
Additional Notes or Comments:						